Understanding the mechanism of salt tolerance in alfalfa (*Medicago sativa* L.)

A Thesis Submitted to the College of Graduate and Postdoctoral Studies

In Partial Fulfillment of the Requirements

For the Degree of Doctor of Philosophy

In the Department of Plant Sciences

University of Saskatchewan

Saskatoon

by

SURENDRA BHATTARAI

PERMISSION TO USE

In presenting this dissertation in partial fulfilment of the requirements for a Postgraduate degree from the University of Saskatchewan, I agree that the Libraries of this University may make it freely available for inspection. I further agree that permission for copying of this dissertation in any manner, in whole or in part, for scholarly purposes may be granted by the professor or professors who supervised my dissertation work or, in their absence, by the Head of the Department or the Dean of the College in which my dissertation work was done. It is understood that any copying or publication or use of this dissertation or parts thereof for financial gain shall not be allowed without my written permission. It is also understood that due recognition shall be given to me and to the University of Saskatchewan in any scholarly use which may be made of any material in my dissertation.

Requests for permission to copy or to make other use of the material in this thesis in whole or part should be addressed to:

Head of the Department of Plant Sciences
College of Agriculture and Bioresources
University of Saskatchewan
51 Campus Drive
Saskatoon, Saskatchewan S7N 5A8, Canada

OR

Dean
College of Graduate and Postdoctoral Studies
University of Saskatchewan
116 Thorvaldson Building, 110 Science Place
Saskatoon, Saskatchewan S7N 5C9, Canada

ABSTRACT

Alfalfa (*Medicago sativa* L.) is an important perennial forage legume characterized by its wide adaptability, high forage yield, good quality, and resistance to frequent cuttings. It is often used for pasture, hay, silage, dehydrated products, seed production, and soil improvement. Alfalfa is moderately tolerant to salinity, but its productivity decreases under saline growth condition. Understanding of the salt tolerance mechanism and identification of genes responsible for salt tolerance is critical for the development of salt tolerant alfalfa cultivars. We investigated the morphological, physiological and genetic variation of salt tolerant 'Halo' and salt intolerant 'Vernal' alfalfa cultivars. The specific objectives of the study were: 1) to determine seed germination and post-germination performance of alfalfa cultivars to different salinity stresses, 2) to compare the distribution and accumulation of organic compounds and elements in different tissues of the two alfalfa cultivars under five different salinity stresses, and 3) to identify differentially expressed gene(s) in leaf and root tissues at 12 dS m^{-1}. The response of the alfalfa cultivars to salinity was studied for 12 weeks in five gradients of salt stresses (Electrical conductivities of 0 dS m^{-1}, 4 dS m^{-1}, 8 dS m^{-1}, 12 dS m^{-1} and 16 dS m^{-1}) in a sand based hydroponic system in the College of Agriculture and Bioresources greenhouse at the University of Saskatchewan, using a split-plot arrangement with a randomized complete block design. Elements and organic compounds in leaf, stem, and root tissues were studied using Fourier transform infrared and micro-X-ray fluorescence spectromicroscopy techniques at the Canadian Light Source, as well as using a lab based inductively coupled plasma-mass spectroscopy analysis. RNA-Seq analysis of leaf and root tissues of 'Halo' and 'Vernal' alfalfa were studied at three time points of 0h (control), 3h and 27h after salt treatment of 12 dS m^{-1}. Seed germination percentage and seed vigor were significantly ($P<0.001$) reduced by salt stress. 'Halo' showed significantly greater germination percentage and seed vigor than 'Vernal' at 16 dS m^{-1}, but no difference was found at the other four salt gradients. Salt stress significantly ($P<0.05$) reduced plant height, crude protein, shoot and root biomass, root to shoot ratio. Root tissue of 'Halo' had significantly higher chlorine concentration than leaf tissue at 8 dS m^{-1}, while root tissue of 'Vernal' had significantly lower chlorine concentration than leaf

tissue at 8 dS m^{-1} and 12 dS m^{-1}. The leaf and stem tissue of 'Halo' had higher amide concentration than 'Vernal' at all salt gradients. The distribution of chlorine in salt tolerant cultivar 'Halo' was relatively uniform in the leaf surface and vascular bundles of the stem. RNA-Seq study identified 156 differentially expressed genes in leaf and 322 in roots of the two alfalfa cultivars. This study identified 14 (leaf) and 9 (root) candidate genes consistently expressed in 'Halo' under salt stress, indicating potential genes for marker development. We conclude that "low ion accumulation in the shoot" was a likely tolerance mechanism up to 8 dS m^{-1}, and "tissue tolerance" at 12 dS m^{-1} in tolerant alfalfa. Taken together, the finding of this research and genomic resources generated by this study can be used to develop new salt tolerant alfalfa cultivars.

ACKNOWLEDGEMENTS

I would like to express my sincere gratitude to my supervisor Dr. Bill Biligetu for this opportunity to work with him and for continuous encouragement and guidance throughout my time in the graduate program. This study would not be possible without his suggestions, guidance, and patience. I am also very grateful to my advisory committee members, Drs. Bruce E. Coulman, Yong-Bi Fu, Karen K. Tanino, Chithra Karunakaran, and Tom Warkentin for their valuable advice throughout my graduate program. I would like to thank my external examiner Dr. Long-Xi Yu, United States Department of Agriculture, for his time, effort, and knowledge.

I would like to acknowledge Dr. Fu for allowing me to conduct my RNA-Seq work in his lab, Dr. Karunakaran for allowing me to carry out my synchrotron experiment in her lab, Dr. Yuguang Bai for allowing me to use his lab equipment during my germination experiment, and Dr. Rosalind Bueckert for allowing me to use her lab equipment during my greenhouse experiment. My thanks are also extended to Gregory Peterson and Carolee Horbach at Agriculture and Agri-Food Canada, Saskatoon Research and Development Center for their help during RNA-Seq work, Eldon Simens and Jackie Bantle at the College of Agriculture and Bioresources greenhouses at the University of Saskatchewan and undergraduate student Siyang Shen for their help during my greenhouse study. I would like to thank Drs. Na Liu, Scott Rosendahl, Stuart Read, Renfei Feng, Peter Blanchard, David Muir, and Jarvis Stobbs at the Canadian Light Source for their help during my synchrotron study, data collection and analysis. I would like to thank Barry Goetz and Rocky Kundu for their technical help, and Dr. Raju Soolanayakanahally for his constructive comments. Special thanks go to Dashnyam Byambatseren, Cailin McHardy, Kiran Baral, Dilip Biswas, Samuel Tandoh, Amarjargal Gungaabayar, Chaowei Han, Hu Wang, Kaitlyn Klutz, and Shanna Orloski of the Forage Breeding Group for their help. I appreciate the support I have received from Raju Chaudhary, Sandesh Neupane, Bikash Poudel, Saket Adhikari, Anuja Thapa, Fangqin Zeng, Endale Tafesse, Zalalem Taye, and my fellow graduate students at the Department of Plant Sciences at the University of Saskatchewan.

I am grateful for the financial support provided by the Natural Sciences and Engineering Research Council, F.V. MacHardy Graduate Fellowship in Grasslands Management, Rene Vandeveld Post-Graduate Scholarship, Eric Putt Memorial Scholarship in Plant Sciences, Dr. Guy Lafond Memorial Award and the Seed of the Year Scholarship.

Finally, I would like to extend sincere gratitude to my parents, brother, and sister whose love and encouragement have brought me to this stage. Thanks to my beloved wife for her love and support.

DEDICATION

I dedicate this dissertation to
my mother Man Kumari Neupane,
my father Shankar Prasad Bhattarai &
my wife Sabita Gaire
for their endless love, support and encouragement.

TABLE OF CONTENTS

LIST OF TABLES

LIST OF FIGURES

LIST OF APPENDICES

LIST OF ABBREVIATIONS

ABA	Abscisic acid
ANOVA	Analysis of variance
CLS	Canadian Light Source
CK	Cytokinins
CP	Crude protein
DEGs	Differentially expressed genes
DNA	Deoxyribonucleic acid
dS m^{-1}	deciSiemens per metre
EC	Electrical conductivity
FDR	False discovery rate
FTIR	Fourier transform infrared
g	Grams
GA	Gibberellin
h	Hour
H_2O_2	Hydrogen peroxide
ha	Hectare
ICP-MS	Inductively coupled plasma-mass spectroscopy
IDEAS	Industry, Development, Education, and Students
JA	Jasmonic acid
logFC	Log fold change
Mid-IR	Mid-infrared
MPa	Megapascals
NCBI	National Center for Biotechnology Information
PCA	Principal component analysis
RAPD	Random amplified polymorphic DNA
RCBD	Randomized complete block design
RNA	Ribonucleic acid
ROS	Reactive oxygen species
SA	Salicylic acid
SNP	Single nucleotide polymorphism
VESPERS	Very Sensitive Elemental and Structural Probe Employing Radiation from a Synchrotron
XRF	X-ray fluorescence

Chapter 1: Introduction

Alfalfa (*Medicago sativa* L.), the queen of forages, is characterized by numerous superior traits such as wide adaptability, high forage yield, good forage quality, and resistance to frequent cuttings (Coburn, 1907; Goplen et al., 1982). It is widely cultivated in the Canadian prairies either as a monoculture or in alfalfa-grass mixtures, accounting for 75% of the total national production area (Statistics Canada, 2016). Alfalfa is the main legume forage for the beef and dairy industries of Canada (Canfax Research Services, 2020). To increase the forage production and improve farm profitability it is important to expand current alfalfa production areas to low productive land such as saline regions where annual crop production is limited. Salinization has affected about 6 million ha of agricultural land in the Canadian Prairies (Steppuhn, 1996; Wiebe et al., 2007). Alfalfa is one of a few legumes which can grow in unproductive lands due to its deep tap root system, biological nitrogen fixing capacity and moderate salinity tolerance (Maas and Hoffman, 1977; Goplen et al., 1982). Though a large number of germplasms are available for breeding, alfalfa cultivars with improved salinity tolerance are currently limited. Quantification of morphological and physiological traits and identification of candidate genes are important for new cultivar development. This thesis research was designed to understand the morphological, physiological, and biochemical traits associated with salt tolerance in alfalfa using sand-based hydroponic experiments, cutting-edge synchrotron beamline techniques, as well as the RNA-Seq approach.

It is hypothesized that: 1) alfalfa cultivars with contrasting tolerance to salinity will vary in their morphological and physiological responses at germination and post germination growth and developmental stages; 2) concentration of toxic salt ions such as sodium and chloride in leaf tissue of a salt tolerant alfalfa cultivar will be significantly lower than an intolerant alfalfa cultivar; and 3) a salt tolerant alfalfa cultivar will contain candidate genes for salt tolerance with the consistent expression under salt stress. The objectives of this study were: 1) to determine seed germination and post-germination performance of alfalfa cultivars under different salinity stresses; 2) to compare the distribution and accumulation of organic compounds and elements in different tissues of the two alfalfa cultivars under

different salinity stresses; and 3) to identify differentially expressed gene(s) in leaf and root tissues of the two alfalfa cultivars at 12 dS m^{-1}.

Chapter 2. Literature review

This chapter with some modifications has been published in Agronomy.

Bhattarai, S., Biswas, D., Fu, Y.-B., and Biligetu, B. 2020. Morphological, physiological, and genetic responses to salt stress in alfalfa: a review. Agronomy. 10 (4):577.

For this paper, Surendra Bhattarai reviewed literatures on morphological, physiological, biochemical and genetic responses of alfalfa plants to salt stress, and wrote the manuscript. Drs. Dilip Biswas, Yong-Bi Fu and Bill Biligetu reviewed the manuscript and Surendra Bhattarai did all the revision work.

2.1 Introduction

Alfalfa (*Medicago sativa* L.) is a perennial forage legume that belongs to the sub-family of Papilionoideae. Though diploid forms exist, cultivated alfalfa is predominantly a cross-pollinated, tetraploid (2n = 4x = 32) species (Lesins and Lesins, 1979), which originated in southwestern Asia with Iran as the geographic center of origin (Bolton, 1962; Goplen et al., 1982). Alfalfa is an important forage source for the livestock industries around the world because of its wide adaptability, high yield, good quality, and resistance to frequent cuttings (Coburn, 1907; Goplen et al., 1982). It can be used for pasture, hay, silage, dehydrated products, seed production, and soil improvement (Coburn, 1907; Goplen et al., 1982). Globally, alfalfa is grown on about 30 million ha (Yuegao and Cash, 2009). In Canada, more than four million ha alfalfa is produced either in monoculture or in mixture with grasses (Statistics Canada, 2016), while approximately seven million ha is grown in the United States (USDA-NASS, 2018). Alfalfa is a moderately saline tolerant legume (Maas and Hoffman, 1977). A number of alfalfa cultivars with improved salt tolerance have been developed using conventional breeding approaches (Flowers, 2004). However, genetic improvement of salt tolerance in alfalfa is challenging, mainly as the response of alfalfa plants to salt stress is physiologically and genetically complex because it is controlled by multiple genes and involves various biochemical and physiological mechanisms (Flowers, 2004).

Soil salinity is one of the most influencing stressors that limits agricultural production. Saline soil is characterized by an excess concentration of soluble salts (chloride, sulfate, and carbonate of sodium, calcium, magnesium, potassium) in the root zone, making it difficult for plants to extract water and nutrients from the soil causing plant injury and reducing agricultural production (Szabolcs, 1989). Specifically, soil with an electrical conductivity (EC) of the saturation extract more than 4 dS m^{-1} [approximately 40mM sodium chloride (NaCl)] in the root zone at 25 °C with 15% of exchangeable sodium is known as saline soil (Shrivastava and Kumar, 2015). Salinization is long known as a common environmental phenomenon worldwide (Kassas, 1987; Thomas and Middleton, 1993) and is becoming a global issue of land degradation, with more prevalence in arid and

semi-arid regions (Tanji, 1990) as shown in Figure 2.1. More than 6% of the world's total land area is salt affected, either by salinity (397 million hectares) or by the associated conditions of sodicity (434 million hectares) (FAO, 2005). Due to salt build-up over time, the United Nations Food and Agricultural Organization (FAO) has estimated that 0.25–0.50 million ha of irrigated lands are becoming unsuitable for cultivation annually (Martinex and Manzur, 2005). Though saline soil contains a range of dissolved salts including NaCl, Na_2SO_4, $MgSO_4$, $CaSO_4$, $MgCl_2$, KCl, and Na_2CO_3, many studies have focused on NaCl as this is the most prevalent salt (Rengasamy, 2002; Munns and Tester, 2008). In the Canadian Prairies, sulfate of Na^+, Ca^{2+} and Mg^{2+} are the primary salts while chlorides are also present to a lesser extent (Keller and Van der Kamp, 1988; Florinsky et al., 2000). Under an iso-conductive state, alfalfa biomass yield did not differ between chloride and sulfate salts (Soltanpour et al., 1999; Cornacchione and Suarez, 2017). The critical concentration of salt which alfalfa can tolerate was ~4.37 dS m^{-1} (sea water), ~1.56 dS m^{-1} (sodium chloride), ~2.18 dS m^{-1} (sodium sulfate), ~0.55 dS m^{-1} (sodium carbonate) (Ahi and Powers, 1938). The development of crop cultivars resistant to soil salinity is one of the most effective strategies for maintaining sustainable crop production.

Understanding the mechanisms conferring salt tolerance and identification of heritable traits for screening for improved salt tolerance are crucial for alfalfa breeding. It is also important to identify and characterize genes responsible for salt tolerance in alfalfa for the development of molecular markers for precise screening in breeding and genetic improvement.

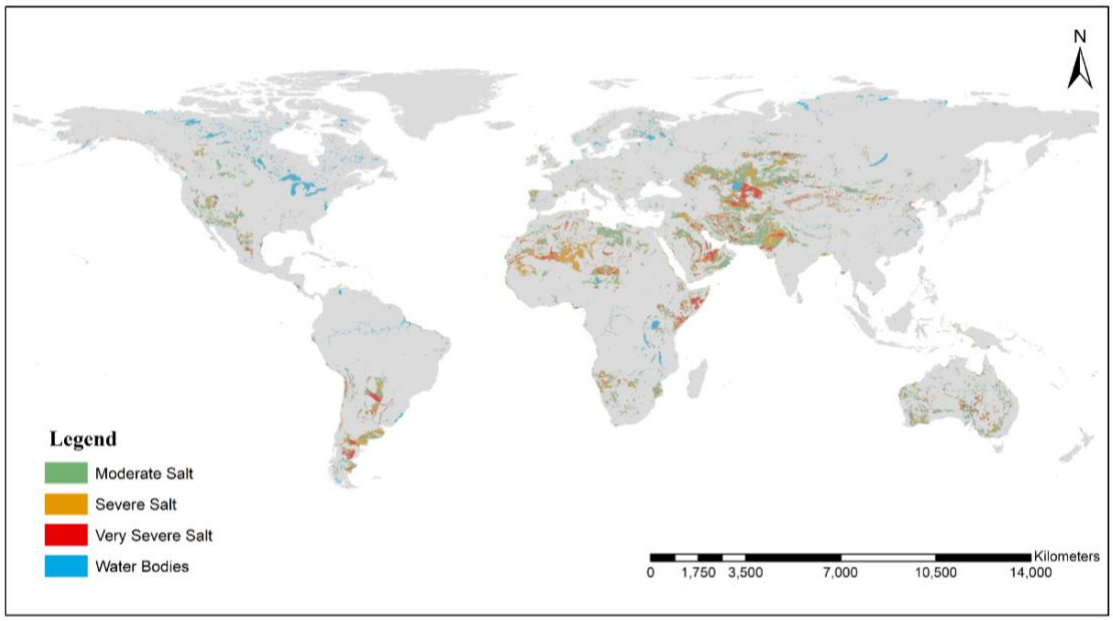

Figure 2.1. Global salt-affected regions and their severity levels.
(Data source: Harmonized World Soil Database v 1.2, (FAO, 2008)).

2.2 Effect of salt stress on morphology, growth, forage yield and nutritive value

Salt stress reduces plant growth by influencing turgor, photosynthesis, and activity of specific enzymes (Munns, 1992). The influence can occur in two phases: the first phase is governed by osmotic effect due to high salt concentration in root zones, whereas the second phase is governed by toxic effects due to high salt accumulation in leaf tissues (Munns, 2005) (Figure 2.2). The presence of high root zone salt concentration causes higher osmotic pressure in soil solution than in plant cells, reducing the ability of plants to uptake water and essential minerals like potassium and calcium (Munns et al., 2006). In severe salt stress, soil solution becomes hyper-osmotic, causing the root cells to lose water, which results in severe wilting or plant senescence (Munns, 2002). Osmotic stress initially reduces leaf growth and eventually causes a reduction in shoot development and reproductive growth (Munns and Tester, 2008), primarily due to water deficit in plant tissues induced by osmotic stress (Munns, 2002). Salt stress induces decreased photosynthetic rate due to osmotic stress-induced partial stomatal closure (Munns and Tester, 2008). Sodium ion absorbed by plant roots, if present at a high concentration in cytosol, can be harmful to the plants (Tuteja, 2007). Since sodium and potassium ions are both monovalent cations, they compete for uptake by the plant under fully hydrated saline condition (Schachtman and Liu, 1999), resulting in the deficiency of potassium, an essential macronutrient, required for

normal metabolic functions (Bhandal and Malik, 1998; Munns et al., 2006). Increased concentrations of sodium and chloride ions in the cytoplasm can disrupt cellular processes, exerting damage to photosynthetic apparatus or as well as dehydration of cells (Munns and Tester, 2008; Ashraf and Harris, 2013). Therefore, limiting the absolute amount of sodium in the cytosol and increasing the cellular potassium to sodium ratio are crucial for salt tolerance (Annunziata et al., 2017; Carillo et al., 2019). This means the maintenance of regular photosynthetic rate and stable K^+/Na^+ ratio are important traits for salt tolerance alfalfa cultivars. Development of molecular markers should target the specific traits mentioned above to provide informative markers.

Smith (1993) described three different growth stages at which alfalfa plants may be affected by salinity: germination, seedling growth, and mature plant growth. The seed germination and seedling stages of alfalfa are highly sensitive to salt stress (Peel et al., 2004). Physiological and genetic correlation might exist between germination and mature growth stages of alfalfa growth, however indirect selection of salt tolerance based on early stage performance had generally been unsuccessful (Johnson et al., 1992). During the germination stage, salt tolerance is expressed by the ability of the seed to germinate and the seedling to survive, whereas in later development stages tolerance is usually measured by the degree of growth reduction relative to growth under no or low salinity (Lauchli and Grattan, 2007). During germination stages, salt stress reduces seed germination either by creating osmotic potential, thereby preventing water imbibition and uptake or by toxic effect of salt ions on embryo viability (Llanes et al., 2005). Likewise, during post germination stages, salt ions in the root zone causes osmotic stress causing inhibition of water uptake, cell expansion and bud development as well as disturbing cell turgor causing wilting and ultimate death of the plants (Munns and Tester, 2008). In extreme cases the root zone soil solution might be hyperosmotic causing roots to lose water rather than absorbing.

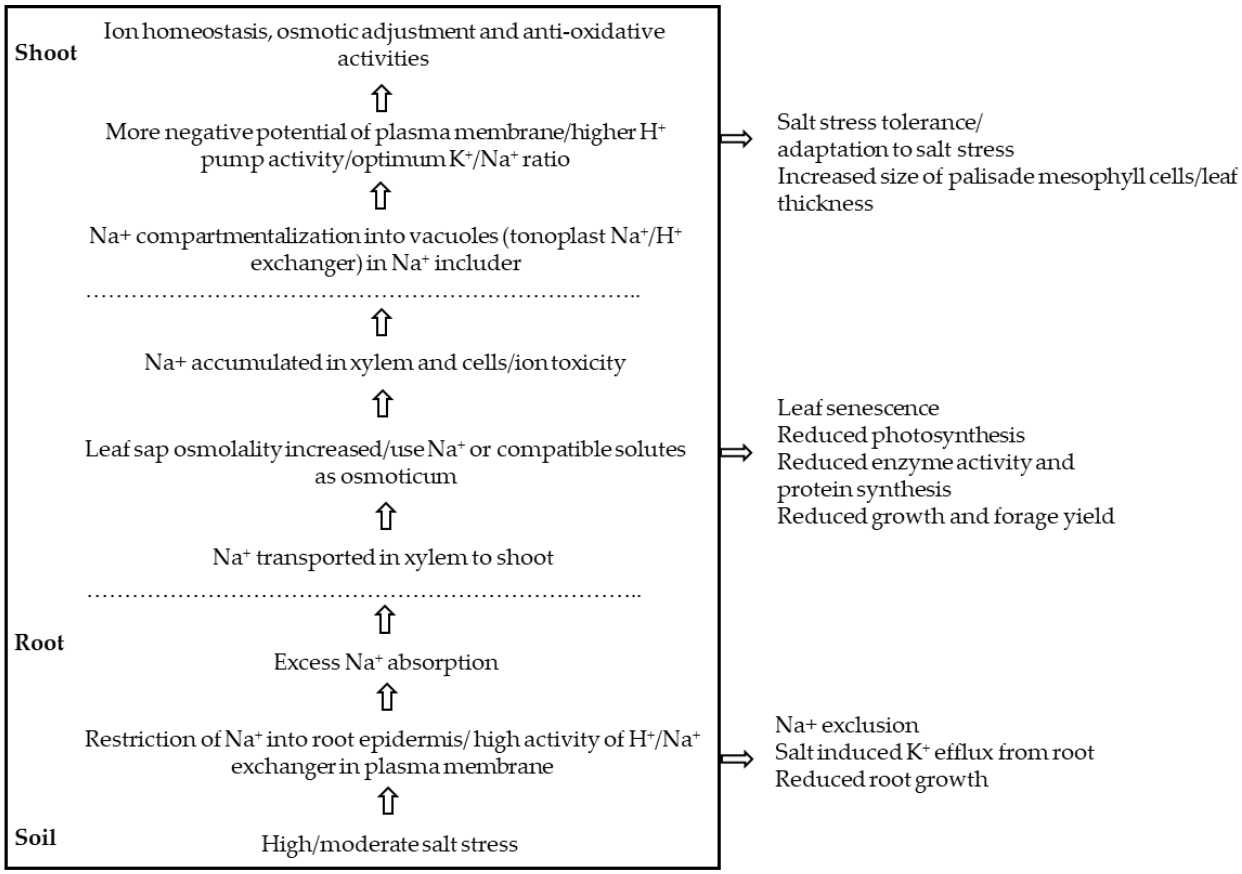

Figure 2.2. Summary of salt stress tolerance in alfalfa.

Though many soluble salts exist in the natural environment, the majority of the research studies on alfalfa salt tolerance used NaCl solution, with few studies evaluating the response of alfalfa biomass production under a mixture of different salts (Soltanpour et al., 1999; Cornacchione and Suarez, 2017). Alfalfa seed germination is more susceptible to $CaCl_2$ and NaCl salts and more resistant to KCl (Azhdari et al., 2010). Salt stress can significantly reduce germination and seed vigor of alfalfa (Azhdari et al., 2010; Soltani et al., 2012). The effect of Na_2SO_4 solution on alfalfa plants from emergence to maturity was examined and it was found that relative emergence (%) decreased dramatically at 12.7 dS m^{-1}, with no surviving plants at 30 dS m^{-1} (Cornacchione and Suarez, 2015). In another study, a mixture of $CaCl_2$, NaCl, $MgSO_4$, and Na_2SO_4 was used to obtain required EC levels to evaluate alfalfa seeding emergence (Steppuhn et al., 2012). In this study, alfalfa seedlings emerged equally under the 1.5 dS m^{-1} and 8.0 dS m^{-1} treatments but the emergence decreased 3–30% at 15.6 dS m^{-1} except for a few tolerant cultivars (Steppuhn et al., 2012). In the past, many breeding efforts have been targeted toward improved seed germination of alfalfa under salt stress, but the selection for salt tolerance should focus on

the whole life cycle of alfalfa rather than on a particular growth stage, as there is no clear correlation between seed germination and post germination performance (Al-Niemi et al., 1992; Johnson et al., 1992).

The shoot growth of alfalfa had been found to be more adversely affected by salinity than root growth (Torabi and halim, 2010). A study on 15 alfalfa populations under salt stress imposed by $MgSO_4$, Na_2SO_4, $CaCl_2$, NaCl, and KCl revealed root biomass per plant at 18.3 dS m^{-1} and 24.5 dS m^{-1} EC was reduced by 18% and 49%, while the shoot biomass was reduced by 50% and 73%, respectively (Cornacchione and Suarez, 2017). Under chloride and sulfate salinity, the average shoot biomass of alfalfa during first, first + second, and first + second + third cuts decreased by 50%, 44%, and 38% at 8.0 dS m^{-1} and by 80%, 73% and 67% at 15.6 dS m^{-1}, respectively (Steppuhn et al., 2012). Salt stress in alfalfa caused a reduction in relative growth rate (Shannon et al., 1994; Khavarinejad and Chaparzadeh, 1998). Moderate NaCl salt stress (9±0.2 dS m^{-1}) reduced plant height, leaf and stem masses of alfalfa by 32, 34, and 35%, respectively (Valizadeh et al., 2013). Sibole et al. (2003) reported that stem and petiole growth was sensitive to NaCl salt stress in the two different salt tolerant Mediterranean *Medicago* species. As compared to the salt stress imposed by NaCl, other saline solutions containing Ca^{2+} and K^+ ions not only have low toxic effects on plants, but also, they can mitigate the negative effects on a plant under salt stress (Hanley et al., 2020; Tootoonchi and Gettys, 2019).

Though a reduction in growth rate and shoot mass were common, high genetic diversity existed among alfalfa populations under salt stress (Steppuhn et al., 2012; Cornacchione and Suarez, 2017; Sandhu et al., 2017), suggesting an adequate genetic variation for further selection for improved salt tolerance. Lei et al. (2018a) compared the performance of seven alfalfa cultivars under NaCl stress and found that the growth rate of salt tolerant cultivars was less affected than salt intolerant cultivars under a high salt stress of ~50 dS m^{-1}. However, in another study, no significant variation in both shoot and root biomasses was observed between salt-tolerant and intolerant alfalfa cultivars under NaCl stress (Bertrand et al., 2015). Differences among studies might be due to the genetic backgrounds of the alfalfa, as the studies used different salt-tolerant cultivars.

The forage nutritive value was affected by salinity and varied among cultivars (Robinson et al., 2004). Salt stress up to 20 dS m^{-1} increased the leaf-to-stem ratio of alfalfa and its crude protein (CP) (Al-Khatib et al., 1992), and reduced acid detergent fiber and neutral detergent fiber (Robinson et al., 2004; Suyama et al., 2007). The reduction of stem height may be the main factor causing changes in alfalfa nutritive value, as it increases leaf-to-stem ratio.

2.3 Effect of salt stress on physiological responses in alfalfa

The mechanisms underlying the ability of alfalfa seedlings to tolerate salt stress are very complex involving processes like photosynthesis, detoxifying and antioxidants, secondary metabolism, and ion transport (Xiong et al., 2017). Salinity altered photosynthetic pigments (i.e. chlorophyll content), therefore it reduced the maximum photochemical efficiency of alfalfa genotypes (Shone and Gale, 1983; Smethurst et al., 2008) and increased dark respiration rate in alfalfa (Khavarinejad and Chaparzadeh, 1998). Salinity reduced membrane stability, relative water content and growth parameters and increased lipid peroxidation, proline and H_2O_2 contents in leaf tissue of alfalfa (Chaparzadeh and Mehrnejad, 2013). In fact, studies have shown that an increased level of proline content was associated with improved salt tolerance (Torabi and Halim, 2010; Campanelli et al., 2013). In addition, effective osmoregulation in salt tolerant alfalfa cultivar is also associated with increased levels of sucrose and pinitol in leaves and a high accumulation of starch in roots (Bertrand et al., 2015). The pinitol accumulation is a characteristic of halophytic plants growing in a saline environment. Anower et al. (2013) characterized the physiological traits of two alfalfa half-sib (HS) families, HS-A and HS-B, selected for improved salt tolerance. Under salt treatment, HS-B showed greater leaf number (72%) and stem length (44%), and HS-A displayed better leaf production (84%) compared to the unselected initial population. This improved growth is associated with 208% and 78% greater accumulation of chlorophyll content in HS-B and HS-A, respectively. An increase in protein concentration in salt tolerant alfalfa cultivars had been reported in previous studies (Robinson et al., 2004; Suyama et al., 2007), which may be associated with an increase in chlorophyll and enzyme activities in the leaves. It is common for plant breeders to measure the plant vigor and shoot

mass to determine the performance of alfalfa under salt stress. However, this analysis could be enhanced by the determination of leaf-to-stem ratio and certain physiological traits such as chlorophyll content and protein concentration.

2.4 Effect of salt stress on oxidative stress and anti-oxidative activities

Salinity induces oxidative stress in plants at the sub-cellular level (Acosta-Motos et al., 2017). Salt stress increases the accumulation of superoxide radicals (O_2^-) and hydrogen peroxide (H_2O_2) in cell compartments including chloroplast and mitochondria (Acosta-Motos et al., 2017). Therefore, lipid peroxidation and protein oxidation occur in the apoplastic space. Increase in peroxidase reduces H_2O_2 to water using various substrates as an electron donor in salt tolerant alfalfa (Babakhani et al., 2011; Ashrafi et al., 2015), suggesting that the analysis of antioxidant enzymes could be useful in understanding the salt tolerance of alfalfa. During seed germination and seedling growth, increased salt stress also increased the activities of superoxide dismutase, catalase, and ascorbate peroxidase and the increase was higher in salt tolerant alfalfa cultivars (Wang and Han, 2009; Ashrafi et al., 2015). Under salt stress, the unsaturated fatty acids of plant membranes are decomposed to malondialdehyde, and the rate of lipid peroxidation in terms of malondialdehyde can be used as a biochemical indicator to evaluate the salt tolerance of cultivars (Jain et al., 2010; Annunziata et al., 2017). The salt tolerance of alfalfa was also improved by melatonin application which acted as an antioxidant in scavenging H_2O_2 and enhanced antioxidant enzymes activities (Cen et al., 2020). Under salt stress, the salt tolerant alfalfa showed less severe cell membrane damage and lower accumulation of reactive oxygen species (ROS) than salt sensitive cultivars (Quan et al., 2016).

2.5 Effect of salt stress on hormone regulation in alfalfa

The protective response of plants to both abiotic and biotic stresses is primarily regulated by phytohormones such as abscisic acid (ABA), auxin, cytokinins (CK), jasmonate, gibberellin (GA), salicylic acid (SA) and ethylene (Ryu and Cho, 2015). Munns and Tester (2008) proposed that leaf growth reduction is affected by long distance signaling regulated by hormones or their precursors. Salt stress increased production of ABA which is a plant stress hormone regulating plant development processes. This increasing ABA concentration

in plants helps in plant adaptation to low water availability by closing stomata and accumulation of osmoprotectants, but high ABA level leads to growth retardation (Ryu and Cho, 2015). Salinity stress increased the concentration of ABA in both tolerant and intolerant alfalfa cultivars, but the rate of increment was higher in intolerant alfalfa cultivars (Lei et al., 2018a). The reduction in plant growth rate due to salt stress might be due to auxin level alteration. Over production of indole-3-acetic acid results in salt tolerance in *Medicago truncatula* (Bianco and Defez, 2009). CK plays an important role in plant development and shoot differentiation as well as salt tolerance. The reduction in supply of CK from root to shoot could inhibit leaf growth (van der Werf and Nagel, 1996; Rahayu et al., 2005). Seed priming with CK showed enhanced seed germination in wheat (*Triticum aestivum* L.) under salt stress (Iqbal et al., 2006). GA are associated with seed germination, leaf expansion, stem elongation and flowering (Magome et al., 2004). Jasmonates like jasmonic acid (JA) activates plant defense against pathogens and abiotic stresses like salinity (Cheong and Choi, 2003). JA content increased under salt stress in a tolerant alfalfa cultivar and SA content was not changed by salt stress in both tolerant and non-tolerant alfalfa cultivars (Lei et al., 2018a). Over expression of alfalfa ethylene response factor (*MsERF*) enhanced salt tolerance in transgenic *Arabidopsis*. Ethylene is a key plant hormone for many developmental processes affected by biotic and abiotic stresses. Plant hormones such as ethylene and auxin can enhance root growth (Boerjan et al. 1995). Ethylene, GA3 application showed increasing alfalfa seed germination under salt stress (Basalah and Mohammad, 1999). Application of 5mM GA3 improves the germination of alfalfa seed under salinity through enhancing the activities of antioxidant enzymes and reducing the membrane damage (Younesi and Moradi, 2014).

2.6 Effect of salt stress on ion uptake in alfalfa plants

Under salt stress, about 98% of the ions in soil solution are excluded from the root in most plants, with the rest transported to the shoot tissues (Munns, 2005). Epidermal cells of root tips are the primary site for ion uptake through the plasma membrane; the uptake of salt ions into roots and translocation to the shoot is primarily attributed to transpiration by the plant (Munns, 2002). To prevent tissue ion toxicity, the ion exclusion mechanism can

restrict excessive ion transport from root to shoot. The ion exclusion mechanism includes: (1) minimal uptake of particular toxic ions by the root and maximization of ion efflux to the soil; (2) restricting excessive ion loading into xylem; (3) increasing the ion retrieval from xylem to other tissues like root and stem; and (4) increasing the ion transport from shoot to root through phloem (Tilbrook and Roy, 2014). High concentrations of sodium and chloride ions in leaves generally lead to leaf senescence; however, the tissue tolerance to such a stress is genotype specific (Munns, 2002). Tolerance to high concentrations of sodium and chloride ions in leaves can be achieved by intercellular partitioning of ions, thus avoiding their accumulation in the photosynthetic organelles (Munns and Tester, 2008). For example, salt tolerant species can sequestrate ions into cell vacuoles in leaves (Munns and Tester, 2008; Roy et al., 2014). Thus, comparison of leaf injury scores under high salt stress can be used as a morphological marker for identifying salt tolerant genotypes in early phases with similar LD_{50} values (median lethal dose to kill 50% of population) (Peel et al., 2004).

Salt stress can lead to nutritional imbalances due to competitive absorption and translocation of elements, which may result in reduced physiological activity (Marschner, 1995). This might in part explain the plant growth reduction and low shoot mass of alfalfa at high salt stress, as discussed in the previous section. The high concentrations of sodium and chloride ions in soil solution may decrease calcium, potassium, and magnesium concentrations in alfalfa (Ashrafi et al., 2018) and also decrease nitrogen accumulation (Pessarakli et al., 1991; Khan et al., 1994). High salt stress increased the concentrations of sodium, total sulfur, chloride, magnesium, and phosphorus, but it decreased the concentrations of potassium and calcium in the shoot of alfalfa genotypes (Cornacchione and Suarez, 2015). The maintenance of the K^+/ Na^+ ratio through Na^+ exclusion from the root epidermis and NaCl induced K^+ efflux from the root causes the deficiency of macronutrients (nitrogen and potassium), reducing plant production and productivity.

Knowledge of the biochemical composition of plant tissues is crucial for salt tolerance studies, as cutting-edge synchrotron-based approaches can help plant scientists to quantify the biochemical compounds and image their structures with minimal sample modification

(Vijayan et al., 2015). The synchrotron is a powerful facility that accelerates charged particles such as electrons in a large ring-like trajectory at relativistic (near-light) speed (Vijayan et al., 2015), where the energy of electron generates light ranging from infrared to soft and hard X-rays at high intensities (Duncan and Williams, 1983). In recent years, synchrotron techniques have been employed to study a number of plant biotic and abiotic stresses leading to the identification of heat tolerant field pea (*Pisum sativum* L.) genotypes (Lahlali et al., 2014; Jiang et al., 2015a), drought tolerance traits in spring wheat (*Triticum aestivum* L.) (Willick et al., 2017), and *Fusarium* head blight tolerance in wheat (Lahlali et al., 2015, 2016). A comprehensive study on ion localization in sub-cellular levels using synchrotron beamlines would provide further insights into salt tolerance in alfalfa.

Table 2.1. Number of differently expressed genes (DEGs), proteins and their functions in salt tolerant and intolerant alfalfa cultivars.

Alfalfa genotype	Tissue	Salt stress	Total number of differentially expressed genes/proteins	Major pathway/function	Reference
NM-801 (tolerant), Vernal (intolerant)	root	2-week-old seedlings treated with ~5, ~10 dS m^{-1} NaCl for 3 days	83	Ion homeostasis, protein turnover and signaling, protein folding, cell wall components, carbohydrate and energy metabolism, reactive oxygen species regulation and detoxification, and purine and fatty acid metabolism.	(Rahman et al., 2015)
Zhongmu-1 (*M. sativa*, tolerant), Jemalong A17 (*M. truncatula*, intolerant)	root	1-month-old seedlings treated with ~30 dS m^{-1} NaCl for 8h	93 (tolerant) 30 (intolerant)	Molecule binding and catalytic activity. Defense against oxidative stress, metabolism, photosynthesis, protein synthesis and processing, and signal transduction.	(Long et al., 2016)
AZ-88NDC (intolerant), AZ-GERM SALT-II (tolerant)	root	1-week-old seedlings treated with ~15 dS m^{-1} NaCl for 7 days	288/273 and 468/337 up-/down regulated in intolerant and tolerant, respectively	Response to stress, kinase activity, hydrolase activity, oxidoreductase activity, extracellular region.	(Postnikova et al., 2013)
Zhongmu No. 1 (tolerant)	root	12-day-old seedlings treated with ~25 dS m^{-1} NaCl for 1, 3, 6, 12, 24 h	8861 at one or more time points	Iron ion transport, ion homeostasis, antiporter, signal perception, signal transduction, transcriptional regulation and antioxidative defense.	(Luo et al., 2019)
Zhongmu No. 1 (tolerant)	root, shoot	1-week-old seedlings treated with ~10, ~20 dS m^{-1} NaCl for 7 days	26 (shoot) 35 (root)	Photosynthesis (31%), and stress and defense (20%) in the shoot. Defense (26%), metabolism (17%), and protein translation, processing, and degradation (17%) in the root.	(Xiong et al., 2017)

CW064027, Bridgeview (tolerant), Rangelander (intolerant)	shoot	4th-cut treated with 1.53, 8, 15.6 dS m^{-1} maintained by sulphate- based sodium, calcium, and magnesium salts	685/527, 368/139 up-/down regulated in CW064027 and Bridgeview at control, 537/949, 375/1045 up-/down regulated in CW064027 and Bridgeview at 8 dS m^{-1}, 1129/1196, 843/1516 up-/down regulated in CW064027 and Bridgeview at 15.6 dS m^{-1}	Redox-related genes, B-ZIP transcripts, cell wall structural components, lipids, secondary metabolism, auxin and ethylene hormones, development, transport, signaling, heat shock, proteolysis, pathogenesis-response, abiotic stress, RNA processing, and protein metabolism.	(Gruber et al., 2017)
Zhongmu-1 (tolerant), Xingjiang Daye (intolerant)	leaf	30-day-old plants treated with ~50 dS m^{-1} NaCl for 7 days	1125 and 2237 between cultivars at control and stress, respectively	Response to stimulus, reactive oxygen species, responding to stress, response to hormone and other stress-responsive processes.	(Lei et al., 2018a)

2.7 Proteome and transcriptome analyses of salt stressed alfalfa

Several transcriptome and proteome studies have been conducted to understand salinity stress in alfalfa. After a three-day salt treatment, a proteomic study on the root of two weeks old seedlings found 83 differentially expressed proteins in alfalfa cultivars with contrasting tolerance to salinity (Table 2.1) (Rahman et al., 2015). These proteins are involved in ion homeostasis, protein turnover, and signaling, protein folding, cell wall components, carbohydrate, and energy metabolism, ROS regulation and detoxification, and purine and fatty acid metabolism. Proteins such as peroxidase, protein disulfide-isomerase, nicotinamide adenine dinucleotide synthetase, and isoflavone reductase were significantly upregulated in salt tolerant alfalfa cultivar 'nonomu' (Rahman et al., 2015). The proteomic analysis of 30-day old alfalfa seedling roots treated with ~30 dS m^{-1} NaCl for 8 hrs found 93 and 30 differentially expressed proteins in salt tolerant alfalfa ('Zhongmu-1') and salt sensitive *Medicago truncatula* ('Jemalong A17'), respectively (Table 2.1) (Long et al., 2016). These proteins primarily play a role in molecule binding and catalytic activities. Xiong et al. (2017) identified 26 (shoot) and 35 (root) differentially abundant proteins in salt-stressed alfalfa compared to alfalfa that had experienced no salt treatment. Similarly, proteomic analysis of osmo-primed alfalfa seeds that germinated under salinity stress contained 94 proteins with different responses to salt treatments (Yacoubi et al., 2013). These proteins were functionally classified as protein destination and storage (seed storage proteins and small heat-shock proteins), cell growth/division (late embryogenesis abundant proteins and seed maturation proteins), metabolism (methionine synthase, cysteine synthase and haem oxygenase), disease and defense (glutathione S-transferase).

Transcriptomic approaches have been employed in alfalfa to understand gene expression associated with salt stress (Table 2.1) (Jin et al., 2010a; Postnikova et al., 2013; Quan et al., 2016; Gruber et al., 2017; Lei et al., 2018a; Luo et al., 2019). Eighty-two unique transcripts were found from salt stressed seedlings of alfalfa by samplings at different time intervals from 10 min to 24 hrs, including 24% that were proteins related to plant metabolism and 9% that were related to abiotic stress (Jin et al., 2010a). Arshad et al. (2017) found that the over-expression of microRNA156 in alfalfa resulted in increased biomass production, stem number, concentration of crude protein, and reduced uptake of Na^+ under salt stress. In another transcriptome study, there were 876 and 1303 differentially expressed genes (DEGs) under salt stress in root tissues of one-week-old seedlings in salt intolerant and tolerant alfalfa genotypes, respectively, with 604

DEGs specific to salt tolerant type (Postnikova et al., 2013). Similarly, RNA-Seq analysis displayed 2237 and 1125 DEGs between 'Zhongmu-1' (salt tolerant) and 'Xingjiang Daye' (salt intolerant) in the presence and absence of salt stress, among which were many genes that are involved in stress-related pathways (Table 2.1) (Lei et al., 2018a). After a salt treatment, the number of DEGs in 'Xingjiang Daye' (19,373 DEGs) compared with the control treatment was about four times that in 'Zhongmu-1' (4833 DEGs). Compared with 'Xingjiang Daye', 'Zhongmu-1' maintained a more stable expression of genes related to the ROS, calcium pathways, phytohormone biosynthesis, and Na^+ /K^+ transport (Lei et al., 2018a). The transcriptome responses of salt tolerant ('211609') and salt intolerant ('Xinjiang Daye') alfalfa cultivars revealed significantly higher expression levels of *NHX1, ZFG*, *CBF4,* and *HSP23* genes in '211609' than in 'Xinjiang Daye' (Quan et al., 2016). In addition, a transcriptomic analysis of alfalfa roots under ~25 dS m^{-1} NaCl identified 8861 NaCl regulated DEGs in alfalfa (Luo et al., 2019). These DEGs were categorized in 13 gene ontology categories including: oxidoreductase activity, oxidation-reduction process, structural constituent of cytoskeleton, hydrolase activity, carbohydrate metabolic process, negative regulation of catalytic activity, polysaccharide catabolic process, iron ion binding, transmembrane transporter activity, cytoskeleton, trehalose biosynthetic process, protein polymerization, and ion homeostasis (Luo et al., 2019). In previous transcriptomic studies, an individual alfalfa genotype was sampled as a replicate for RNA-Seq analysis. As alfalfa is generally seeded as a synthetic population in the field, it may be more suitable to use a group of genotypes as a replicate for a transcriptomic study. Therefore, 100 alfalfa genotypes were divided into four independent replicates to represent an alfalfa population and alfalfa and researchers found 50% of DEGs were down regulated in a salt intolerant population (Gruber et al., 2017). The functions of the genes down-regulated in a salt intolerant alfalfa cultivar were grouped into cell wall structural components, lipids, secondary metabolism, auxin and ethylene hormones, transport, signaling, and pathogenesis-response, abiotic stress (Gruber et al., 2017). The transcriptome analysis identified many annotated sequences homologous to genes involved in osmolyte synthesis (beta-amylase, fructose-1, 6-bisphosphate, aldolase, and sucrose synthase) and ion homeostasis (H^+-PPase, cation/H^+ exchanger3, Ca-related channel, sodium symporter, nitrate and K^+ channels, p translocator, and metal transporters) (Jin et al., 2010a; Gruber et al., 2017; Lei et al., 2018a). In summary, a large number of candidate genes responsible for salt tolerance in alfalfa have been identified in various

studies, and these candidate genes can be used as a baseline for further genetic analyses of salt tolerance in alfalfa. However, it is essential to identify key genes associated with important morphological and physiological traits (i.e., chlorophyll content, sucrose synthase or plant height), and validate them in different alfalfa breeding populations to apply them in salt-tolerant alfalfa breeding.

2.8 Breeding for salt tolerance

Breeding efforts for salt tolerance in alfalfa are focused on high seed germination under stress to improve stand establishment. There are more than 60 registered alfalfa cultivars with improved salinity tolerance in the USA, representing different fall dormancy categories (Table 2.2) (NAFA, 2020). The majority of the registered cultivars were selected for salinity tolerance at germination stages while only 13 of them were selected for salinity tolerance at mature growth stages. Although some progress has been made through conventional plant breeding, the genetic improvement of salt tolerance in alfalfa has been low due to several factors. Firstly, alfalfa is polyploid and outcrossing in nature (Annicchiarico et al., 2015) and genetic studies of its salt tolerance can be complicated and less informative. Secondly, the perennial growth form and low heritability of salt tolerant traits have further complicated the breeding effort (Allen et al., 1985). Thirdly, as previously stated, there is no clear relationship for salt tolerance between germination stage and post-germination performance (Al-Niemi et al., 1992), indicating a need for whole life cycle selection from germination to the flowering stage.

A number of studies have evaluated the performance of alfalfa germplasm under salt stress (Steppuhn et al., 2012; Jiang et al., 2015b; Azzam et al., 2019; Benabderrahim et al., 2020). The genetic variability among nine alfalfa populations in response to sulfate salt revealed a high relative shoot mass of 8 dS m^{-1} in 'Halo' alfalfa, which had a lower seed emergence than that of 'Rugged' (Steppuhn et al., 2012). Benabderrahim et al. (2020) studied the genetic diversity of 36 alfalfa populations from Tunisia using 12 agronomic and physiological traits and identified three salt-tolerant types. Jiang et al. (2015b) have applied random amplified polymorphic DNA (RAPD) markers and clustered 25 salt-tolerant alfalfa populations into nine clusters, suggesting that salt-tolerant alfalfa germplasm possess a certain genetic diversity which can be utilized in salt-tolerant breeding. Azzam et al. (2019) identified a highly salt-tolerant alfalfa population by screening 16 alfalfa populations using RAPD and inter simple sequence repeat markers. Therefore, the available genotypic diversity for salt tolerance in alfalfa provides an opportunity

for plant breeders to select and develop superior salt-tolerant cultivars. However, there is still a lack of well-characterized genetic materials and common phenotyping protocols for parental selection. Due to the spatial heterogeneity of soil properties and seasonal variation in rainfall, it is difficult to perform plant screening for salinity tolerance in the field (Munns and James, 2003). Thus, early phase screening in controlled environments is a feasible option before testing the advanced lines in a saline field with the use of proper salinity induction.

Table 2.2. Salt tolerant alfalfa cultivars and their fall dormancy (FD) and growth stages (G, germination and/or F, forage production) for salt tolerance (ST).
[Source: National Alfalfa and Forage Alliance, (2020)].

Cultivar	FD	ST	Variety	FD	ST
Foothold	2	G	GUNNER	5	G
Spredor 5	2	G	MPIII Max Q	5	G
Hi-Gest 360	3	G	RR NemaStar	5	G
LegenDairy XHD	3	G	RR Tonnica	5	G
HVX Tundra II	3	G	WL 365HQ	5	G
LegenDairy AA	3	G	6610N	6	G
RR Presteez	3	G	Cisco II	6	G/F
Rugged	3	G	Hi-Gest 660	6	G
WL 336HQ.RR	3	G	Revolt	6	G
6401N	4	G	RRALF 6R200	6	G
6472A	4	G	WL 454HQ.RR	6	G/F
6497R	4	G	6829R	7	G
AFX 457	4	G	AFX 779	7	G
AFX 469	4	G	AmeriStand 715NT RR	7	G/F
AmeriStand 415NT RR	4	G	Sun Titan	8	G
AmeriStand 427TQ	4	G	SW8421S	8	F
AmeriStand 455TQ RR	4	G	WL 535HQ	8	G
AmeriStand 457TQ RR	4	G	WL 552HQ.RR	8	G
AmeriStand 480 HVXRR	4	G	6906N	9	G
Barricade SLT	4	G/F	AFX 960	9	G
DKA40-16	4	G	AmeriStand 901TS	9	G
DKA44-16RR	4	G	LG 9C300	9	G
Integra 8444R	4	G/F	PGI 908-S	9	G/F
Magnum Salt	4	G/F	RRALF 9R100	9	G
Rebound AA	4	G	Sun Quest	9	G
RR Stratica	4	G	SW 9215	9	F
RR VaMoose	4	G	SW 9720	9	F
WL 356HQ.RR	4	G	SW9215RRS	9	G/F
6516R	5	G	WL 656HQ	9	G
6547R	5	G/F	WL 668HQ.RR	9	G
AFX 579	5	G	6015R	10	G
Nimbus	5	F	AFX 1060	10	G

The success of a breeding program lies in the precise phenotyping of the traits of interest (seed germination, ion transport, osmolyte synthesis, signaling, photosynthesis, and protein synthesis) and correlating them with genes or quantitative trait loci for marker-assisted selection (Tiwari and Mamrutha, 2013). A comprehensive breeding platform including high-throughput phenotyping and genotyping is needed for an efficient improvement of salt tolerance in alfalfa. High-throughput phenotyping contributes directly to the genetic gain by evaluating genetic variation more efficiently (Araus et al., 2018). A hyperspectral imaging platform has the potential for the detection of stress responses as it can capture wavelengths within and beyond the visible spectrum (Fahlgren et al., 2015). Hyperspectral cameras detect both spectral and spatial information; each spatially located pixel contains full wavelength (~350–2500 nm) information. Imaging within the visible spectrum (~400–700 nm) can measure the morphological and color properties of plants, while hyperspectral imaging can also study the radiative properties of plant leaves to facilitate the early detection of abiotic stress (Romer et al., 2012; Fahlgren et al., 2015). Hyperspectral imaging has been successfully applied to study the vegetation indices of crops under salt stress (Naumann et al., 2009; Behmann et al., 2014; Sytar et al., 2017). The physiological reflectance index and normalized difference vegetation index are useful for the early detection of salinity stress in plants (Naumann et al., 2009; Behmann et al., 2014). Sytar et al. (2017) reviewed the application of hyperspectral imaging as a fast and reliable technique for the detection of quantitative and qualitative changes in plants to evaluate plant variation under salt stress.

Several studies have focused on the development of molecular markers associated with salt tolerance in alfalfa at different growth stages (Julier et al., 2003; Liu et al., 2006, 2019a; Yu et al., 2016; Liu and Yu, 2017; Azzam et al., 2019). The most significant salt tolerance markers during the germination stage were identified on chromosomes 1, 2, and 4, while the marker located on chromosome 6 overlapped with drought resistance (Zhang et al., 2015; Yu et al., 2016). During alfalfa seed germination, broad-sense heritability for germination rate was observed at 0.60 at 0.5% (~8 dS m^{-1} NaCl) salt concentration, which decreased to 0.24 at 0.75% (~12 dS m^{-1} NaCl) salt concentration and 0.27 at 1.0% (~17 dS m^{-1} NaCl) (Yu et al., 2016). The broad sense heritability for leaf chlorophyll content increased from 0.22 to 0.34 at 8 dS m^{-1} NaCl (Liu and Yu, 2017). As salt tolerant traits are genetically complex and multigene controlled, the development of genome wide markers might be useful for conducting genomic selection based

on predictive breeding values of genotypes. Genomic selection can enhance the genetic gain and reduce breeding cycle length when it increases the selection accuracy (Meuwissen et al., 2001; Fu et al., 2017). The trait prediction accuracy remains generally low in current genomic selection models, even with the aid of dense, genome-wide single nucleotide polymorphism (SNP) markers (Fu et al., 2017). As demonstrated by Fu et al. (2017), salt tolerance-associated SNP markers in alfalfa could be explored to achieve a more accurate trait-specific prediction in genomic selection. This is feasible, as the application of the RNA-Seq technique in alfalfa salinity tolerance studies is relatively common and a large amount of genomic information is already available. With the development of modern breeding techniques, such as high-throughput phenotyping and genotyping-by-sequencing platforms, genomic selection can enhance the salt-tolerance breeding of alfalfa at a reasonable cost.

Chapter 3. Tissue specific changes in elements and organic compounds of alfalfa (*Medicago sativa* L.) cultivars differing in salt tolerance under salt stress

3.1 Abstract

Soil salinity is a global concern and often the primary factor contributing to land degradation, limiting crop growth and production. Alfalfa (*Medicago sativa* L.) is a low input high value forage legume with a wide adaptation. Germination and seedling stages of alfalfa are highly sensitive to salt stress, while mature plants show intermediate tolerance. Examining the impact of salinity stress during development and localizing tissue-specific responses will be important to understanding physiological changes of alfalfa to tolerate salinity stress. The responses of two contrasting alfalfa cultivars (salt tolerant 'Halo', salt intolerant 'Vernal') were studied for 12 weeks in five gradients of salt stress (electrical conductivities of 0, 4, 8, 12 and 16 dS m^{-1}) in a sand based hydroponic system in the greenhouse. To our knowledge, this is the first comprehensive study on accumulation and localization of elements and organic compounds in leaf, stem and root tissues of alfalfa under salt stress using synchrotron beamlines. Salt stress had a negative ($P<0.05$) effect on germination, shoot biomass yield, root to shoot ratio of the two alfalfa cultivars. Plant height of both cultivars at 16 dS m^{-1} was 50% of the control treatment. The pattern of chlorine accumulation for 'Halo' was root>stem$\underline{\sim}$leaf at 8 dS m^{-1}, and root$\underline{\sim}$leaf>stem at 12 dS m^{-1}, potentially preventing an elemental overload injury in leaf tissues. In contrast, for 'Vernal', it was leaf>stem$\underline{\sim}$root at 8 dS m^{-1} and leaf>root$\underline{\sim}$stem at 12 dS m^{-1}. The distribution of chlorine in 'Halo' was relatively uniform in the leaf surface and vascular bundles of the stem. Amide concentration in the leaf and stem tissues was higher for 'Halo' than 'Vernal' at all salt gradients. Both cultivars accumulated higher concentrations of carbohydrates at 12 dS m^{-1} than the control. The carbohydrates and amides in salt stressed stems of 'Halo' were mainly localized in the phloem. This study determined that low ion accumulation in the shoot was a common strategy in salt tolerant alfalfa up to 8 dS m^{-1} of salt stress, which was then replaced by shoot tissue tolerance at 12 dS m^{-1} or higher salt stress.

3.2 Introduction

Soil salinity is one of the most significant abiotic stresses contributing to land degradation and limiting plant growth (Munns and Tester, 2008). Soil is considered saline when it has electrical conductivity (EC) of 4 dS m^{-1} or greater [approximately 40 mM sodium chloride (NaCl)] at

25°C, containing 15% of an exchangeable sodium soil (Shrivastava and Kumar, 2015). Approximately 6% of the world's total land area is salt affected, either by salinity (397 million hectares) or associated conditions of sodicity (434 million hectares) (FAO, 2005). In North America, salinization has threatened the agricultural productivity in the Great Plains, affecting more than 10 million hectares (Steppuhn et al., 2012). The development of salt tolerant crop cultivars is an important strategy for sustainability of agricultural production.

The primary cause of salt stress on plants is a combination of osmotic and ionic stresses because of high sodium and chlorine concentrations in the root zone (Hasegawa et al., 2000). Three mechanisms of salinity resistance have been identified: tolerance to osmotic stress; ion exclusion by roots to prevent toxic ion accumulation in plant tissues and; tissue tolerance by compartmentalization of toxic ions at the cellular and intra-cellular levels to avoid high concentration in the cytoplasm (Munns and Tester, 2008; Roy et al., 2014). Plants under salt stress accumulate compatible solutes like amino acids, amides, proline, and soluble carbohydrates to reduce osmotic stress and dehydration at high salt levels (Bohnert et al., 1995; Chen et al., 2007; Lee et al., 2008). Under salt stress, high concentrations of salt ions in the root zone interfere with the uptake of other elements like potassium, nitrogen, calcium and phosphorus, causing nutritional imbalance (Ashrafi et al., 2018). Therefore, plant growth and development are inhibited because of insufficient osmotic adjustment and the toxic effect of sodium or chlorine under a continuous salt stress (Flowers et al., 2015).

Alfalfa (*Medicago sativa* L.), also called lucerne, is the most important forage legume in the world due to its numerous superior traits such as wide adaptability, high forage yield and quality, and tolerance to frequent harvests (Coburn, 1907; Goplen et al., 1982). It is considered to be a low-input, high-value forage crop for the livestock industries, because of its biological N fixation and protein-rich attributes. This plant has a long history of cultivation and is widely grown as a forage crop in the world from sub-tropical to the subarctic areas (Goplen et al., 1982). Globally, alfalfa is grown on about 30 million ha (Yuegao and Cash, 2009). Alfalfa is a moderately saline tolerant crop (Maas and Hoffman, 1977), but its yield dramatically decreases with the increase of salinity (Johnson et al., 1992).

Previous studies reported that superior growth of alfalfa genotypes under salt stress was associated with salt ion exclusion from the shoot based on the salt ion concentrations in leaves (Kapulnik et al., 1989), shoot, and root tissues (McKimmie and Dobrenz, 1991). Based on higher

sodium concentration in the root than in the shoot tissue, Cornacchione and Suarez (2017) concluded that alfalfa restricts sodium translocation to shoots. However, in other studies, the increase of salt concentration resulted in lower sodium concentration in the roots than in shoots of alfalfa (Ashraf et al., 1986; Wang and Han, 2007; Mezni et al., 2010). In other species, compartmentalization of sodium into the vacuole in the cytoplasm improved salt tolerance in *Arabidopsis thaliana* (Apse et al., 1999), *Salicornia europaea* (Lv et al., 2012), and *Ipomoea batatas* (Fan et al., 2015). The seed germination and seedling stages of alfalfa are highly sensitive to salt stress (Peel et al., 2004), and a majority of previous studies focused on screening for high seed germination of alfalfa in saline substrate (Steppuhn et al., 2012). However, Al-Niemi et al. (1992) and Johnson et al. (1992) determined no relationship between alfalfa seed germination and shoot growth under salt stress. Katerji et al. (2012) reported the ability to emerge in saline conditions is not always an indicator of salt tolerance. Though many studies have been conducted to understand the response of alfalfa to salt stress, there is no comprehensive study to understand the mechanisms of salt tolerance in alfalfa at different growth stages and in different tissues. Additionally, no studies have applied synchrotron beamline methods in evaluation of salt tolerance of alfalfa. Synchrotrons accelerate charged particles such as electrons in a large ring-like trajectory at relativistic (near light) speed (Vijayan et al., 2015), where energy of electrons generates light ranging from infrared to soft and hard X-rays at high intensities (Duncan and Williams, 1983). Synchrotron radiation is a powerful tool in material and biomedical sciences, but it is still underutilized in agricultural science.

We hypothesized that alfalfa cultivars with contrasting tolerance to salinity varied in their phenotypic and physiological responses, as well as the accumulation and distribution of organic compounds and elements, but the tolerant cultivar under salt stress would have greater performance and lower chlorine concentration in leaf tissue than the intolerant cultivar. This study aimed to compare several physiological aspects of salt tolerance from germination to maturity in two alfalfa cultivars with contrasting salt tolerance. The response of alfalfa cultivars to salt stress was determined by evaluating seed vigor and phenotypic and physiological traits at different gradients of salt concentrations (maintained by NaCl and measured as EC) in a sand-based hydroponic system under greenhouse conditions, as well as using synchrotron spectromicroscopy techniques and inductively coupled plasma-mass spectroscopy (ICP-MS).

3.3 Materials and Methods

3.3.1 Plant material and salt treatments

Two alfalfa cultivars with contrasting tolerance to salinity were chosen for the study. Cultivar 'Halo' was registered in the United States as PGI 427 in 2007. It is a synthetic cultivar selected for improved salinity tolerance, as demonstrated under greenhouse conditions (Steppuhn et al., 2012; Bertrand et al., 2015; www.aosca.org) (hereafter referred to as the tolerant cultivar). Cultivar 'Vernal' is a synthetic cultivar developed at the University of Wisconsin in 1956 and selected for adaptation to the northern states of the United States and Canada (Graber, 1956). It was considered as a salinity susceptible type (Peel et al., 2004; Rahman et al., 2015) (hereafter referred to as the intolerant cultivar). The experiment was conducted on five gradients of salt concentration: 0 dS m^{-1}, 4 dS m^{-1}, 8 dS m^{-1}, 12 dS m^{-1}, and 16 dS m^{-1} EC maintained by NaCl. The corresponding water potential of each salinity level is 0 MPa (0 dS m^{-1}), -0.144 MPa (4 dS m^{-1}), -0.288 MPa (8 dS m^{-1}), -0.432 MPa (12 dS m^{-1}), and -0.576 MPa (16 dS m^{-1}), respectively. Two separate experiments were conducted to understand the physiological response of alfalfa to varying salt concentrations from germination to the early flowering growth stages with each experiment repeated twice.

3.3.2 Experimental design and response measurements

3.3.2.1 Germination test

The germination test was carried out in a germination cabinet (Conviron CMP 6010, China) under day/night (12/12 h) temperatures of 20/10°C. Twenty-five alfalfa seeds were imbibed on top of two layers of filter paper (Whatman 597) in 9 cm diameter sterilized plastic Petri dishes moistened with 5 ml distilled water or 5 ml of respective saline concentrations. The Petri dishes were enclosed and sealed in polyethylene bags to prevent desiccation. Seeds with a radical length greater than 2mm were considered to be germinated. Germination counts were made daily for seven days, cumulatively without removing the germinated seeds. After 14 days, the seedling length of each germinated seed was measured. The experiment was conducted in a randomized complete block design with four replications and the whole experiment was repeated twice. Seed vigor was calculated using following equation (3.1):

$$\text{Seed vigor} = \text{germination percentage} \times \text{seedling length} / 100$$ (Abdul-Baki and Anderson, 1973) …… (3.1)

3.3.2.2 Greenhouse study

A greenhouse experiment was carried out in the College of Agriculture and Bioresources greenhouse at the University of Saskatchewan (45 Innovation Blvd., Saskatoon, SK) using a split-plot arrangement with a randomized complete block design (RCBD) with four replications. Salt treatment was considered as a main plot factor and alfalfa cultivar was treated as a sub-plot factor. For each replication, 15 randomly selected seeds of each alfalfa cultivar were seeded at a depth of 2 cm in three 1.5 L pots filled with 20-grit silica sand (Lane Mountain Company, Valley, WA). Each pot was thinned to two seedlings after five weeks. Silica sand was used in this study because it is an inert, stable medium for plant growth, with a minimal ion-binding potential. In the greenhouse, natural light was supplemented with high pressure sodium halogen lamps to a total of 490–550 μM s^{-1} m^{-2} PAR with a 16 h photoperiod. A temperature of 21/16°C (day/night) was maintained during the study. For salt treatments, each replication was arranged in a 20 × 40 × 60 cm dimensional plastic tray that was connected to a tank containing one-fifth strength Hoagland's No. 2 Basal Salt Mixture (Sigma-Aldric, Oakville, ON) (Hoagland and Arnon, 1950) dissolved in distilled water. Nutrients and desired salt solutions in the tanks were replaced every 4 weeks. Salt concentrations were achieved by adding NaCl (Fisher Scientific, Toronto, ON). The EC levels of the nutrient solutions were checked weekly using ECTestr 11+ (Eutech Instruments, Singapore) and adjusted to ensure consistent salt concentration over time. All pots were irrigated by flooding the trays twice a day for a period of 2 min each using a pre-set automatic timer. Water in the trays was drained completely back to the tank after each irrigation. Salt treatments were applied after 4 weeks of sowing. To avoid osmotic shock, EC level was gradually increased during three transition weeks starting on the first day with 4 dS m^{-1} for all salt treated pots and increased by 4 dS m^{-1} in weekly intervals until reaching final targeted concentrations. The whole experiment was repeated twice in the greenhouse.

Plant height of all individual plants was measured five times at 14 day intervals beginning on the day 28 after seeding. Chlorophyll content was determined for all individual plants after 11 weeks of growth. Three fully expanded randomly selected leaflets from each individual plant were measured for chlorophyll content using a Chlorophyll Meter SPAD-502 (Konica Minolta Sensing, Japan), and then values were averaged for each plant. Whole plants were manually harvested at the soil surface at the early flowering stage after 12 weeks of growth (Kalu and Fick, 1981). After removing the sand, roots were gently rinsed using tap water, shade dried and

weighed. The shoot and root samples were dried at 60°C for 48 h in a forced air oven and weighed for dry matter determination. Root to shoot ratio was calculated using dry weights. The salt stress tolerance index was determined based on shoot dry weight using the following equation (3.2):

$Stress\ tolerance\ index = (Yc \times Ys)/(\widehat{Yc})^2$ (Fernandez, 1992) ……..... (3.2)

where, Yc and Ys are mean shoot dry weight of alfalfa cultivars under control and salt stress, respectively, and $\widehat{Yc}$ is the shoot dry weight means of both alfalfa cultivars under the control treatment.

Crude protein (CP) content was determined for shoot samples at the early flowering stage after 12 weeks of growth. The dried samples were ground in a Willey Mill (Thomas-Wiley, Philadelphia, PA) to pass through a 1-mm mesh screen (Cyclone Mill, UDY Mfg, Fort Collins, CO). The ground samples were stored in plastic bags prior to CP determination. Nitrogen content was determined using a LECO CN628 Element Analyzer (LECO, St. Joseph, MI). Crude protein was calculated using equation (3.3):

CP = nitrogen concentration (%) × 6.25 ……. (3.3)

The relative water content of alfalfa leaflets was determined after 11 weeks of growth. Briefly, five fully expanded young leaflets per replication were placed in pre-weighed petri dishes. The petri dishes were placed in an ice box during transportation from the greenhouse to lab. The petri dishes with samples were weighed to determine the fresh weight (FW) immediately before being hydrated to full turgidity by floating leaflets in deionized water for 48 h at 4°C. After hydration, samples were removed from the water and surface moisture was removed immediately using tissue paper and weighed to obtain full turgid weight (TW). The samples were oven dried for 48 h at 60°C and weighed after cooling down in a desiccator for dry weight (DW) determination. Relative leaf water content was calculated using equation (3.4):

Relative leaf water content (%) = [(FW-DW) / (TW-DW)] × 100 …….. (3.4)

3.3.2.3 Analysis of organic compounds and elements

Fourier transform infrared (FTIR) and X-ray fluorescence (XRF) spectromicroscopy analyses were conducted at the Canadian Light Source (CLS) (Saskatoon, Canada) to study organic compounds and elements in different alfalfa tissues. FTIR data were collected at the mid-infrared (Mid-IR) beamline in the range of 4000-800 cm^{-1} wavenumber using an Agilent Cary 670

spectrometer with a Cary 620 Microscope. This microscope has two detectors, a liquid nitrogen cooled mercury cadmium telluride and a 128 × 128 pixel Focal Plane Array (FPA) for recording spectroscopy and spectromicroscopy data, respectively. Micro-XRF data were collected from the Very Sensitive Elemental and Structural Probe Employing Radiation from a Synchrotron (VESPERS) and Industry, Development, Education, and Students (IDEAS) beamlines. The VESPERS beamline uses a pink beam which operates in the energy range of 6–30 keV and uses Si (111) crystal monochromator, Kirkpatrick-Baez focusing mirror, and Vortex ®-ME4 4-element (bulk spectroscopy) or 1-element (mapping) dispersive silicon drift detector (Hitachi, Troy, MI, USA). The IDEAS beamline uses a Ge (220) crystal in the monochromator and a KETEK, and the incident energy of the beam was set at 13.4 keV for all samples.

3.3.2.3.1 Bulk analysis of organic compounds and elements

Leaf, stem and root of the two alfalfa cultivars were sampled for a bulk spectroscopy experiment at the vegetative stage after 10 weeks after sowing. For bulk analysis, all of the plant tissues were sampled from only four salt gradients (0 dS m^{-1}, 4 dS m^{-1}, 8 dS m^{-1} and 12 dS m^{-1}), as plant mortality was too high to have an adequate number of samples at 16 dS m^{-1}. In total, 72 samples (two cultivars × four salinities × three tissues × three technical replications) were used for the bulk analysis. The leaf, stem and root tissues from three biological replicates were pooled and immediately freeze-dried for 24 hours using a FreeZone Triad Cascade Benchtop Freeze Dryer (Labconco, Kansas City, MO). The samples were cryoground at 3000 rpm for 2 minutes using a Geno/Grinder 2010 (SPEX SamplePrep, LLC, UK) to obtain fine ground samples of <20 microns in size. The samples were pelletized with a 13 mm stainless steel pellet die using a hydraulic pellet press, Auto-CrushIR (PIKE Technologies Inc., Wisconsin, US), at continuous pressure of 2.5 ton for 3 seconds, 4 tons for 3 seconds and 6.5 tons for 3 seconds to form a pellet. The pelletizing die was rinsed with acetone after each sample preparation to avoid contamination. The prepared pellets were stored in a vacuum desiccator prior to the analysis.

For bulk analysis using FTIR spectroscopy, approximately 98 mg of homogeneously mixed potassium bromide (KBr) and the ground sample (1–2% sample concentration) were mixed and pelletized. For bulk XRF data collection using VESPERS beamline, about 80mg of the powdered sample were pelletized. Synchrotron XRF beamlines used in this study had high energy therefore were not able to detect sodium ion in alfalfa tissue. Therefore, the bulk samples used in XRF spectroscopy were also analyzed using Inductively Coupled Plasma-Mass Spectroscopy (ICP-

MS) (Agilent 7500ce, Palo Alto, CA, USA) with two technical replicates to further confirm the accuracy of XRF spectroscopy for element quantification in alfalfa as well as to determine K^+/Na^+ and Ca^{2+}/Na^+ ratio.

3.3.2.3.2 Mapping of organic compounds and elements

For *in situ* analyses, mid-IR, VESPERS and IDEAS beamlines were used to study leaf and stem samples collected from two salt gradients (0 and 12 dS m^{-1}) 10 weeks after sowing and stored at –80°C prior to the analysis. There were four samples from each tissue for mapping experiment. To be consistent for stem location, the stems were sectioned about 3 cm above the crown region. The samples were held in a tube filled with deionized water which was flash frozen in liquid nitrogen. The ice blocks with the samples were then mounted onto pre-cooled specimen discs covered with glycerol until the specimen was completely frozen. The specimen disc was then inserted into a specimen head and sectioned using a cryostats microtome Leica CM 1950 (Leica Biosystems, Nussloch, Germany). Stem samples were sectioned to the thickness of 8 microns and mounted on calcium fluoride discs for analysis using FTIR spectroscopy with a mid-IR beamline. The stem samples were sectioned to a thickness of 80 microns and mounted on Kapton polyimide films for analysis using XRF spectroscopy at VESPERS beamline with step size of 0.005 mm × 0.005 mm. The abaxial surface of the leaflet was attached to Kapton polyimide films with an adaxial surface facing beam and scanned using XRF spectroscopy at IDEAS beamlines using a step size of 0.2 mm × 0.2 mm.

3.3.3 Data analyses

All the germination and post-germination data were normalized to be a fraction of the control treatment (distilled water with no salt) before statistical analysis. In the mixed procedure with a standard split-plot test format, experimental run was considered as a random effect, analysis of variance (ANOVA) for all traits in the germination test and plant growth study was performed using SAS software version 9.4 (http://www.sas.com). Salt tolerance index of two alfalfa cultivars were compared using Welch two-sample t-test.

Bands associated with different functional groups within the infrared spectrum (4000-800 cm^{-1}) were identified. The amides region of FTIR spectrum is detectable within the wavenumber range from 1706-1530 cm^{-1} consisting of two prominent bands of amide I (1650 cm^{-1}; C=O and C-N stretching) and amide II (1550 cm^{-1}; N-H bending and C-N stretching) vibration; however, in the present study amide I and II overlapped and were not distinguishable (Wetzel et al., 2003;

Barth, 2007; Türker-Kaya and Huck, 2017; Lei et al., 2018b). Likewise, the carbohydrate structures (C-O and C-C stretching vibration and C-O-H deformation) are detectable within the wavenumber range of 1200-980 cm^{-1} (Kacurakova et al., 2000; Lei et al., 2018b). Lipid structures (vibration absorption of C-H) are detectable within the wavenumber range from 3000-2800 cm^{-1} and represent C-H asymmetric (2918 cm^{-1}) or symmetric (2848 cm^{-1}) stretching vibration belonging to CH_2 and intensity of the CH_3 (2954 cm^{-1}) groups (Lei et al., 2018b; Liu et al., 2019b). The FTIR data were analyzed using Orange version 3.16 (Demsar et al., 2013). The FTIR data were preprocessed using rubber band baseline correction followed by Gaussian smoothing of 3 points and the raw spectra normalized first using sample weight and then by vector normalization.

All micro-XRF bulk data were normalized to incident beam energy (I_0). The spectra were analyzed using PyMCA version 5.3.1 (Sole et al., 2007) and the areas of element specific peaks were integrated. Overlapping peaks were deconvoluted before area calculation (Figure 3.1). The calibration and configuration fit were developed in the PyMca including input measures of incident X-ray beam energy, detector type, and instrumental geometry. The SigmaPlot 13.0 software was used to produce the images using normalized spectra as well as for principal component analysis (PCA). A Pearson correlation coefficient between bulk analysis by XRF and ICP-MS was calculated.

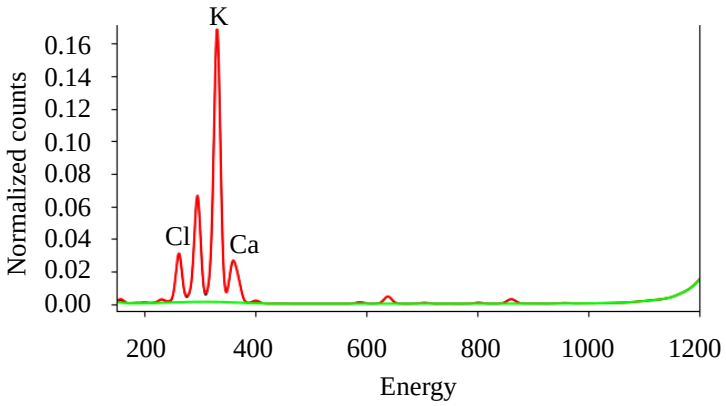

Figure 3.1. Overlapping and deconvolution of element peaks of the leaf tissue of alfalfa cultivar 'Halo' grown under 12 dS m^{-1} salinity before area calculation in PyMca.

3.4 Results

3.4.1 Effects of salinity on seed germination and plant growth rate

Salt stress had a negative ($P<0.001$) effect on seed germination and seed vigor of the two alfalfa cultivars. In the control with no salt, 'Vernal' showed a numerically higher germination percentage and seed vigor than 'Halo' but at 16 dS m^{-1} 'Halo' showed a significantly greater germination and seed vigor than 'Vernal' (Figure 3.2a, b). Alfalfa growth rate declined with the increased salt levels, and this decrease was evident even at the low salt level of 4 dS m^{-1} (Figure 3.2c). At 12 dS m^{-1}, 'Vernal' had a significantly higher growth rate than 'Halo' at the 6th week, but the growth rate of 'Vernal' was numerically lower than 'Halo' after the 10th week of the experiment (Figure 3.2c).

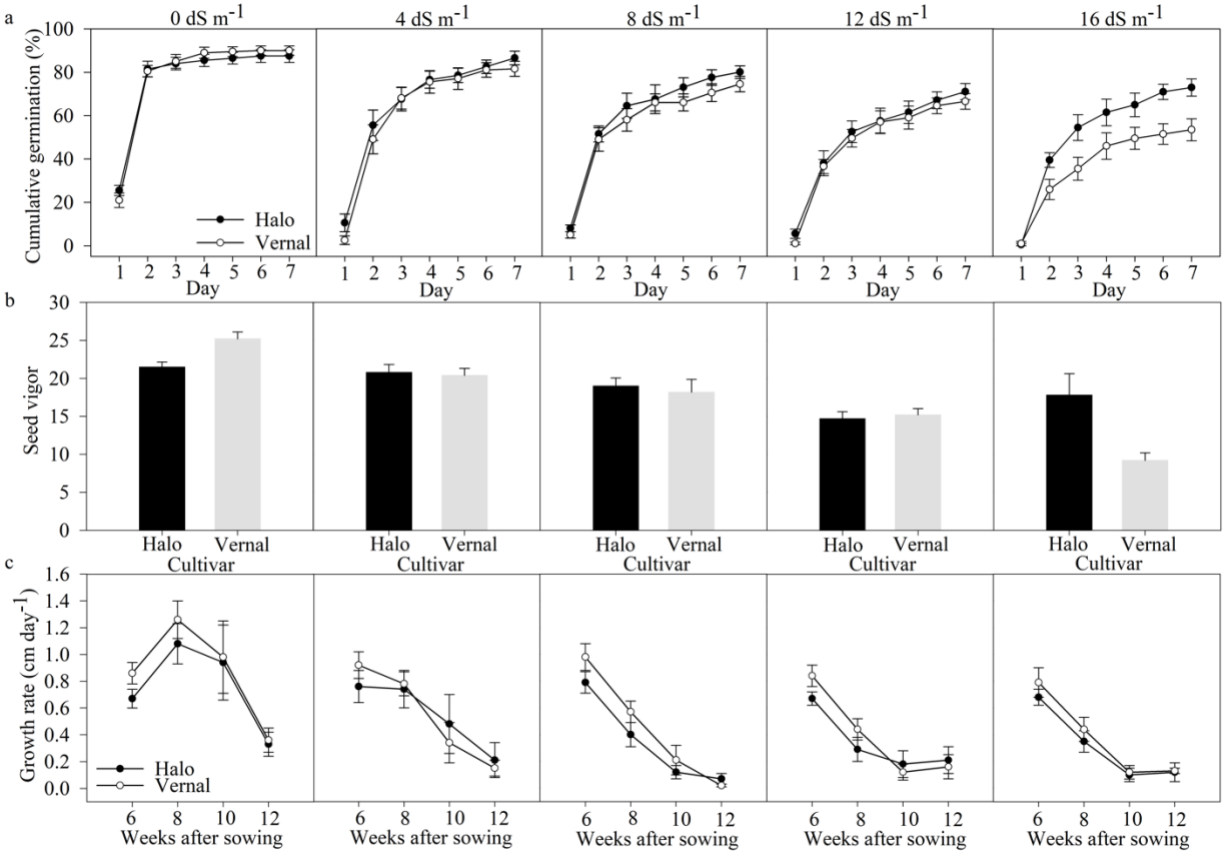

Figure 3.2. Cumulative germination (%; **a**), seed vigor (**b**), and growth rate (cm day^{-1}; **c**) of two alfalfa cultivars under five gradients of salt stress (0, 4, 8, 12, and 16 dS m^{-1}) (Error bars represent standard error of means, n=8).

3.4.2 Effect of salinity on shoot, root biomass, and salt tolerance index

Salt treatment significantly reduced shoot and root biomass as well as root to shoot ratio ($P<0.05$) of the two cultivars at the flowering stage, but no significant difference was found between these cultivars (Table 3.1). From 0 dS m^{-1} to 4 dS m^{-1} of salinity, the root to shoot ratio increased, which then gradually decreased with the increase of salt stress from 4 dS m^{-1} to 12 dS m^{-1} (Table 3.1). Only 34% of alfalfa plants survived at 16 dS m^{-1}, and thus, biomass yield was not reported at this salt stress level. 'Halo' had a numerically higher but non-significant ($P>0.05$) salt tolerance index than 'Vernal' with indices of 0.61 and 0.53 at 4 dS m^{-1}, 0.39 and 0.30 at 8 dS m^{-1}, 0.38 and 0.28 at 12 dS m^{-1}, respectively.

Table 3.1. Mean values of two experimental runs and analysis of variance of the traits measured at post germination stages of two alfalfa cultivars.

Cultivars	Salinity[1]	Shoot biomass (g plant^{-1})	Root biomass (g plant^{-1})	Root to shoot ratio	Chlorophyll[2] (SPAD values)	Crude Protein[3] (%)	Relative water content[4]
Halo	0 dS m^{-1}	4.4±1.4	2.5±1.2	0.5±0.1	51.4±3.1	14.0±2.2	80.8±6.1
	4 dS m^{-1}	2.0±0.5	1.8±0.5	2.1±0.9	49.8±4.7	14.6±0.9	74.5±3.4
	8 dS m^{-1}	1.3±0.3	1.0±0.2	1.1±0.2	46.2±4.0	18.1±1.2	74.4±1.7
	12 dS m^{-1}	1.4±0.4	0.9±0.1	0.9±0.3	44.7±6.5	21.7±0.9	74.0±2.5
	16 dS m^{-1}	-	-	-	40.5±4.8	-	-
Vernal	0 dS m^{-1}	3.9±1.0	1.7±0.4	0.5±0.1	48.7±2.5	14.4±2.0	82.3±3.6
	4 dS m^{-1}	2.2±0.6	2.4±0.8	1.4±0.4	54.0±2.3	13.4±0.7	77.4±1.0
	8 dS m^{-1}	1.2±0.3	1.2±0.5	1.1±0.2	48.1±4.4	15.9±0.7	70.4±4.5
	12 dS m^{-1}	1.2±0.4	0.8±0.2	1.0±0.1	41.3±6.7	20.0±0.9	75.8±3.3
	16 dS m^{-1}	-	-	-	43.5±3.5	-	-
Salinity		<0.001	0.05	0.03	0.12	<0.001	0.07
Cultivar		0.25	0.97	0.28	0.97	0.27	0.81
Salinity : Cultivar		0.98	0.77	0.67	0.87	0.79	0.73

[1]Salt stress was applied after 4 weeks of growth.
[2]Chlorophyll content was measured after 11 weeks of growth.
[3]Crude protein was determined from whole shoot tissue (leaf and stem) at early flowering stage after 12 weeks of growth.
[4]Relative water content of fully expanded young leaflets was measured after 11 weeks of growth.
Data are means ± standard error of mean (n=8). Values are means of two experimental replications.

3.4.3 Effect of salinity on chlorophyll content, crude protein and relative water content

There was no significant difference between the two cultivars for leaf chlorophyll content ($P=0.97$) after 12 weeks of growth and for crude protein concentration ($P=0.27$) in shoot tissue at flowering stage of growth (Table 3.1). However, crude protein concentration of alfalfa cultivars significantly increased with salt stress ($P<0.001$) (Table 3.1). Relative water content of fully expanded young leaflets was similar ($P=0.81$) between the two cultivars (Table 3.1).

3.4.4 Effect of salinity on organic compound composition and distribution as revealed by FTIR

The integrated peak areas for carbohydrate and lipid in leaf tissue of 'Halo' increased at 4 dS m^{-1} compared to the no salt control, and then decreased with the increase of salt concentrations from 4-12 dS m^{-1} (Figure 3.3). However, concentration of carbohydrate in the leaves of 'Vernal' increased from 0-12 dS m^{-1}. 'Halo' had higher amide concentration in the leaves than 'Vernal' at all salt levels. Leaf tissue of 'Halo' at the highest salt stress showed higher amides than 'Vernal' but had lower carbohydrates and lipids.

In stem tissue, 'Vernal' significantly increased integrated peak areas of carbohydrate and lipid compounds under salt stress while 'Halo' maintained or slightly reduced the concentrations of these compounds (Figure 3.3). Amide concentration in stem tissues was higher for 'Halo' than 'Vernal' at all salt stress levels. Stem tissue of 'Halo' at the highest salt stress showed higher carbohydrates and amides than 'Vernal', but it had lower lipids.

In root tissue, integrated peak areas of carbohydrate, amides, and lipid compound were lower than the controls for 'Halo' and 'Vernal' at 8 and 12 dS m^{-1} with an exception of lipid concentration for 'Vernal'. 'Halo' under the highest salt stress had higher amides, lower carbohydrates and lipids in root tissue than 'Vernal' (Figure 3.3).

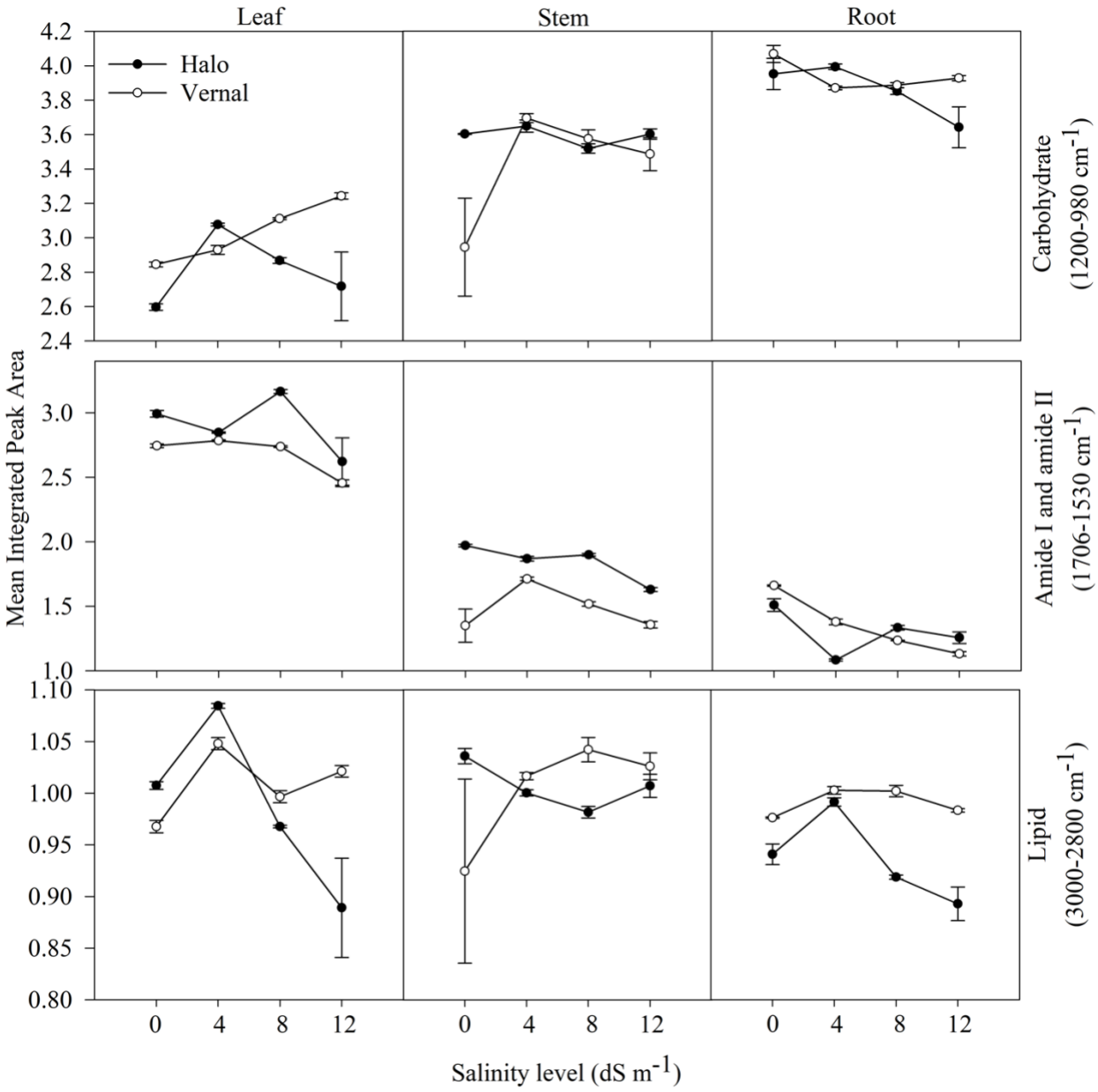

Figure 3.3. Spectroscopic characteristics of carbohydrate (1200-980 cm^{-1}), amide I and II (1706-1530 cm^{-1}) and lipid (3000-2800 cm^{-1}) regions of leaf, stem and root tissues sampled 10 weeks after sowing of two alfalfa cultivars under salt stress as revealed by FTIR spectroscopy. (Note: salt stress was applied after 4 weeks of sowing; Error bar represents standard error of means, n=3).

For the FTIR spectra in stem tissue, compared to 'Halo' (Figure 3.4a), 'Vernal' showed greater shifts from the control in integrated peak areas of all biomolecules under salt stress (Figure 3.4b). The spectra (4000–800 cm^{-1}) were analyzed using principal component analysis (PCA). The first two principal components explained 83.6% of variation associated to salt stress

in stem tissue (Figure 3.4), 75% in leaf tissue (Figure 3.5), and 79.5% in root tissue (Figure 3.6). PC1 distinguished all the samples from 'Vernal' stems at no salt control treatment, while PC2 distinguished the two cultivars (Figure 3.4c). Likewise, in leaf and root tissue PC1 partially distinguished the two cultivars and PC2 clustered samples according to salinity levels (Figure 3.5 and 3.6).

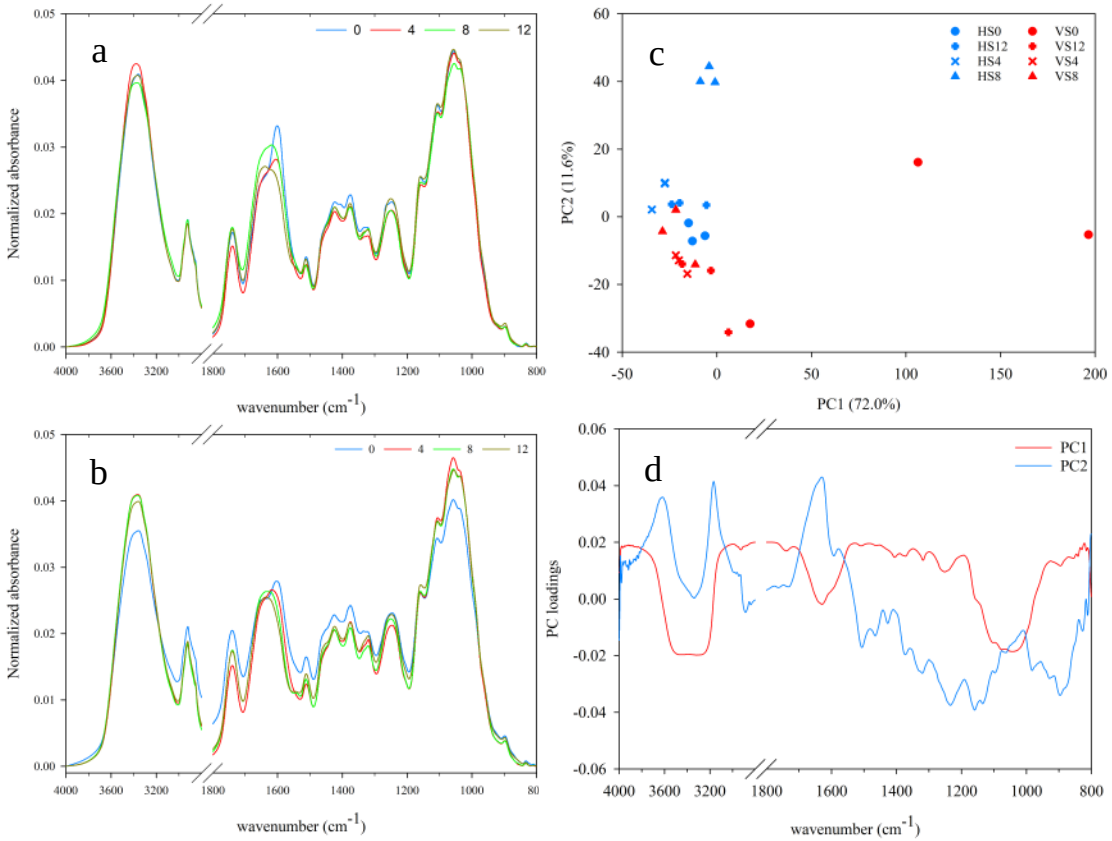

Figure 3.4. Principal components analysis of Fourier-transformed infrared (FTIR) spectra (4000–800 cm^{-1}) collected from the stem tissues of two alfalfa cultivars with contrasting salinity tolerance grown at four gradients (0, 4, 8, and 12 dS m^{-1} electrical conductivities) of salt stress. Average infrared spectra were collected from a. 'Halo', b. 'Vernal', c. principal component analysis, and d. principal component loadings.
[HS0, Halo stem 0 dS m^{-1}; HS12, Halo stem 12 dS m^{-1}; HS4, Halo stem 4 dS m^{-1}; HS8, Halo stem 8 dS m^{-1}; VS0, Vernal stem 0 dS m^{-1}; VS12, Vernal stem 12 dS m^{-1}; VS4, Vernal stem 4 dS m^{-1}; VS8, Vernal stem 8 dS m^{-1}; PC1, first principal component; PC2, second principal component].

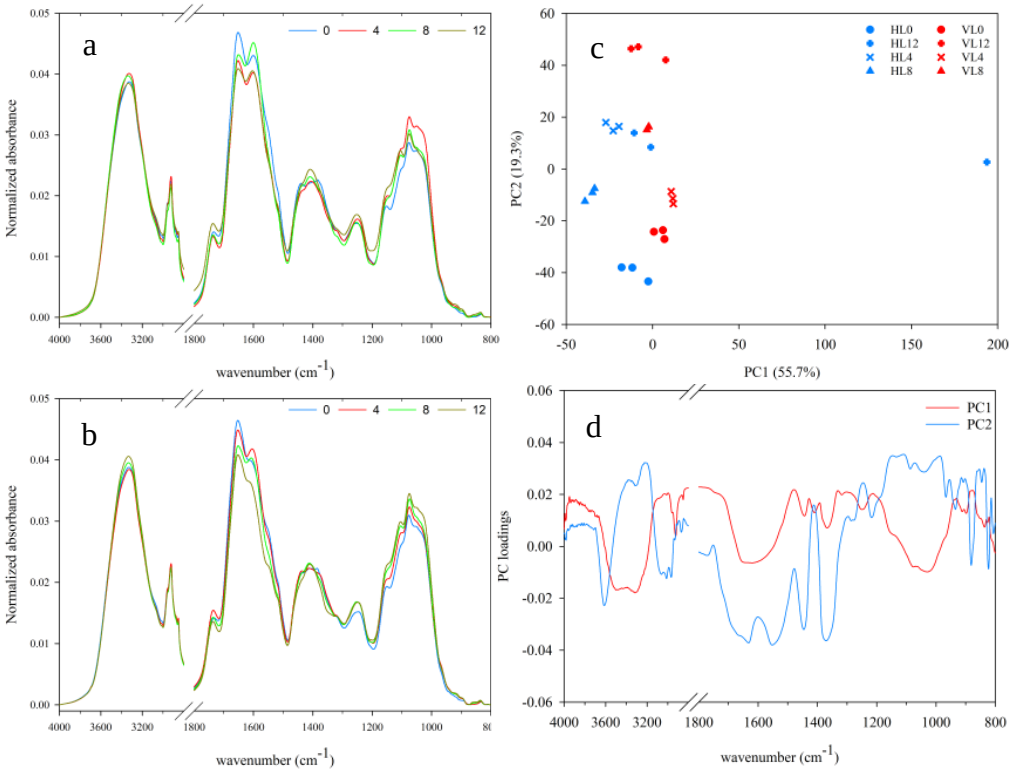

Figure 3.5. Principal components analysis of Fourier-transformed infrared (FTIR) spectra (4000–800 cm^{-1}) collected from the leaf tissues of two alfalfa cultivars with contrasting salinity tolerance grown at four gradients (0, 4, 8, and 12 dS m^{-1} electrical conductivities) of salt stress. Average infrared spectra were collected from a. 'Halo', b. 'Vernal', c. principal component analysis, and d. principal component loadings.
[HL0, halo leaf 0 dS m^{-1}; HL12, halo leaf 12 dS m^{-1}; HL4, halo leaf 4 dS m^{-1}; HL8, halo leaf 8 dS m^{-1}; VL0, vernal leaf 0 dS m^{-1}; VL12, vernal leaf 12 dS m^{-1}; VL4, vernal leaf 4 dS m^{-1}; V8, vernal leaf 8 dS m^{-1}; PC1, first principal component; PC2, second principal component].

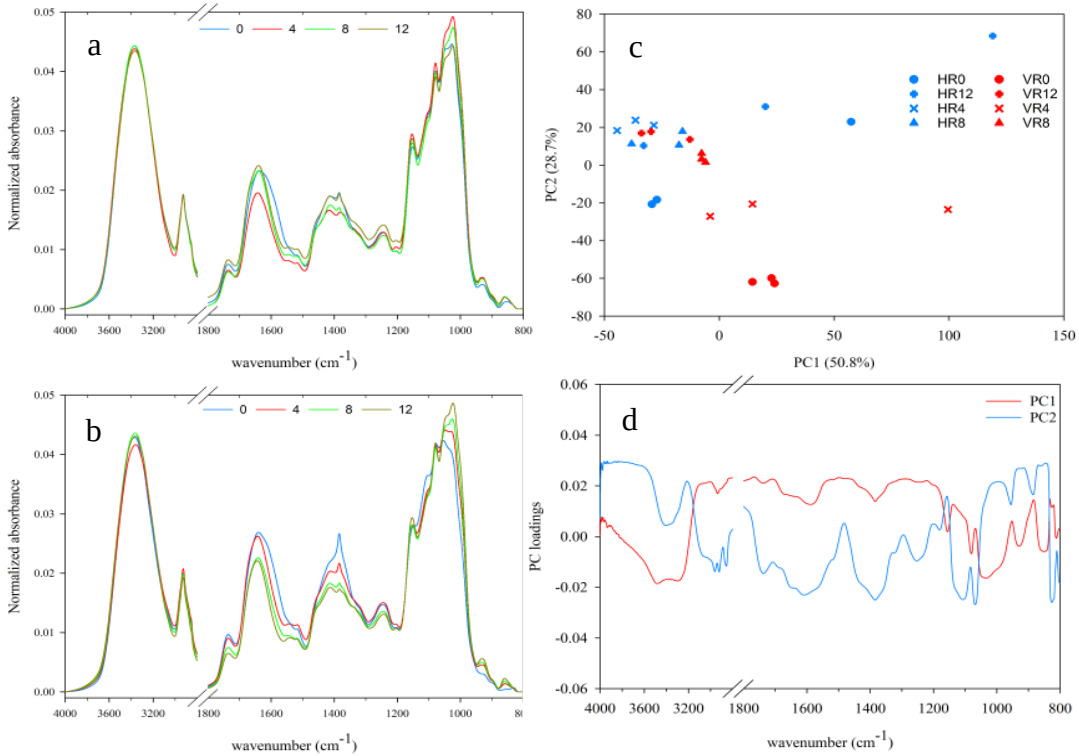

Figure 3.6. Principal components analysis of Fourier-transformed infrared (FTIR) spectra (4000–800 cm^{-1}) collected from the root tissues of two alfalfa cultivars with contrasting salinity tolerance grown at four gradients (0, 4, 8, and 12 dS m^{-1} electrical conductivities) of salt stress. Average infrared spectra were collected from a. 'Halo', b. 'Vernal', c. principal component analysis, and d. principal component loadings.
[HR0, halo root 0 dS m^{-1}; HR12, halo root 12 dS m^{-1}; HR4, halo root 4 dS m^{-1}; HR8, halo root 8 dS m^{-1}; VR0, vernal root 0 dS m^{-1}; VR12, vernal root 12 dS m^{-1}; VR4, vernal root 4 dS m^{-1}; VR8, vernal root 8 dS m^{-1}; PC1, first principal component; PC2, second principal component].

The stem cross-section samples used for *in situ* study using the FTIR spectromicroscopic mapping technique are shown in Figure 3.7a. The distribution of carbohydrate, lipid and amide regions in the cross-section of stem tissue were further localized using FTIR spectromicroscopy data (Figure 3.7b, c, d). The distribution of carbohydrate in 'Halo' at 12 dS m^{-1} showed higher concentration in xylem and phloem tissues while the concentration of carbohydrate was localized mainly in xylem tissues for 'Vernal'. The distribution of amides in stem tissue of both alfalfa cultivars showed more localized in phloem tissue (Figure 3.7c). The distributions of lipid (Figure 3.7d) in stem tissue showed that both cultivars accumulated more lipid in both xylem and phloem tissues in 'Halo' and largely in xylem tissue in 'Vernal'.

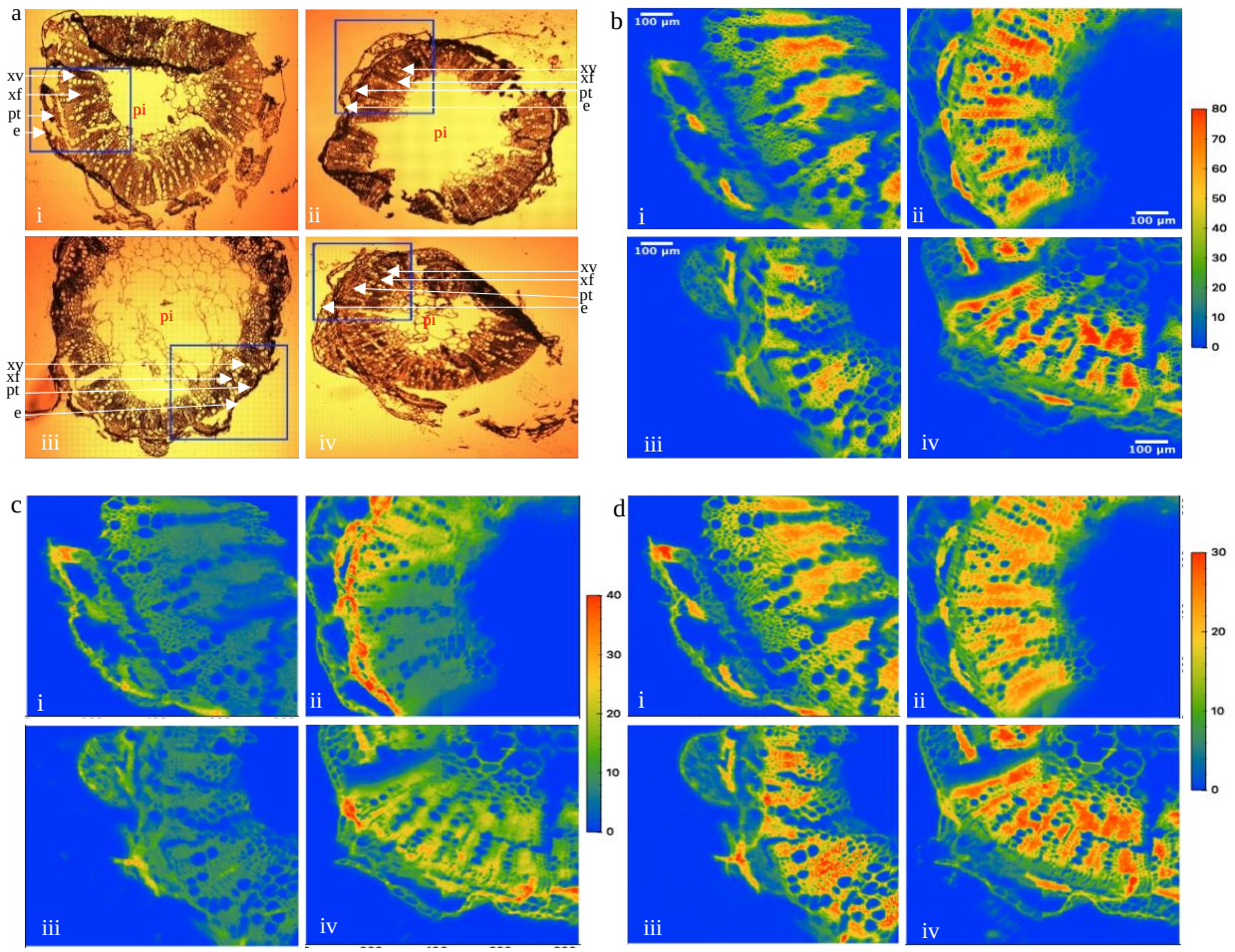

Figure 3.7. Images of a) stem cross-section samples for FTIR spectromicroscopy study; b) distribution of carbohydrate structures (1200-980 cm^{-1}) and c) amide I and amide II region (1706-1530 cm^{-1}) d) lipid (3000-2800 cm^{-1}) in two alfalfa cultivars with different tolerances to salt stress.
(i. Halo control at 0 dS m^{-1} ii. Halo at 12 dS m^{-1} EC iii. Vernal control at 0 dS m^{-1} iv. Vernal at 12 dS m^{-1} EC; Gradient bar represents integrated absorption peak area; e, epidermis; pt, phloem tissue; xv, xylem vessels; xf, xylem fibre; pi, pith).

3.4.5 Effect of salinity on elemental composition and distribution

3.4.5.1 XRF spectroscopy results

The integrated peak areas by bulk measurement for chlorine, potassium, and calcium of the leaf, stem and root tissues of the two cultivars using the VESPERS beamline are shown in Table 3.2. There was a significant ($P<0.01$) interaction effect of salt, cultivar, and tissue for integrated peak areas of the three measured elements. The mean integrated peak area of chlorine in leaf tissue under salt stress for 6 weeks was significantly higher for ‘Vernal’ than ‘Halo’ at salt concentrations of 8 dS m^{-1} and 12 dS m^{-1}. The pattern of chlorine ion distribution at 8 dS m^{-1} was

root>stem~leaf for ‘Halo’ and leaf>stem~root for ‘Vernal’. The pattern of chlorine ion distribution at 12 dS m^{-1} was altered to root~leaf>stem for ‘Halo’ and leaf>root~stem for ‘Vernal’. The chlorine concentration in stem tissue of ‘Halo’ gradually increased with the increase of salt stress while ‘Vernal’ showed a sharp increase in chlorine concentration at 8 dS m^{-1} followed by a decrease at 12 dS m^{-1}. The integrated peak area of potassium significantly ($P<0.001$) decreased with increasing salt stress in both cultivars. Similarly, stem and root tissues also showed a reduced concentration of potassium with increasing salt stress in both alfalfa cultivars. In leaf tissue, ‘Halo’ had significantly higher potassium concentration than ‘Vernal’ at 12 dS m^{-1} while there was non-significant variation between two cultivars in other tissues. The integrated peak area of calcium was the highest in leaf tissue followed by stem and root tissues. Calcium concentration was significantly ($P=0.002$) affected by the interaction of cultivar, tissue and salinity. In leaf tissue, calcium concentration significantly decreased with increasing salt stress, but the concentration was not different between the two cultivars. In stem and root tissues, calcium concentration showed no significant changes with increasing salt stress (Table 3.2).

The *in situ* study on element distribution in leaves of the two cultivars at 0 dS m^{-1} and 12 dS m^{-1} under the IDEAS beamline showed differential distribution with increasing salt stress. ‘Halo’ accumulated chlorine in the whole leaf surface relatively uniformly, while ‘Vernal’ accumulated high concentrations in discrete small areas towards the leaf tip (Figure 3.8a). This was consistent with the leaf injury pattern of ‘Vernal’ observed in the greenhouse. Under salt stress, leaf tissue of ‘Halo’ accumulated more potassium in the mid-rib and veins while the potassium concentrated to the leaf tip in ‘Vernal’ (Figure 3.8b) which is similar to chlorine accumulation (Figure 3.8a). In leaf tissue, the distribution of calcium was observed mainly concentrated in leaf veins in both cultivars (Figure 3.8c).

In stem tissue at 12 dS m^{-1} both cultivars localized chlorine in the xylem and phloem tissues (Figure 3.9a). Distribution of potassium in stem tissue showed ‘Halo’ reduced potassium in the epidermal layer under salt stress (Figure 3.9b). Under salt stress conditions stem tissue of both alfalfa cultivars showed a distribution of potassium more in the phloem tissue (Figure 3.9b, ii, iv). In stem tissue, a pattern of hotspots of calcium accumulation was observed in the phloem tissue and epidermal region in both cultivars (Figure 3.9c).

Table 3.2. Mean values and analysis of variance of integrated absorption peak areas of elemental concentration in leaf, stem and root tissues of alfalfa cultivars after 10 weeks of sowing exposed to salt stress after 4 weeks of sowing at different salt gradients as revealed by bulk measurement using synchrotron based XRF spectroscopy (n=3).

Tissue	Salinity	Cultivars	Chlorine	Potassium	Calcium
Leaf	0 dS m^{-1}	Halo	149^{j1}	91668^{a}	109489^{a}
		Vernal	240^{j}	85220^{ab}	107722^{a}
	4 dS m^{-1}	Halo	4374^{fgh}	73371^{bc}	51746^{bc}
		Vernal	3556^{hi}	78765^{ab}	63189^{b}
	8 dS m^{-1}	Halo	5145^{efg}	35279^{efghi}	59662^{bc}
		Vernal	11004^{a}	41097^{ef}	48929^{cd}
	12 dS m^{-1}	Halo	9278^{b}	58838^{cd}	38619^{de}
		Vernal	11952^{a}	40099^{efg}	33172^{efg}
Stem	0 dS m^{-1}	Halo	43^{j}	84043^{ab}	30636^{efg}
		Vernal	128^{j}	90597^{a}	31806^{efg}
	4 dS m^{-1}	Halo	2994^{hi}	39991^{efgh}	24993^{fgh}
		Vernal	2642^{i}	29255^{fghi}	23442^{gh}
	8 dS m^{-1}	Halo	5263^{ef}	33160^{efghi}	34475^{efg}
		Vernal	8150^{bc}	22592^{i}	36147^{ef}
	12 dS m^{-1}	Halo	7299^{cd}	24847^{hi}	24795^{fgh}
		Vernal	6498^{de}	25818^{ghi}	33155^{efg}
Root	0 dS m^{-1}	Halo	90^{j}	61149^{c}	9788^{i}
		Vernal	425^{j}	70319^{bc}	10255^{i}
	4 dS m^{-1}	Halo	3752^{ghi}	35417^{efghi}	8950^{i}
		Vernal	2873^{i}	45871^{de}	16989^{hi}
	8 dS m^{-1}	Halo	7875^{bcd}	35173^{efghi}	6251^{i}
		Vernal	8034^{bc}	33227^{efghi}	8136^{i}
	12 dS m^{-1}	Halo	9254^{b}	27305^{fghi}	6685^{i}
		Vernal	7566^{cd}	22283^{i}	9102^{i}

Salinity	<0.001	<0.001	<0.001
Cultivar	<0.001	0.268	0.148
Tissue	<0.001	<0.001	<0.001
Salinity : Cultivar	<0.001	0.004	0.016
Salinity : Tissue	<0.001	<0.001	<0.001
Cultivar : Tissue	<0.001	0.027	0.076
Salinity : Cultivar : Tissue	<0.001	<0.001	0.002

[1]Means with the same lower case letters within the column for each treatment are not significantly different (P > 0.05).

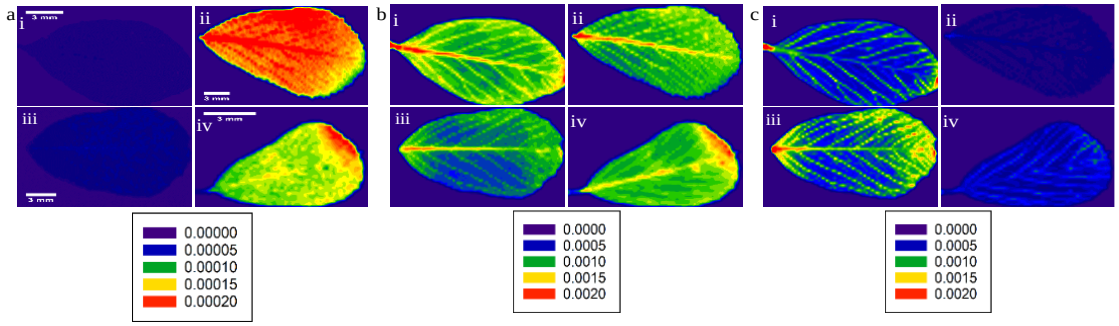

Figure 3.8. Distribution of chlorine (a), potassium (b), calcium (c) ions in leaf tissues of two alfalfa cultivars as revealed by synchrotron based XRF spectroscopy at IDEAS beamline in the Canadian Light Source.
(i. Halo control at 0 dS m^{-1} ii. Halo at 12 dS m^{-1} EC iii. Vernal control at 0 dS m^{-1} iv. Vernal at 12 dS m^{-1} EC; Index bar represents integrated absorption peak area).

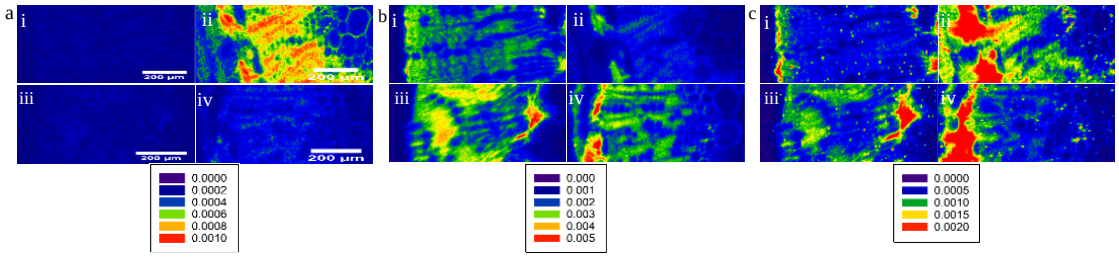

Figure 3.9. Distribution of chlorine (a), potassium (b), calcium (c) ions in stem cross-section of two alfalfa cultivars as revealed by synchrotron based XRF spectroscopy at VESPERS beamline in the Canadian Light Source.
(i. Halo control at 0 dS m^{-1} ii. Halo at 12 dS m^{-1} EC iii. Vernal control at 0 dS m^{-1} iv. Vernal at 12 dS m^{-1} EC; Index bar represents integrated absorption peak area).

3.4.5.2 ICP-MS results

The Pearson correlation analysis between mean integrated areas of elements by XRF with ionome data by ICP-MS showed significant correlations for chlorine ($P<0.001$; $r=0.81$), potassium ($P<0.001$; $r=0.70$), and calcium ($P<0.001$; $r=0.92$). The analysis of variance showed that the ratios of K^+/Na^+ and Ca^{2+}/Na^+ significantly ($P<0.001$) decreased under salt stress, compared to the no salt control in all tissues (Table 3.3). Leaf tissue had the highest concentrations of K^+/Na^+ and Ca^{2+}/Na^+ followed by stem and root tissues. The ratio of K^+/Na^+ in leaf ($P<0.001$) and root ($P<0.001$) tissues was significantly different between the two cultivars but was similar in stem tissue ($P=0.26$). The ratio of Ca^{2+}/Na^+ in root tissue ($P<0.001$) was significantly different between the two cultivars, but it was similar for leaf and stem tissues. Compared to their no salt controls, the percent reduction in K^+/Na^+ in leaf tissues of 'Halo' was greater than 'Vernal' at all salt stress conditions, while in root tissue 'Vernal' showed greater reduction than 'Halo' at 8 dS m^{-1}. Similarly, leaf tissue of 'Halo' showed higher reduction for

Ca^{2+}/Na^{+} than 'Vernal' at 4 dS m^{-1} and 12 dS m^{-1}, while stem and root tissues showed higher reduction for 'Vernal' at 8 dS m^{-1} (Table 3.3).

Table 3.3. Mean values and analysis of variance of K+/Na+ and Ca2+/Na+ ratio in leaf, stem and root tissues of alfalfa cultivars after 10 weeks of sowing exposed to salt stress after 4 weeks of sowing at different salt gradients as revealed by ICP-MS (n=2).

		Leaf		Stem		Root	
Salinity	Cultivars	K^{+}/Na^{+}	Ca^{2+}/Na^{+}	K^{+}/Na^{+}	Ca^{2+}/Na^{+}	K^{+}/Na^{+}	Ca^{2+}/Na^{+}
0 dS m^{-1}	Halo	50.45[a1]	47.46[a]	36.09[a]	15.34[a]	7.71[b]	0.91[b]
	Vernal	23.46[b]	36.27[a]	32.43[a]	17.18[a]	11.70[a]	1.35[a]
4 dS m^{-1}	Halo	0.73[c]	0.79[b]	1.15[b]	0.67[b]	0.75[c]	0.13[d]
		(99)	(98)	(97)	(96)	(90)	(85)
	Vernal	1.57[c]	1.21[b]	1.74[b]	0.75[b]	1.15[c]	0.39[c]
		(93)	(97)	(95)	(96)	(90)	(71)
8 dS m^{-1}	Halo	0.72[c]	0.39[b]	0.75[b]	0.45[b]	0.85[c]	0.10[d]
		(99)	(99)	(98)	(97)	(89)	(89)
	Vernal	0.74[c]	0.34[b]	0.76[b]	0.37[b]	0.85[c]	0.11[d]
		(97)	(99)	(98)	(98)	(93)	(92)
12 dS m^{-1}	Halo	0.39[c]	0.24[b]	0.39[b]	0.20[b]	0.48[c]	0.09[d]
		(99)	(99)	(99)	(99)	(94)	(90)
	Vernal	0.45[c]	0.24[b]	0.42[b]	0.25[b]	0.76[c]	0.15[d]
		(98)	(99)	(99)	(99)	(94)	(89)
Salinity		<0.001	<0.001	<0.001	<0.001	<0.001	<0.001
Cultivar		<0.001	0.063	0.265	0.315	<0.001	<0.001
Salinity : Cultivar		<0.001	0.052	0.150	0.410	<0.001	0.001

[1]Means with the same lower case letters within the column for each treatment are not significantly different (P > 0.05); the values in parentheses represent percent reduction compared to the control of each cultivar at each tissue.

3.5 Discussion

To our knowledge, this study is the first comprehensive study on accumulation and localization of elements and organic compounds at the tissue level in response to salt stress in alfalfa using synchrotron beamlines. The results obtained support the hypothesis that low ion accumulation in the shoot was a common strategy in alfalfa up to 8 dS m^{-1} of salt stress.

We utilized the FTIR at the Mid-IR beamline and Micro-XRF from the VESPERS and IDEAS beamlines enabling spatial localization and semi-quantitative assessment of organic compounds and elements in different alfalfa tissues. FTIR spectroscopy showed both cultivars generally

reduced their concentration of amides under the salt stress levels; however, concentration of amides was higher for 'Halo' than 'Vernal' at all stress levels in leaf and stem tissues. High amide concentration is associated with stress tolerance in plants as amides are involved in many biochemical processes (Mansour, 2000). This may also be important for osmotic adjustment and energy allocation under alfalfa salt stress as salt stimulated accumulation of amino acids and organic osmotica (carbohydrates) in plant tissues is an effective mechanism of physiological adaptation to salt stress in non-halophytes (Hellebust, 1976; Munns et al., 1982). Our results showed that under salt stress, the distribution of amides was concentrated in phloem tissue of 'Halo' (Figure 3.7c, ii) but less so in 'Vernal' (Figure 3.7c, iv). Also, amide concentration was the highest in leaf tissue followed by stem and root tissue in 'Halo'. This suggests that salt tolerant alfalfa actively transports osmolytes to the root tissues which might play a role in osmotic adjustment. Protein concentrations increased in both cultivars at the 8 and 12 dS m^{-1} stress levels, but it was not different between the two cultivars. An increase in protein concentration in salt tolerant alfalfa cultivars has been reported in previous studies (Robinson et al., 2004; Suyama et al., 2007; Ferreira et al., 2015).

In the present study, the cultivar 'Vernal' showed higher accumulation of carbohydrates than 'Halo' in leaf and root tissues under salt stress of 8 dS m^{-1} and 12 dS m^{-1}. A similar result was observed by Rathert (1984) and Kafi et al. (2003) in root and leaf of salt sensitive bush bean (*Phaseolus vulgaris* L.) and wheat (*Triticum aestivum* L.), respectively, who found an inverse correlation between salt tolerance and soluble carbohydrate content. A reduction of the carbohydrate in 'Halo' under salt stress in our study might be a result of stress-induced starch degradation. Leaf starch degradation was found to be important for osmotic stress tolerance in plants (Thalmann et al., 2016). Gao et al., (2019) found carbohydrate metabolism in alfalfa leaves to accumulate soluble sugar was associated with salt tolerance in alfalfa. The carbohydrates were distributed in xylem and phloem tissues of salt stressed stem tissue of 'Halo' (Figure 3.7b, ii) while they were only observed in xylem tissue in 'Vernal' (Figure 3.7b, iv) which indicated that 'Halo' was actively transporting carbohydrates to and from leaf tissue while such transport was limited for 'Vernal'.

We hypothesized that the chlorine concentration in leaf tissue of the salt tolerant alfalfa cultivar would be significantly lower than the intolerant alfalfa cultivar. Rahman et al. (2015) found ion exclusion in alfalfa roots under salt stress. Our study suggests the mechanism as "low

salt ion accumulation in the shoot" at 8 dS m^{-1} and "shoot tissue salt ion tolerance" at 12 dS m^{-1} based on chlorine concentration in leaf, stem and root tissues of the two alfalfa cultivars. Chlorine ion accumulation under increasing salt stress was significantly higher in leaf tissues for 'Vernal' than 'Halo' at 8 dS m^{-1} and 12 dS m^{-1} which is in agreement with another salt tolerant alfalfa cultivar 'Salado' (Cornacchione and Suarez, 2015). However, as revealed by XRF spectroscopy, the pattern of chlorine ion accumulation of tissues varied between the two cultivars. In salt tolerant cultivar 'Halo', root tissue had significantly higher chlorine concentration than leaf tissue at 8 dS m^{-1} but root and leaf tissues had the same concentration at 12 dS m^{-1}, while salt intolerant cultivar 'Vernal' showed significantly higher chlorine concentration in leaf tissue than root tissue at both salinity levels of 8 dS m^{-1} and 12 dS m^{-1}. A similar pattern of sodium ion accumulation in root, stem and leaf was observed in salt tolerant alfalfa 'Zhongmu No.1' under 12 dS m^{-1} salt stress (Wang and Han, 2007). Cornacchione and Suarez (2017) also stated that salt tolerant alfalfa maintained lower concentration of salt ions in shoot tissue. Maintenance of low sodium and chlorine in leaf tissue has been considered as a strategy for salt tolerance in barley (*Hordeum vulgare* L.) (Shen et al., 2016).

Based on VESPERS beamline results, mean integrated peak area of potassium was higher in leaves of 'Halo' at 12 dS m^{-1} than in 'Vernal', indicating its ability to maintain higher potassium ions under salt stress. Potassium and sodium, being monovalent cations, are generally considered as being competitive elements for root uptake and transport in the plant (Schachtman and Liu, 1999). The retention of potassium under salt stress was considered to be crucial for salt tolerance of glycophytic plants (Wu et al., 1996; Zhu et al., 1998; Chen et al., 2007), and a salt-tolerant barley cultivar had a higher ability to retain potassium than sensitive cultivars (Wu et al., 2013; Shen et al., 2016). Wei et al. (2020) proposed Ca^{2+}/Na^{+} ratio as a critical marker for evaluating saline-alkaline tolerance in alfalfa; we also found the ratio was significantly reduced with increase in salt stress, but the ratio did not differentiate the two alfalfa cultivars in our study (Table 3.3). The distribution of chlorine in 'Vernal' (Figure 3.8a, iv) showed a high concentration in the leaf tip, but in 'Halo', there was a more uniform distribution of chlorine ion in leaf tissue avoiding high concentration in small areas (Figure 3.8a, ii), preventing visible symptoms of salt injury. There was uniform distribution of chlorine in both xylem and phloem in 'Halo' (Figure 3.9a, ii) suggesting that salt tolerance is associated with avoiding high

concentration of chlorine in leaf, which was also supported by the results of bulk analysis at 12 dS m^{-1}.

During the germination stage, salt tolerance is expressed by the ability of the seed to germinate and the seedling to survive, whereas in later development stages, tolerance is usually measured by the degree of growth reduction relative to growth under the control of no salt (Lauchli and Grattan, 2007). We hypothesized that seed germination and shoot and root development of the two cultivars would be similar under control conditions, but the salt tolerant alfalfa cultivar would have greater performance under salt stress. The cultivar 'Halo' was selected for tolerance to salt stress at both germination and flowering stages (Steppuhn et al., 2012), while 'Vernal' was a salt intolerant cultivar (Peel et al., 2004; Rahman et al., 2015). In the present study, the seed vigor of 'Halo' was significantly higher than 'Vernal', but only at the highest salt stress (i.e.16 dS m^{-1}). 'Halo' and 'Vernal' were not different in dry shoot and root biomass or root to shoot ratio under the different levels of salt stress, which was in agreement with the findings of Bertrand et al. (2015) for which the authors compared 'Halo' with a salt intolerant alfalfa cultivar 'Apica'. Steppuhn et al., (2012) reported that 'Halo' showed significantly higher mean relative shoot biomass at 8 and 15.6 dS m^{-1} compared to the intolerant alfalfa cultivar 'Rangelander'. Although our study found non-significant differences between the two cultivars for shoot and root biomass after 12 weeks of growth, we speculate that this difference may be evident at high salinity (>16 dS m^{-1}), or long-term exposure to salt stress. This is possible because at 12 dS m^{-1}, root biomass of 'Halo' was numerically higher than 'Vernal', and the rate of root biomass reduction from 8 dS m^{-1} to 12 dS m^{-1} was much smaller for 'Halo' as compared to a sharp decrease of root biomass for 'Vernal', meaning 'Halo' can maintain a relatively stable root system. A large root system is generally associated with high plant vigor (Cornacchione and Suarez, 2017), and larger root biomass also enables better extraction of water against osmotic gradients thereby increased salt tolerance (Cornacchione and Suarez, 2015), as well as the retention of toxic ions in the roots limiting their translocation to the shoots (Hsiao and Xu, 2000; Acosta-Motos et al., 2017).

In our study, we also found that 'Halo' was slightly superior to 'Vernal' for maintaining leaf relative water content under salt stress compared to their controls, although both alfalfa cultivars showed reduction in relative leaf water content due to salt stress. The reduction of relative leaf water content was also reported by Li et al. (2010), but surprisingly, both cultivars in our study

maintained more than 70% relative water content under all stress levels. This suggests that alfalfa is able to maintain cell turgor pressure (Acosta-Motos et al., 2017) and withstand certain levels of osmotic stress. Maintenance of relative leaf water content indicates that alfalfa plants are able to prevent water loss (Anower et al., 2013), thereby mitigating salt ion toxicity by a dilution effect. The decrease in chlorophyll content with salt stress has been considered as a typical symptom of oxidative stress (Gill and Tuteja, 2010). Our results suggest that alfalfa does not undergo chlorophyll reduction significantly with increasing salt stress, at least until 12dS m^{-1}. However, Ashrafi et al. (2015) found an increase of chlorophyll content for salt tolerant alfalfa at about 6 dS m^{-1} and 12 dS m^{-1} while it decreased for salt intolerant alfalfa.

Sanders (2020) highlighted that plant response to salt stress should not only be considered at the cellular level. In the present study, we found that the most important differences between salt tolerant and intolerant alfalfa cultivars were seed vigor, and the elemental and organic compound accumulation and distribution in different tissues. This study demonstrated effectiveness of FTIR and XRF spectroscopy in identifying salt tolerant alfalfa genotypes based on salt ions and organic compound concentrations in alfalfa tissues. This study examined the low ion accumulation in the shoot as a mechanism in salt tolerant alfalfa based on salt ion accumulation in different tissues. Further research investigating the localization of salt ions at cellular and intracellular levels and identification of genes involved in Na^+ and Cl^- transport in vacuoles for tissue tolerance will be crucial for further understanding the salt tolerant mechanism. At salt concentration of 8 dS m^{-1}, the salt tolerant alfalfa showed significantly higher amide I and amide II concentration and lower concentration of carbohydrate and lipid in leaf tissue as compared to the salt intolerant alfalfa cultivar, suggesting the energy expenditure of salt tolerant alfalfa to cope with salt stress. Teakle and Tyerman (2010) suggested that the mechanism of Cl^- transport is energy demanding which appears true in alfalfa based on our findings, where salt tolerant alfalfa restricts the transportation of Cl^- to the leaf tissue and the transported Cl^- was uniformly distributed throughout the leaf tissue protecting the leaf mesophyll cells. Identification of genes for energy budgeting such as maintenance requirements, growth requirements, and increased demands related to acclimation under salt stress would add more information to understanding the salt tolerance mechanism in alfalfa. The approach in this paper may support the development of salt tolerant crops, which could improve agriculture production and productivity in saline regions. For the successful indirect selection for salt tolerance traits in alfalfa we found seed

vigor and the concentration of salt ions and organic compounds can be used as physiological and biochemical markers.

Chapter 4. Transcriptome analysis revealed differentially-expressed genes in leaves and roots of two alfalfa (*Medicago sativa* L.) cultivars with different salt tolerance

4.1 Abstract

Alfalfa (*Medicago sativa* L.) production decreases under salt stress. Identification of genes associated with salt tolerance in alfalfa can help develop molecular markers for genetic improvement. In this study, gene expression analysis using RNA-Seq technique was performed to identify the differentially expressed genes (DEGs) associated with salt stress in two alfalfa cultivars: salt tolerant 'Halo' and salt intolerant 'Vernal'. Leaf and root tissues were sampled for RNA extraction at 0h, 3h, and 27h of 12 dS m^{-1} salt stress maintained by NaCl. This study generated a total of 381 million clean reads, which were then assembled to 436,358 transcripts. The transcripts corresponded to 299,032 genes with N50 of 858 bp. This study identified 156 DEGs in leaf and 322 DEGs in roots of the two alfalfa cultivars. In leaf tissue, 'Halo' had 31 and 21 DEGs at 3h and 27h of salt stress, while 'Vernal' had 19 and 45, respectively. In root tissue, 'Halo' maintained 32 and 36 DEGs at 3h and 27h, while the number of DEGs was 60 and 17 for 'Vernal'. This study identifies fourteen (leaf) and nine (root) salt responsive candidate genes consistently expressed in 'Halo' compared to 'Vernal' under salt stress. The genes were involved in signaling, osmotic adjustment, DNA topology, ion homeostasis, and metal transport. In addition, 10 novel salt responsive transcripts were also identified. Alfalfa genomic information obtained in this study would be useful for molecular marker development for alfalfa genetic improvement.

4.2 Introduction

Alfalfa (*Medicago sativa* L.) is an important forage legume in the world. Cultivated alfalfa is an outcrossing autotetraploid (2n=4x=32) with a genome size of 800–1000 Mb (Blondon et al., 1994). Alfalfa is regarded as moderately tolerant to salinity (Maas and Hoffman, 1977). However, alfalfa yield reduced by approximately 6-7% for each dS m^{-1} increase above salinity of 2 dS m^{-1} (Johnson et al., 1992). To stabilize alfalfa production under saline regions, the development of superior salt tolerant cultivars becomes an important breeding goal. Identification of candidate genes for salt tolerance can increase the accuracy of genetic selection as this is a low heritable trait (Gregorio and Senadhira, 1993). Salt tolerance is controlled by multiple genes, involving different signaling pathways, osmotic tolerance, ion transport,

compartmentalization of salt ions in vacuoles, the synthesis of plant hormones and photosynthesis (Munns and Tester, 2008).

Next-generation sequencing (NGS) technologies have been used to identify candidate genes involved in salt tolerance of alfalfa. Transcriptome studies in the 1-week old root tissue of alfalfa under salt stress found 1165 DEGs, including 86 transcription factors which are responsible for stress tolerance, kinase, hydrolase, and oxidoreductase activities (Postnikova et al., 2013). Luo et al. (2019) identified 8861 DEGs in 12-day old seedlings of alfalfa under salt stress, which are responsible for ion homeostasis, antiporter, signal perception, signal transduction, transcriptional regulation, and antioxidative defense. Lei et al. (2018a) found 2237 DEGs between salt tolerant and intolerant alfalfa cultivars and found a salt tolerant alfalfa cultivar maintained relatively stable expression of genes responsible for reactive oxygen species (ROS) and Ca^{2+} pathway, phytohormone biosynthesis and Na^{+}/K^{+} transport under stress. Gruber et al. (2017), using bulked genotypes as replications, studied transcriptomes in alfalfa and found genes responsible for numerous functions in a salt intolerant alfalfa cultivar. In recent years, genetic modification of certain genes controlling salt tolerance have also been conducted in alfalfa. Overexpression of salt responsive genes or transcription factors had improved salt tolerance in transgenic alfalfa. Such genes include *Alfin1* (Winicov, 2000), *AVP1* (Bao et al., 2009), *GmDREB1* (Jin et al., 2010b), *SsNHX1* (Li et al., 2011), *TaNHX2* (Zhang et al., 2012), *GsCBRLK* (Bai et al., 2013), *GsZFP1* (Tang et al., 2013), *OsAPX2* (Zhang et al., 2014a), *SeNHX1* (Zhang et al. 2014b), *AtNDPK2* (Wang et al., 2014), *AgcodA* (Li et al., 2014), and *GsWRKY20* (Tang et al., 2014).

Tissue specific protein induction is regulated during salinity stress and is unique to roots and shoots (Ramagopal, 1987a). Thus, there should be tissue specific transcriptomic responses (Ramagopal, 1987b; Kumar et al., 2017; Villarino et al., 2017). Although the root is the first receptor of salt stress (Postnikova et al., 2013; Luo et al., 2019), leaf tissue is the main energy source for plant growth and stress tolerance during active growth and developmental stages. Most of the earlier transcriptome studies in alfalfa salt tolerance mainly focused on single time point sampling of root tissue at the seedling stage after salt stress (summarized in Chapter 2, Table 2.1). However, understanding pattern of gene expression over time in different tissues are necessary for the understanding of genetic control under salt stress between the two cultivars. The objectives of this study were to simultaneously analyze gene expressions of leaf and root

tissues of two alfalfa cultivars with different tolerance to salinity after exposing them to 12 dS m^{-1} of EC salt stress for 0h, 3h, and 27h.

4.3 Materials and Methods

4.3.1 Plant material and salt treatment

Two alfalfa cultivars, 'Halo' and 'Vernal', were chosen for the study. Cultivar 'Halo' was selected for improved salinity tolerance in lab condition (Steppuhn et al., 2012), and cultivar 'Vernal' was considered as a salinity susceptible cultivar (Peel et al., 2004; Rahman et al., 2015). Four genotypes (biological replicates) of each cultivar were grown from seeds in the College of Agriculture and Bioresources greenhouse at the University of Saskatchewan (45 Innovation Blvd., Saskatoon, SK) for 12 weeks. Six identical clones of each biological replicate were produced by stem cutting. Salt stress of 12 dS m^{-1} was applied on 4 weeks old seedlings developed by stem cuttings. Leaf and root samples were collected immediately before salt treatment (control, 0 h), and at 3 h and 27 h of salt treatments. The samples were immediately frozen in liquid nitrogen and then stored at –80 °C until total RNA extraction.

4.3.2 Tissue sample and RNA isolation

About 100 mg of tissue samples were disrupted using TissueLyser II and total RNA was extracted with RLT buffer using the Qiagen RNeasy Plant Mini Kit (Qiagen Inc, Mississauga, ON, Canada) according to the manufacturer's protocol. DNase treatment was performed using the Ambion DNA-free DNase treatment and removal reagents (Life Technologies, Carlsbad, CA, USA) to remove contaminant genomic DNA from the isolated total RNA. Nanodrop 2000 (Thermo Fisher Scientific, Wilmington, DE, USA) was used to measure the total RNA concentration. RNA integrity number was evaluated using RNA 6000 Nano labchip on 2100 Agilent Bioanalyzer (Agilent Technologies, Waldbronn, Germany).

4.3.3 Library preparation and sequencing

Poly (A) RNA was purified from total RNA using Magnosphere MS150 OligodT beads according to the manufacturer's protocol. The RNA samples were subsequently used in cDNA library preparation. Two cDNA libraries were prepared using Lexogen's SENSE mRNA-Seq Library Prep Kit V2 (Lexogen, Vienna, Austria). To avoid technical error, two technical replicates of each treatment were divided into two cDNA libraries. The technical replicates represent two clones of the same genotype (biological replicate) by separately extracting RNA.

Thus, 96 samples (2 cultivar × 2 tissue type × 3 time point × 8 replicate) were collected for the study. The cDNA libraries were sequenced using Illumina HiSeq v4 system at the National Research Council of Canada, Saskatoon, Canada. Raw reads were deposited in the National Center for Biotechnology Information (NCBI) and received BioProject ID PRJNA657410.

4.3.4 *De Novo* assembly, differential gene expression analysis and annotation

The quality of the raw sequence was assessed using the FastQC software (Schmieder and Edwards, 2011). The raw reads were cleaned by removing adapters and low-quality sequences using Trimmomatic v.0.36 based on the default setting of paired-end mode, phred 33 and threads 6 (Bolger et al., 2014).

De novo assembly of the alfalfa transcriptome was accomplished following the online instructions of Trinity (Grabherr et al., 2011; Haas et al., 2013). The quality of alfalfa *de novo* transcriptome assembly was checked using perl script "TrinityStats.pl" of the Trinity pipeline. The *de novo* assembly of alfalfa RNA-Seq libraries was used as a reference. The alignment-based qualification method RSEM (Li and Dewey, 2011) was used to estimate transcript abundance using trinity pipeline "align_and_estimate_abundance.pl" with each RNA-Seq library separately aligned to the reference using Bowtie (Langmead et al., 2009). Then the gene counts matrix was generated using trinity pipeline "abundance_estimates_to_matrix.pl". The DEGs were analyzed using the R Bioconductor package, edgeR (Robinson et al., 2010) from trinity pipeline "run_DE_analysis.pl". The threshold of false discovery rate (FDR) $\leq$ 0.001 and the Log fold change (LogFC) $\geq$ 2 were used to determine the significance of gene expression differences.

The fasta file for the longest isoform for each DEGs were extracted from trinity assembly using perl script "get_longest_isoform_seq_per_trinity_gene.pl" of the Trinity pipeline for putative function analysis by nucleotide blast against non-redundant protein sequences of Leguminosae (taxid:3803) in the NCBI database.

4.4 Results

4.4.1 *De Novo* assembly

Total 407,911,014 raw reads were generated using the Illumina HiSeq sequencing platform. The reads were reduced to 93.5% (clean read) by eliminating reads with length lower than 36bp (Table 4.1). *De novo* assembly generated 436,358 transcripts, which corresponds to 299,032 genes, with N50 length of 858 bp and GC content of 42.05% (Table 4.1). The minimum and

maximum lengths of the assembled genes were 198 bp and 13,741 bp, respectively. A dendrogram of differentially expressed genes showed that the difference between technical replicates was smaller than biological replicates, which was expected (Appendix 1).

Table 4.1. Summary statistics of sequencing data and the combined *de novo* transcriptome assembly of alfalfa.

Read processing	
Raw reads	407,911,014
Processed reads	381,482,398
Trinity *de novo* assembly	
Total assembled bases	270,888,810
Number of Transcripts	436,358
Number of transcripts with predicted genes	299,032
Average contig length (bp)	620
Median contig length (bp)	379
Transcript N50 (bp)	858
GC content (%)	42.05

4.4.2 Detection and annotation of differentially expressed genes

In leaf tissue, there were 156 DEGs between the two alfalfa cultivars (Figure 4.1a, b; Appendix 2). Of these DEGs, 22, 31, and 21 DEGs were specific to ‘Halo’, and 18, 19, and 45 DEGs unique to ‘Vernal’ at 0h, 3h, and 27h of salt stress, respectively.

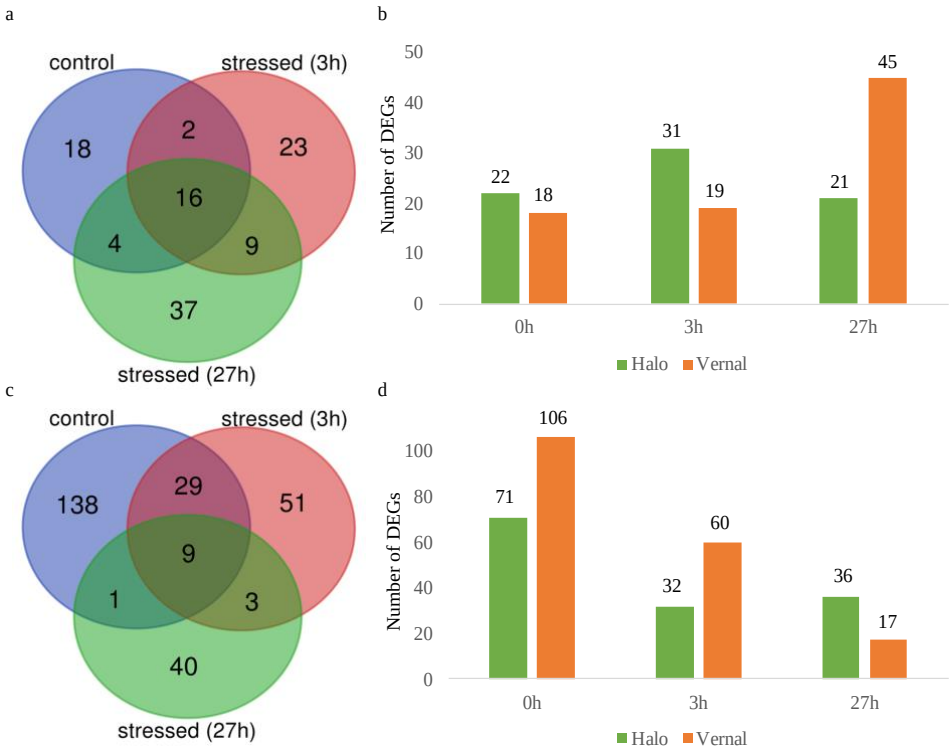

Figure 4.1. Differentially expressed genes (DEGs) between salt tolerant 'Halo' and intolerant 'Vernal' alfalfa cultivars in leaf and root tissues at three different time-points: control (0h), 3h and 27h after salt stress. a) Venn diagram for the number of DEGs in leaf tissue of two alfalfa cultivars ('Halo' vs. 'Vernal') at three different time-points (0h, 3h, and 27h). Numbers in each intersection represent the number of DEGs detected in both time points. b) number of DEGs identified in leaf tissue at each time-point (0h, 3h, and 27h) between tolerant and intolerant alfalfa cultivars. (Green; DEGs with higher expression in 'Halo' than 'Vernal', Orange; DEGs with higher expression in 'Vernal' than 'Halo'). c) Venn diagram for the number of DEGs in root tissue of two alfalfa cultivars ('Halo' vs. 'Vernal') at three different time-points (0h, 3h, and 27h). Numbers in each intersection represent the number of DEGs detected in both time points. d) number of DEGs identified in root tissue at each time-point (0h, 3h, 27h) between tolerant and intolerant alfalfa cultivars. (Green; DEGs with higher expression in 'Halo' than 'Vernal', Orange; DEGs with higher expression in 'Vernal' than 'Halo').

In root tissue, 322 DEGs were identified between the two alfalfa cultivars (Figure 4.1c, d; Appendix 3). Of these DEGs, 71, 32, and 36 DEGs were significantly expressed in 'Halo' at 0h, 3h, and 27h, respectively, whereas 106, 60, and 17 DEGs were specific to 'Vernal'. The number of DEGs in leaf tissue was slightly reduced for 'Halo' between 3h and 27h, while the number of DEGs more than doubled in 'Vernal' (Figure 4.1b). In root tissue, 'Halo' showed a slight increase in the number of DEGs from 3h to 27h of salt stress, but it was decreased to about one third in 'Vernal' (Figure 4.1d).

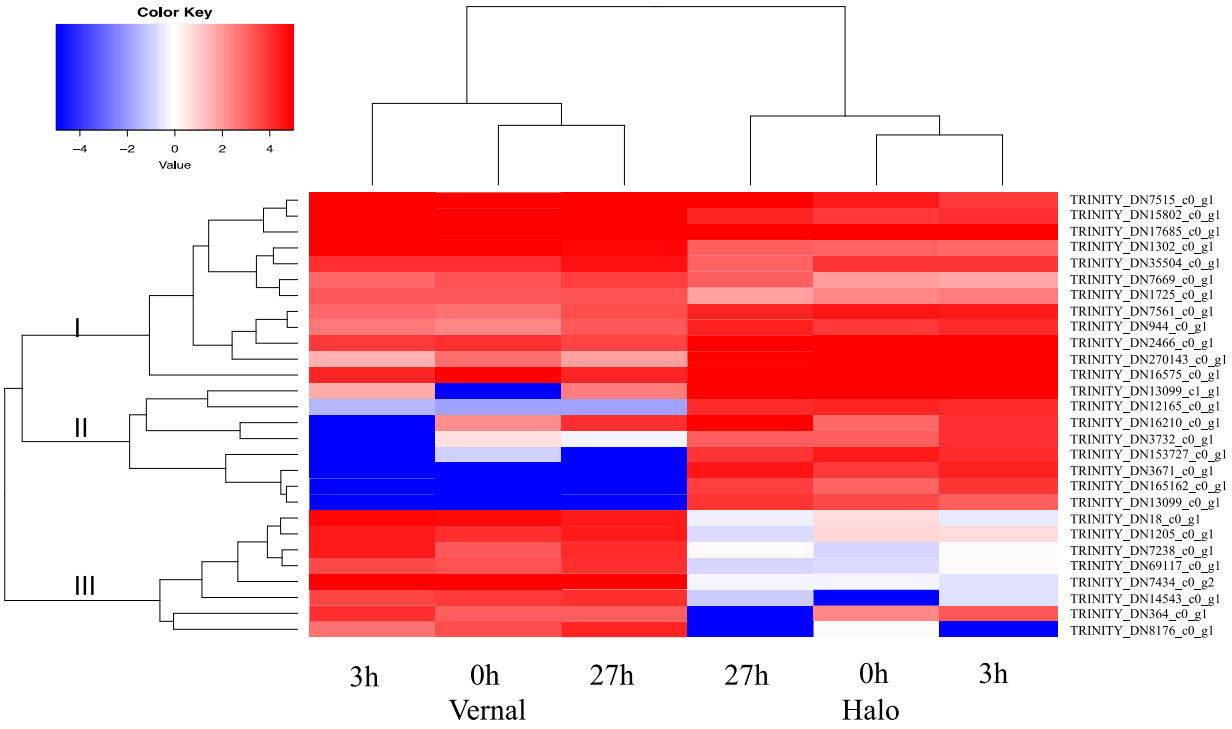

Figure 4.2. Heatmap of relative expression (logTPM) of the top 25% of differentially expressed genes in leaf tissue of two alfalfa cultivars, ‘Halo’ and ‘Vernal’, in response to salt stress. Each column represents an experimental sample and each row represents a gene. Gene expression differences are shown in different colors with blue color representing low expression and red color representing high expression. TPM, transcript per million value.

Out of 156 DEGs expressed in leaf tissue, 109 DEGs were expressed at all three time points (0h, 3h, and 27h); a heatmap of 25% of 109 DEGs is shown in Figure 4.2. Likewise, of 322 DEGs expressed in root tissue, 271 DEGs were expressed at all three time points; a heatmap of 25% of 271 DEGs is shown in Figure 4.3. The heatmap showed clear distinct clustering of DEGs in the two alfalfa, but the pattern was similar between the leaf and root samples (Figures 4.2 and 4.3). For ‘Halo’, samples from 0h and 3h were closely clustered, while samples after 27h showed distinct clustering. However, for ‘Vernal’, samples from 0h and 27h were closely clustered and samples from 3h were separately clustered, indicating a different pattern for gene expression.

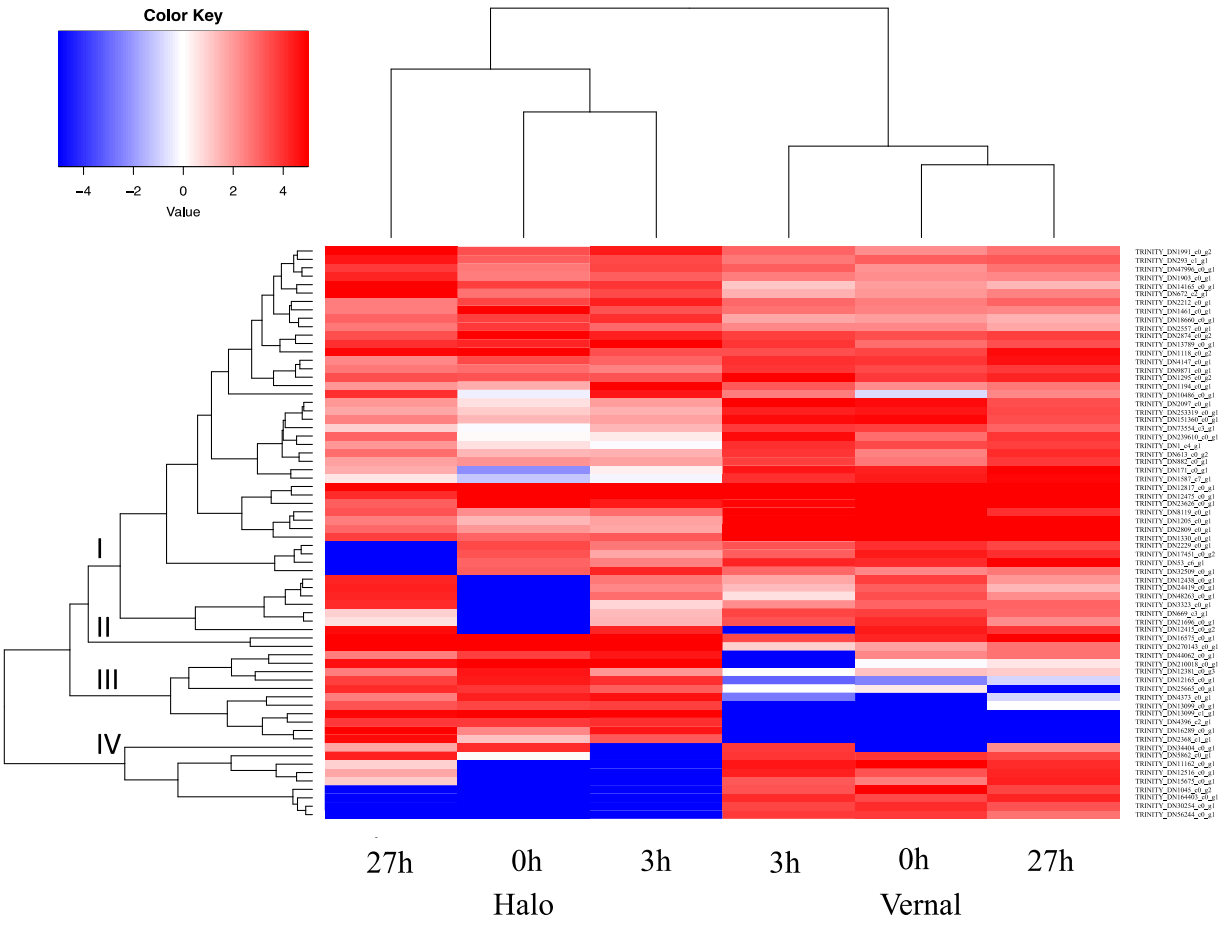

Figure 4.3. Heatmap of relative expression (logTPM) of the top 25% of differentially expressed genes in root tissue of two alfalfa cultivar ‘Halo’ and ‘Vernal’ in response to salt stress. Each column represents an experimental sample and each row represents a gene. Gene expression differences are shown in different colors with blue color representing low expression and red color as high expression. TPM, transcript per million value.

In leaf tissue, DEGs showed three distinct clusters with the first cluster containing genes with high TPM value in both cultivars, indicating common genes for salt tolerance. The second cluster comprised of eight DEGs highly expressed in leaf tissue of ‘Halo’ and the third cluster consisted of highly expressed eight genes of ‘Vernal’ (Figure 4.2). In root tissue, DEGs showed four clusters, with first cluster containing several sub-clusters of genes with high TPM value in both cultivars. The second cluster comprised of two genes (TRINITY_DN270143_c0_g1, TRINITY_DN16575_c0_g1), which showed exceptionally high TPM values in ‘Halo’, responding to the increased salt stress. The third cluster consisted of 11 genes highly expressed in ‘Halo’. The fourth cluster included nine genes highly expressed in ‘Vernal’ (Figure 4.3).

4.4.3 Candidate genes for salt tolerance in alfalfa

The candidate genes responsible for salt tolerance in alfalfa were classified into two major groups: 1) genes consistently expressed under salt stress (3h and 27h) in 'Halo', and 2) the genes consistently expressed at all three time points in 'Halo'. In the first group, there were five genes (three in leaf; two in root) consistently expressed at both 3h and 27h of salt stress. In the second group, there were 11 genes in leaf and seven genes in root expressed consistently at all three time points. Interestingly, there were six of these genes commonly expressed in both leaf and root tissues (Table 4.2). Of these six genes, compared between the two cultivars, TRINITY_DN12165_c0_g1, homologous gene of GTP cyclohydrolase (*GCH*), showed about eight times higher expression in 'Halo', TRINITY_DN10576_c0_g1, homologous gene of dnaJ protein ERDJ2A (*ERDJ2A*), showed more than six times high expression in 'Halo'. TRINITY_DN462_c0_g2, homologous gene of ribosomal RNA small subunit methyltransferase nep-1, showed more than seven times expression in 'Halo', TRINITY_DN16575_c0_g1, homologous gene of protein IAA-LEUCINE RESISTANT 2 (*ILR2*), showed about eight times higher expression in leaf tissue of 'Halo' and 11 times higher expression in root. The putative function of two of six genes (TRINITY_DN13099_c0_g1, TRINITY_DN270143_c0_g1) were unknown.

Eight genes showed high expression in leaf tissue of 'Halo' (Table 4.3) while there were three genes in root tissue (Table 4.4) as compared to 'Vernal'.TRINITY_DN274030_c0_g1, homologous gene of DNA gyrase subunit B (*MtGyrB*), showed about eight times higher expression in leaf tissue of 'Halo' than in 'Vernal'. TRINITY_DN34220_c0_g1, homologous gene of replication factor A protein had a consistent expression of more than five times in leaf tissue of 'Halo'. TRINITY_DN3671_c0_g1, homologous gene of histone H2A.6-like, showed the highest expression around nine times in leaf of 'Halo' compared to 'Vernal'. TRINITY_DN4000_c0_g1, homologous gene of putative non-specific serine/threonine protein kinase, showed seven times higher expression in leaf tissue of 'Halo'. TRINITY_DN165162_c0_g1 showed consistent expression (> 7 times) at the three time points in leaf tissue of 'Halo', but no homology was retrieved upon performing BLASTX against non-redundant protein sequences of Leguminosae in the NCBI database. In addition, no homology was found for one of seven genes (TRINITY_DN13099_c1_g1) specific to root tissue of 'Halo'.

Table 4.2 List of six salt responsive candidate genes highly expressed in both leaf and root tissues of salt tolerant alfalfa cultivar 'Halo'.

Gene ID	Putative function[1]	Nr ID[2]	log_2FC[3] (Leaf)			log_2FC (Root)		
			0h	3h	27h	0h	3h	27h
TRINITY_DN462_c0_g2	ribosomal RNA small subunit methyltransferase nep-1 [*Medicago truncatula*]	XP_013454067.1	7.07	7.19	7.66	8.06	7.20	7.52
TRINITY_DN10576_c0_g1	dnaJ protein ERDJ2A [*Medicago truncatula*]	XP_024632012.1	7.09	8.08	6.83	6.59	7.28	6.46
TRINITY_DN16575_c0_g1	protein IAA-LEUCINE RESISTANT 2 [*Trifolium medium*]	MCI04234.1	7.36	7.36	7.98	8.11	9.78	10.73
TRINITY_DN12165_c0_g1	GTP cyclohydrolase [*Arachis hypogaea*]	QHO24156.1	7.95	8.75	8.08	9.31	8.86	7.68
TRINITY_DN270143_c0_g1	NA	-	7.50	7.50	8.42	7.72	9.33	10.98
TRINITY_DN13099_c0_g1	NA	-	8.12	7.33	8.71	8.25	8.37	5.48

[1]NA represents no homology retrieved upon performing BLASTX.
[2]Nr ID is the protein accession number in NCBI non redundant protein database.
[3]log_2FC stands for log Fold Change, where it is log base 2.

Table 4.3 List of eight salt responsive candidate genes highly expressed only in leaf tissue of salt tolerant alfalfa cultivar 'Halo'.

Gene ID	Putative function[1]	Nr ID[2]	log_2FC[3]		
			0h	3h	27h
TRINITY_DN34220_c0_g1	replication factor A protein [*Trifolium pratense*]	PNY01153.1	5.98	5.22	5.6
TRINITY_DN4000_c0_g1	putative non-specific serine/threonine protein kinase [*Medicago truncatula*]	RHN41153.1	7.39	7.09	7.66
TRINITY_DN274030_c0_g1	DNA gyrase subunit B, putative [*Medicago truncatula*]	AES88004.1	7.97	7.91	8.14
TRINITY_DN3671_c0_g1	histone H2A.6-like [*Arachis duranensis*]	XP_015953769.1	8.51	9.20	9.54
TRINITY_DN165162_c0_g1	NA	-	7.30	8.51	8.43
TRINITY_DN2664_c0_g1	NA	-	-	6.80	5.22
TRINITY_DN153727_c0_g1	NA	-	-	8.81	8.65
TRINITY_DN129905_c0_g1	NA	-	-	5.52	6.11

[1]NA represents no homology retrieved upon performing BLASTX.
[2]Nr ID is the protein accession number in NCBI non redundant protein database.
[3]log_2FC stands for log Fold Change, where it is log base 2.

Table 4.4 List of three salt responsive candidate genes highly expressed only in root tissue of salt tolerant alfalfa cultivar 'Halo'.

Gene ID	Putative function[1]	Nr ID[2]	log_2FC[3]		
			0h	3h	27h
TRINITY_DN2368_c1_g1	hypothetical protein VIGAN_01442200 [*Vigna angularis* var. *angularis*]	BAT76424.1	-	7.70	10.12
TRINITY_DN13099_c1_g1	NA	-	11.10	11.02	10.28
TRINITY_DN2664_c2_g2	NA	-	-	7.58	7.86

[1]NA represents no homology retrieved upon performing BLASTX.
[2]Nr ID is the protein accession number in NCBI non redundant protein database.
[3]log_2FC stands for log Fold Change, where it is log base 2.

4.5 Discussion

This study generated important genomic resources that can be used to characterize genes associated with salt tolerance in alfalfa breeding materials and develop molecular markers for salt tolerant selection. First, 436,358 transcripts were identified. Second, 156 DEGs in leaf and 322 DEGs in root were identified between the two alfalfa cultivars. It is also evident that the number of DEGs between the two cultivars were different with the increase of salt exposure time. Third, this study was able to determine candidate genes consistently expressed under salt stress in the salt tolerant cultivar, and also identified a few genes which previously have not been reported.

Due to polyploidy and its out-crossing nature, alfalfa genomic studies have encountered many challenges (Liu et al., 2013) as compared to homogenous cultivars such as wheat (Feldman and Levy, 2005) and soybean (*Glycine max*) (Gill et al., 2009). To overcome certain technical difficulties, this study has sampled identical clones at different time points and in different tissues. Unlike previous alfalfa transcriptome studies, two technical replicates for each treatment were included to minimize technical error. Furthermore, this study also focused on both leaf and root tissues of alfalfa cultivars to capture tissue specific gene expression. The transcriptome study generated ~381 million high quality reads which likely represents most of the genome of *Medicago sativa*. This is supported by the assembly of 436,358 transcripts, which were comparable with earlier reports (Zeng et al., 2017; Lei et al., 2018a). The transcript N50 value representing 50% of the transcript was 858bp, suggesting that sequencing results are reliable. These findings demonstrated the effectiveness of the RNA-Seq technique to study transcriptional variation in response to salt stress in alfalfa.

There were six candidate genes commonly expressed in leaf and root tissues of ‘Halo’ under salt stress. High expression of putative non-specific serine/threonine protein kinase in ‘Halo’ leaf tissue might be involved in maintaining ion homeostasis. Because serine/threonine type protein kinase was encoded by *Salt Overly Sensitive 2 (SOS2)* gene, which is essential for intracellular Na^+ and K^+ homeostasis and plants salt tolerance (Liu et al., 2000). Histone H2A.6-like and replication factor A protein were highly expressed in leaf tissue of ‘Halo’, which might play a role in binding, replication, repair, and recombination of DNA under stress conditions (Longhese et al., 1994; Luo et al., 2017). *MtGyrB*, an essential gene for the control of DNA topology and

genome maintenance, was found highly expressed in leaf tissue of salt tolerant 'Halo'. Confalonieri et al., (2014) reported that this gene was responsible for osmotic stress tolerance in *Medicago truncatula*. Heat shock protein acts as a molecular chaperone and protects plants against abiotic stresses by keeping cell protein in a functional state and maintaining cellular homeostasis (Haq et al., 2019). In this study, the high expression of heat shock proteins in leaf tissue of 'Halo' suggested their role in salt tolerance, in agreement with a previous study by Gruber et al. (2017). DnaJ proteins (*ERDJ2A*), which are also called heat shock proteins (Fan et al., 2017), were observed highly expressed in both leaf and root tissues of 'Halo' at all time points in the study. Similar to this, over-expression of DnaJ proteins exhibited salt tolerance in *Arabidopsis* (Zhichang et al., 2010).

GCH was found highly expressed in both leaf and root tissues of 'Halo'. The first step of the pterin branch of folate synthesis pathway was mediated by *GCH* (Basset et al., 2002). Folic acids are known as natural antioxidants (Asensi-Fabado and Munné-Bosch, 2010) and are also involved in proline synthesis in plants under stress (Burguieres et al., 2007). A higher synthesis of proline was found responsible for an osmotic adjustment (Ashraf and Foolad, 2007). Exogenous application of folic acid was found responsible for salt stress resistance in barley by alleviating the salt-induced inhibition and improving seed germination and vigor of barley under salt stress (Kilic and Aca, 2016). Although no significant DEGs related to Na^+ transport was observed as the candidate genes in our sequencing results, some genes homologous to ion transport and transmembrane protein were differentially expressed under salt stress in both alfalfa cultivars. Finally, TRINITY_DN270143_c0_g1 and TRINITY_DN16575_c0_g1 (*ILR2*) showed exceptionally higher expression in both leaf and root tissues of 'Halo', suggesting that these genes could serve as potential markers for salt tolerance in alfalfa. In addition, the heatmap of leaf tissue showed additional salt responsive DEGs closely clustered with candidate genes, including three genes [TRINITY_DN16210_c0_g1 (MLP-like protein), TRINITY_DN3732_c0_g1 (putative lipid-transfer protein DIR1), TRINITY_DN13099_c1_g1 (no homology)] in the second cluster of leaf tissue. Likewise, there were an additional seven genes [TRINITY_DN44062_c0_g1 (putative naringenin-chalcone synthase), TRINITY_DN210018_c0_g1 (hypothetical protein MtrunA17_Chr1g0149151), TRINITY_DN4373_c0_g1 (hypothetical protein MTR_4g051502), TRINITY_DN25665_c0_g1 (elongation factor 1-beta), TRINITY_DN16289_c0_g1 (unknown), TRINITY_DN12381_c0_g3

(hypothetical protein TSUD_262640), and TRINITY_DN4396_c2_g1 (no homology)] in the second and third clusters of the heatmap generated for root tissue.

The result showed higher number of DEGs in root tissue than leaf tissue which might be due to root tissue being first receptor of salt stress. We found that the salt tolerant alfalfa cultivar 'Halo' showed few fluctuations in the number of DEGs in leaf tissue with the increase of salt exposure time, while the number of DEGs in the intolerant alfalfa increased at 27h of salt stress. In roots, however, the number of DEGs in the salt tolerant alfalfa slightly increased from 3h to 27h of salt stress, but the opposite trend was observed for the intolerant cultivar. We speculate that such earlier activation of salt responsive genes and maintenance of the number of DEGs might be a key characteristic for salt tolerance in alfalfa. In addition, the increase of the number of DEGs in 'Halo' roots may indicate a transcriptional reprogramming at 27h to cope with prolonged salt stress. The heatmap also showed close clustering of DEGs expressed at 0h and 3h in both leaf and root tissues of 'Halo' suggesting that 'Halo' experiences almost no salt stress within 3h while the DEGs in 'Vernal' at 3h were separately clustered from the control (0h). However, in 'Halo', DEGs after 27h are separately clustered from control and 3h salt treatment, suggesting unique gene expression at 27h of salt stress, and are likely salt responsive genes.

In conclusion, our study identified important genes for osmotic tolerance, ion homeostasis, transport, and signaling, and found 10 additional novel salt responsive transcripts. This transcriptome study provided a comprehensive set of tissue specific, genomic information on between the two alfalfa cultivars with different tolerances to salinity. The genomic resources generated can be used to develop molecular markers for salt tolerance selection.

Chapter 5. General discussion

Development of a salt tolerant alfalfa cultivar is an important breeding goal for the Canadian prairies due to the increasing threat of salinization in agriculture land. Characterization of salt tolerance is a complex task as it is controlled by multiple genes involving various biochemical and physiological processess (Flowers, 2004). Although some progress has been made in the development of salt tolerant cultivars, genetic improvement of this trait in alfalfa has been limited due to its polyploidy, outcrossing, perennial growth nature and low heritability (Allen et al., 1985; Al-Niemi et al., 1992; Annicchiarico et al., 2015). The present study aimed to understand the mechanisms of salt tolerance in alfalfa using physiological, biochemical, and molecular approaches. The Ph.D. project utilized sand based hydroponic controlled environment experiments to study the agronomic and physiological responses of alfalfa from its germination to the flowering stage under five levels of salt stress. Modern synchrotron facilities and spectromicroscopy were used to investigate the accumulation and distribution of organic compounds and elements in leaf, stem, and root tissues of alfalfa. Furthermore, the RNA-Seq technique was deployed to find the candidate genes responsible for salt tolerance in alfalfa.

'Halo' showed higher germination percentage and seed vigor than 'Vernal' at a salt level of 16 dS m^{-1} and the shoot and root biomass yield showed a non-significant difference between the two cultivars (Chapter 3). Therefore, the first hypothesis "alfalfa cultivars with contrasting tolerance to salinity will vary in their morphological and physiological responses at germination and post germination growth and developmental stages" was partially accepted. The concentration of chloride in leaf tissue of 'Halo' was significantly lower than in 'Vernal' at 8 dS m^{-1} and 12 dS m^{-1} (Chapter 3), therefore the second hypothesis "concentration of toxic salt ions such as sodium and chloride in leaf tissue of a salt tolerant alfalfa cultivar will be significantly lower than an intolerant alfalfa cultivar" was accepted. The third hypothesis "a salt tolerant alfalfa cultivar will contain candidate genes for salt tolerance with consistent expression under salt stress" was accepted as revealed by the RNA-Seq study (Chapter 4).

There are three main mechanisms of salt tolerance in plants. First, osmotic tolerance starts immediately when the salt concentration in the root zone increases to a threshold level; this involves long distance signaling and increases osmotic adjustment. Second, ion exclusion develops over time when salt ions are transported into the plant; this involves accumulation of

toxic ions in root tissues and controlling net ion transport to leaf tissues. Finally, tissue tolerance occurs over time when toxic salt ions accumulate in shoot tissues after being deposited in the transpiration stream; this involves compartmentalization of toxic salt ions at the cellular and intracellular levels to avoid toxic concentrations in the cytoplasm (Munns and Tester, 2008; Roy et al., 2014). We found reduction in growth rate and plant height in alfalfa cultivars under osmotic stress, but non-significance difference between the two alfalfa cultivars might be due to non-limiting soil water availability as indicated by high relative leaf water content (>70%) in both alfalfa cultivars. On the other hand, salt tolerant alfalfa cultivar accumulated significantly higher amide I and II concentrations in leaf, stem and root tissues at high salinity which was found essential for osmotic adjustment. Furthermore, the distribution of amides was found concentrated in phloem tissue suggesting salt tolerance might be attributed to active transport of osmolytes for osmotic adjustments. The carbohydrates were found in xylem and phloem tissues of salt stressed stem tissue of salt tolerant alfalfa (Figure 3.5b, ii) while it was only observed in xylem tissue in intolerant alfalfa (Figure 3.5b, iv) which clearly demonstrates that salt tolerance is associated with active mobilization of carbohydrates. Leaf starch degradation was found to be important for osmotic stress tolerance in plants (Thalmann et al., 2016).

This study found that the salt tolerant alfalfa cultivar 'Halo' adopts mechanism of low ion accumulation in the shoot at 8 dS m^{-1} which is a process requiring a high energy level. Furthermore, we concluded that at 12 dS m^{-1}, the mechanism of salt tolerance was tissue tolerance. At 8 dS m^{-1} of salt stress, salt tolerant alfalfa cultivar accumulated significantly higher chlorine concentration in root tissue than leaf tissue while intolerant cultivar showed leaf tissue had significantly higher chlorine concentration than root tissue (Table 3.2). At 12 dS m^{-1} of salt stress, salt tolerant alfalfa cultivar had same concentration of chlorine in root and leaf tissue at 12 dS m^{-1} (Table 3.2). Though the exact localization of salt ions at the cellular level could not be confirmed using XRF spectromicroscopy, the mapping showed uniform distribution of chloride in both xylem and phloem tissue of stem in the salt tolerant alfalfa cultivar (Figure 3.7a, ii). We assumed that at 12 dS m^{-1} salt tolerant alfalfa cultivar is able to compartmentalize toxic salt ions in cellular and intercellular levels protecting photosynthetic apparatus. The RNA-Seq study identified more DEGs between 'Halo' and 'Vernal' in root tissue than leaf tissues; this might be because roots are the first receptor of salt stress, and the ability of plants to survive in salt stress relies on the root system (Yu et al., 2017). We found eight (leaf) and three (root) tissue specific

candidate genes as well as six common candidate genes expressed in both leaf and roots. Salt responsive genes such as *GCH*, *ERDJ2A*, *ILR2* were found highly expressed in both leaf and root tissues of salt tolerant alfalfa which are involved in osmotic adjustment and metal transport (Basset et al., 2002; Magidin et al., 2003; Fan et al., 2017). Other salt responsive genes significantly expressed in salt tolerant alfalfa were *MLP* and *DIR1*. The genes were also responsible for salt tolerance involved in signalling in other crops (Maldonado et al., 2002; Wang et al., 2016). The candidate genes identified in this study were mainly involved in osmotic tolerance, ion homeostasis, transport, and signaling. We also identified 10 novel salt responsive transcripts previously have not been reported.

This study was conducted in a sand based hydroponic system in the greenhouse, however, in field conditions crops are routinely exposed to a range of abiotic and biotic stresses, therefore, further field scale studies would be useful. This study showed non-significant variations between two cultivars for biomass yield, chlorophyll content, crude protein content, relative leaf water content for 12 weeks of growth, but further research to in field conditions and continous evaluation during regrowth period of perennial crop like alfalfa is critical to understand prolonged effect of salt stress. We found chlorine distribution in both xylem and phloem in stem tissue of both alfalfa cultivars under stress conditions, but a gap remains in our knowledge regarding anion transport under salt stress. In this study, salt stress was applied by adding NaCl, but in natural growth conditions there are multiple salt types. This study found a tissue tolerance mechanism at 12 dS m^{-1} based on physiological and morphological findings and localization of organic compounds and elements in different plant tissues. Future research to understand the localization of organic compounds and elements within cell organelles would be useful to understand the nature of toxic ion compartmentalization in salt tolerant alfalfa.

For the rapid development of salt tolerant crops, a good understanding of the salt stress physiology of plants and the discovery of candidate genes are needed (Munns and Tester, 2008). This thesis provided a comprehensive understanding of salt tolerant mechanisms in alfalfa from germination to post germination stages. This study also provided a set of genomic information including key candidate genes for salt tolerance, facilitating selection of gene for marker development. The findings of this study will contribute to the ongoing investigation of alfalfa salt stress tolerance and for the development of stress tolerant elite cultivars. The development of

alfalfa cultivars with improved tolerance to saline growth conditions will contribute to the increased productivity of marginal land and contribute to global food security.

References

Abdul-Baki, A.A., and Anderson, J.D. 1973. Vigor determination in soybean seed by multiplication. Crop Sci. 3: 630–633.

Acosta-Motos, J.R., Ortuño, M.F., Bernal-Vicente, A., Diaz-Vivancos, P., Sanchez-Blanco, M.J., and Hernandez, J.A. 2017. Plant responses to salt stress: adaptive mechanisms. Agronomy. 7: 18.

Ahi, S.M., and Powers, W.L. 1938. Salt tolerance of plants at various temperatures. Plant Physiol. 13: 767–789.

Al-Khatib, M., McNeilly, T., and Collins, J. 1992. The potential of selection and breeding for improved salt tolerance in lucerne (*Medicago sativa* L.). Euphytica. 65: 43–51.

Al-Niemi, T. S., Campbell, W. F., and Rumbaugh, M.D. 1992. Response of alfalfa cultivars to salinity during germination and post-germination growth. Crop Sci. 32: 976–980.

Allen, S.G., Dobrenz, A.K., Schonhorst, M.H., and Stoner, J.E. 1985. Heritability of NaCl tolerance in germinating alfalfa seeds. Agronomy J. 77: 99–101.

Annicchiarico, P., Barrett, B., Brummer, E.C., Julier, B., and Marshall, A.H. 2015. Achievements and challenges in improving temperate perennial forage legumes. Crit. Rev. Plant Sci. 34: 327–380.

Annunziata, M.G., Ciarmiello, L.F., Woodrow, P., Maximova, E., Fuggi, A., and Carillo, P. 2017. Durum wheat roots adapt to salinity remodeling the cellular content of nitrogen metabolites and sucrose. Front. Plant Sci. 7: 2035.

Anower, R.M., Mott, I.W., Peel, M.D., and Wu, Y. 2013. Characterization of physiological responses of two alfalfa half-sib families with improved salt tolerance. Plant Physiol. Bioch. 71: 103–111.

Apse, M.P., Aharon, G.S., Snedden, W.A., and Blumwald, E. 1999. Salt tolerance conferred by overexpression of a vacuolar Na^+/H^+ antiport in Arabidopsis. Science. 285: 1256–1258.

Araus, J.L., Kefauver, S.C., Zaman-Allah, M., Olsen, M.S., and Cairns, J.E. 2018. Translating high-throughput phenotyping into genetic gain. Trends Plant Sci. 23: 451–466.

Arshad, M., Gruber, M.Y., Wall, K., and Hannoufa, A. 2017. An insight into microRNA156 role in salinity stress responses of alfalfa. Front. Plant Sci. 8: 356.

Asensi-Fabado, M.A., and Munné-Bosch, S. 2010. Vitamins in plants: occurrence, biosynthesis and antioxidant function. Trends Plant Sci. 15:582–592.

Ashraf, M., and Foolad, M.R. 2007. Roles of glycine betaine and proline in improving plant abiotic stress resistance. Environ. Exp. Bot. 59: 206–216.

Ashraf, M., and Harris, P.J.C. 2013. Photosynthesis under stressful environment: an overview. Photosynthetica. 51: 163–190.

Ashraf, M., McNeilly, T., and Bradshaw, A.D. 1986. The response to NaCl and ionic content of selected salt-tolerant and normal lines of three legume forages species in sand culture. New Phytol. 104:463–471.

Ashrafi, E., Razmjoo, J. M., and Zahedi, M. 2018. Effect of salt stress on growth and ion accumulation of alfalfa (*Medicago sativa* L.) cultivars. J. Plant Nutr. 41: 818–831.

Ashrafi, E., Razmjoo, J., Zahedi, M., and Pessarakli, M. 2015. Screening alfalfa for salt tolerance based on lipid peroxidation and antioxidant enzymes. Agron. J. 107: 167–173.

Azhdari, G., Tavili, A., and Zare, M.A. 2010. Effects of various salts on the germination of two cultivars of *Medicago sativa*. Front. Agric. China. 4: 63–68.

Azzam, C.R., Naby, Z.M.A.E., and Mohamed, N.A. 2019. Salt tolerance associated with molecular markers in alfalfa. J. Biosci. Appl. Res. 5: 416–428.

Babakhani, B., Khavari-Nejad, R.A., Hassan Sajedi, R., Fahimi, H., and Saadatmand, S. 2011. Biochemical responses of alfalfa (*Medicago sativa* L.) cultivars subjected to NaCl salinity stress. African J. Biotechnol. 10: 11433–11441.

Bai, X., Liu, J., Tang, L., Cai, H., Chen, M., Ji, W., Liu, Y., and Zhu, Y. 2013. Overexpression of GsCBRLK from *Glycine soja* enhances tolerance to salt stress in transgenic alfalfa (*Medicago sativa*). Funct. Plant Biol. 40: 1048–1056

Bao, A.K., Wang, S.M., Wu, G.Q., Xi, J.J., Zhang, J.L., and Wang, C.M. 2009. Overexpression of the Arabidopsis H+-PPase enhanced resistance to salt and drought stress in transgenic alfalfa (*Medicago sativa* L.). Plant Sci. 176: 232–240.

Barth, A. 2007. Infrared spectroscopy of proteins. Biochim. Biophys. Acta. 1767: 1073–1101.

Basalah, M.O., and Mohammad, S. 1999. Effect of salinity and plant growth regulators on seed germination of *Medicago sativa* L. Pakistan J. Biol. Sci. 2(3): 651–653.

Basset, G., Quinlivan, E.P., Ziemak, M. J., Diaz De La Garza, R., Fischer, M., Schiffmann, S., Bacher, A., Gregory, J.F., 3rd, and Hanson, A.D. 2002. Folate synthesis in plants: the first step of the pterin branch is mediated by a unique bimodular GTP cyclohydrolase I. Proc. Natl. Acad. Sci. U S A. 99(19): 12489–12494.

Behmann, J., Steinrucken, J., and Plumer, L. 2014. Detection of early plant stress responses in hyperspectral images. ISPRS J. Photogramm. Remote Sens. 93: 98–111.

Benabderrahim, M.A., Guiza, M., and Haddad, M. 2020. Genetic diversity of salt tolerance in tetraploid alfalfa (*Medicago sativa* L.). Acta Physiol. Plant. 42: 5.

Bertrand, A., Dhont, C., Bipfubusa, M., Chalifour, F.P., Drouin, P., and Beauchamp, C.J. 2015. Improving salt stress responses of the symbiosis in alfalfa using salt-tolerant cultivar and rhizobial strain. Appl. Soil Ecol. 87: 108–117.

Bhandal, I.S., and Malik, C.P. 1998. Potassium estimation, uptake, and its role in the physiology and metabolism of flowering plant. Int. Rev. Cytol. 110: 205–254.

Bianco, C., and Defez, R. 2009. *Medicago truncatula* improves salt tolerance when nodulated by an indole-3-acetic acid-overproducing *Sinorhizobium meliloti* strain. J. Exp. Bot. 60(11): 3097–3107.

Blondon, F., Marie, D., Brown, S., and Kondorosi, A. 1994. Genome size and base composition in *Medicago sativa* and *M. truncatula* species. Genome. 37: 264–270.

Boerjan, W., Cervera, M.-T., Delarue, M., Beeckman, T., Dewitte, W., Bellini, C., Caboche, M., Van Onckelen, H., Van Montagu, M., and Inze, D. 1995. Superroot, a recessive mutation in Arabidopsis, confers auxin overproduction. Plant Cell. 7: 1405–1419.

Bohnert, H.J., and Nelson, D.E., and Jensen, R.G. 1995. Adaptation to environmental stresses. Plant Cell. 7: 1099–1111.

Bolger, A.M., Lohse, M., and Usadel, B. 2014. Trimmomatic: a flexible trimmer for Illumina sequence data. Bioinformatics. 30: 2114–2120.

Bolton, J.L. 1962. Alfalfa. botany, cultivation and utilization. Leonard Hill Ltd, London and Interscience Publishers, Inc, New York.

Burguieres, E., McCue, P., Kwon, Y.I., and Shetty, K. 2007. Effect of vitamin C and folic acid on seed vigour response and phenolic-linked antioxidant activity. Bioresour. Technol. 98:1393–1404.

Campanelli, A., Ruta, C., Morone-Fortunato, I., and De Mastro, G. 2013. Alfalfa (*Medicago sativa* L.) clones tolerant to salt stress: In vitro selection. Cent. Eur. J. Biol. 8: 765–776.

Canfax Research Services. 2020. Statistical Briefer. Available online: www.canfax.ca [19 July 2020].

Carillo, P., Cirillo, C., De Micco, V., Arena, C., De Pascale, S., and Rouphaelb, Y. 2019. Morpho-anatomical, physiological and biochemical adaptive responses to saline water of *Bougainvillea spectabilis* Willd. trained to different canopy shapes. Agric. Water Manag. 212: 12–22.

Cen, H., Wang, T., Liu, H., Tian, D., and Zhang, Y. 2020. Melatonin application improves salt tolerance of alfalfa (*Medicago sativa* L.) by enhancing antioxidant capacity. Plants. 9: 220.

Chaparzadeh, N., and Mehrnejad, F. 2013. Oxidative markers in five Iranian alfalfa (*Medicago sativa* L.) cultivars under salinity stress. Iran. J. Plant Physiol. 3: 793–799.

Chen, Z., Cuin, T.A., Zhou, M., Twomey, A., Naidu, B.P., and Shabala, S. 2007. Compatible solute accumulation and stress-mitigating effects in barley genotypes contrasting in their salt tolerance. J. Exp. Bot. 58: 4245–4255.

Cheong, J.J., and Choi, Y.D. 2003. Methyl jasmonate as a vital substance in plants. Trends Genet. 19(7): 409–413.

Coburn, F.D. 1907. The book of alfalfa: history, cultivation and merits. its uses as a forage and fertilizer. Orange Judd Co, New York.

Confalonieri, M., Faè, M., Balestrazzi, A., Donà, M., Macovei, A., Valassi, A., Giraffa, G., and Carbonera, D. 2014. Enhanced osmotic stress tolerance in Medicago truncatula plants overexpressing the DNA repair gene MtTdp2α (tyrosyl-DNA phosphodiesterase 2). Plant Cell Tissue Organ Cult. 116: 187–203.

Cornacchione, M.V., and Suarez, D.L. 2015. Emergence, forage production, and ion relations of alfalfa in response to saline waters. Crop Sci. 55: 444–457.

Cornacchione, M.V., and Suarez, D.L. 2017. Evaluation of alfalfa (*Medicago sativa* L.) populations' response to salinity stress. Crop Sci. 57:137–150.

Demsar, J., Curk, T., Erjavec, A., Gorup, C., Hocevar, T., Milutinovic, M., Mozina, M., Polajnar, M., Toplak, M., Staric, A., Stajdohar, M., Umek, L., Zagar, L., Zbontar, J., Zitnik, M., and Zupan, B. 2013. Orange: data mining toolbox in python. J. Mach. Learn. Res. 14: 2349−2353.

Duncan, W., and Williams, G. 1983. Infrared synchrotron radiation from electron storage rings. Appl. Opt. 22: 2914–2923.

Fahlgren, N., Gehan, M.A., and Baxter, I. 2015. Lights, camera, action: high-throughput plant phenotyping is ready for a close-up. Curr. Opin. Plant Biol. 24: 93–99.

Fan, F., Yang, X., Cheng, Y., Kang, Y., and Chai, X. 2017. The DnaJ gene family in pepper (*Capsicum annuum* L.): comprehensive identification, characterization and expression profiles. Front. Plant Sci. 8:689.

Fan, W., Deng, G., Wang, H., Zhang, H., and Zhang, P. 2015. Elevated compartmentalization of Na^+ into vacuoles improves salt and cold stress tolerance in sweet potato (*Ipomoea batatas*). Physiol. Plant. 154: 560–571.

FAO, IIASA, ISRIC, ISS-CSA, JRC. 2008. Harmonized World Soil Database (version 1.2), FAO, Rome, Italy and IIASA, Laxenburg, Austria.

FAO. 2005. Global network on integrated soil management for sustainable use of salt-affected soils. Rome, Italy: FAO Land and Plant Nutrition Management Service. http://www.fao.org/ag/agl/agll/spush

Feldman, M., and Levy, A.A. 2005. Allopolyploidy – a shaping force in the evolution of wheat genomes. Cytogenet Genome Res 109:250–258.

Fernandez, G.C.J. 1992. Effective selection criteria for assessing plant stress tolerance. Pages 257–270. In: Kuo, C.G. (eds) Proceedings of the international symposium on adaptation of vegetable and other food crops in temperature and water stress. AVRDC Publication, Tainan, Taiwan.

Ferreira, J.F.S., Cornacchione, M.V., Liu, X., and Suarez, D.L. 2015. Nutrient composition, forage parameters, and antioxidant capacity of alfalfa (*Medicago sativa* L.) in response to saline irrigation water. Agriculture. 5: 577–597.

Florinsky, I.V., Eilers, R.G., and Lelyk, G.W. 2000. Prediction of soil salinity risk by digital terrain modelling in the Canadian Prairies. Can. J. Soil Sci. 80: 455–463.

Flowers, T.J. 2004. Improving crop salt tolerance. J. Exp. Bot. 55: 307–319.

Flowers, T.J., Munns, R., and Colmer, T.D. 2015. Sodium chloride toxicity and the cellular basis of salt tolerance in halophytes. Ann. Bot. 115: 419–431.

Fu, Y.-B., Yang, M.H., Zeng, F., and Biligetu, B. 2017. Searching for an accurate marker-based prediction of an individual quantitative trait in molecular plant breeding. Front. Plant Sci. 8: 1182.

Gao, Y., Cui, Y., Long, R., Sun, Y., Zhang, T., Yang, Q., and Kang, J. 2019. Salt-stress induced proteomic changes of two contrasting alfalfa cultivars during germination stage. J. Sci. Food Agric. 99: 1384–1396.

Gill, N., Findley, S., Walling, J.G., Hans, C., Ma, J., Doyle, J., Stacey, G., and Jackson, S.A. 2009. Molecular and Chromosomal Evidence for Allopolyploidy in Soybean. Plant Physiology, 151 (3) 1167-1174;

Gill, S.S., and Tuteja, N. 2010. Reactive oxygen species and antioxidant machinery in abiotic stress tolerance in crop plants. Plant Physiol. Biochem. 48: 909–930.

Goplen, B.P, Baenziger, H., Bailey, L.D., Gross, A.T.H., Hanna, M.R., Michaud, R., Richards, K.W., and Waddington, J. 1982. Agriculture Canada: growing and managing alfalfa in Canada, Publication, 1705/E.

Graber, L.F. 1956. Registration of vernal alfalfa. Agronomy J. 48: 587.

Grabherr, M., Haas, B., Yassour, M., Levin, J.Z., Thompson, D.A., Amit, I., Adiconis, X., Fan, L., Raychowdhury, R., Zeng, Q., Chen, Z., Mauceli, E., Hacohen, N., Gnirke, A., Rhind, N., di Palma, F., Birren, B.W., Nusbaum, C., Lindblad-Toh, K., Friedman, N., and Regev, A. 2011. Full-length transcriptome assembly from RNA-Seq data without a reference genome. Nat. Biotechnol. 29: 644–652.

Gregorio, G.B., and Senadhira, D. 1993. Genetic analysis of salinity tolerance in rice (*Oryza sativa* L.). Theoret. Appl. Genetics. 86: 333–338.

Gruber, M., Xia, J., Yu, M., Steppuhn, H., Wall, K., Messer, D., Sharpe, A., Acharya, S., Wishart, D., Johnson, D., Miller, D., and Taheri, A. 2017. Transcript analysis in two alfalfa salt tolerance selected breeding populations relative to a non-tolerant population. Genome. 60: 104–127.

Haas, B., Papanicolaou, A., Yassour, M., Grabherr, M., Blood, P.D., Bowden, J., Couger, M.B., Eccles, D., Li, B., Lieber, M., MacManes, M.D., Ott, M., Orvis, J., Pochet, N., Strozzi, F., Weeks, N., Westerman, R., William, T., Dewey, C.N., Henschel, R., LeDuc, R.D., Friedman, N., and Regev, A. 2013. De novo transcript sequence reconstruction from RNA-seq using the Trinity platform for reference generation and analysis. Nat. Protoc. 8: 1494–1512.

Hanley, M.E., Sanders, S.K.D., Stanton, H.M., Billington, R.A., and Boden, R. 2020. A pinch of salt: Response of coastal grassland plants to simulated seawater inundation treatments. Ann. Bot. 125: 265–275.

Haq, S.U., Khan, A., Ali, M., Khattak, A.M., Gai, W.X., Zhang, H.X., Wei, A.M., and Gong, Z.H. 2019. Heat Shock Proteins: Dynamic biomolecules to counter plant biotic and abiotic stresses. Int. J. Mol. Sci. 20(21): 5321.

Hasegawa, P.M., Bressan, R.A., Zhu, J.K., and Bohnert, H.J. 2000. Plant cellular and molecular responses to high salinity. Annu. Rev. Plant Mol. Plant Physiol. 51: 463–499.

Hellebust, J. A. 1976. Osmoregulation. Annu. Rev. Plant Physiol. 27: 485–505.

Hoagland, D.R., and Arnon, D.L. 1950. The water-culture method for growing plants without soil. Calif. Agric. Exp. Stn. Cir. 347.

Hsiao, T.C., and Xu, L.K. 2000. Sensitivity of growth of roots versus leaves to water stress: Biophysical analysis and relation to water transport. J. Exp. Bot. 51: 1595–1616.

Iqbal, M., Ashraf, M., and Jamil, A. 2006. Seed enhancement with cytokinins: changes in growth and grain yield in salt stressed wheat plants. Plant Growth Regul. 50: 29−39

Jain, M., Tiwary, S., and Gadre, R. 2010. Sorbitol-induced changes in various growth and biochemical parameters in maize. Plant Soil Environ. 56: 263–267.

Jiang, J., Yang, B.L., Xia, T., Yu, S.M., Wu, Y.N., Jin, H., and Li, J.R. 2015b. Analysis of genetic diversity of salt-tolerant alfalfa germplasms. Genet. Mol. Res. 14: 4438–4447.

Jiang, Y., Lahlali, R., Karunakaran, C., Kumar, S., Davis, A.R., and Bueckert, R.A. 2015a. Seed set, pollen morphology and pollen surface composition response to heat stress in field pea. Plant Cell Environ. 38: 2387–2397.

Jin T., Chang Q., Li W., Yin D., Li Z., Wang D., Liu, B., and Liu, L. 2010b. Stress-inducible expression of GmDREB1 conferred salt tolerance in transgenic alfalfa. Plant Cell Tissue Organ Cult. 100 219–227.

Jin, H., Sun, Y., Yang, Q., Chao, Y., Kang, J., Jin, H., Li, Y., and Margaret, G. 2010a. Screening of genes induced by salt stress from alfalfa. Mol. Biol. Rep. 37: 745–753.

Johnson, D.W., Smith, S.E., and Dobrenz, A.K. 1992. Selection for increased forage yield in alfalfa at different NaCl levels. Euphytica. 60: 27–35.

Julier, B., Flajoulot, S., Barre, P., and Cardinet, G. 2003. Construction of two genetic linkage maps in cultivated tetraploid alfalfa (*Medicago sativa*) using microsatellite and AFLP markers. BMC Plant Biol. 3: 9.

Kacurakova, M., Capek, P., Sasinkova, V., Wellner, N., and Ebringerova, A. 2000. FT-IR study of plant cell wall model compounds: pectic polysaccharides and hemicelluloses. Carbohyd. Polym. 43: 195–203.

Kafi, M., Stewart, W.S., and Borland, A.M. 2003. Carbohydrate and proline contents in leaves, roots, and apices of salt-tolerant and salt-sensitive wheat cultivars. Russ. J. Plant Physiol. 50(2): 155–162.

Kalu, B.A., and Fick, G.W. 1981. Quantifying morphological development of alfalfa for studies of herbage quality. Crop Sci. 21: 267–271.

Kapulnik, Y., Teuber, L.R., and Phillips, D.A. 1989. Lucerne (*Medicago sativa* L.) selected for vigor in a nonsaline environment maintained growth under salt stress. Crop Pasture Sci. 40: 1253–1259.

Kassas, M. 1987. Seven paths to desertification. Desert. Control Bull. 15: 24–26.

Katerji, N., Mastrorillib, M., Lahmerc, F.Z., and Oweis, T. 2012. Emergence rate as a potential indicator of crop salt-tolerance. Europ. J. Agronomy. 38: 1–9.

Keller, C.K., and Van der Kamp, G. 1988. Hydrogeology of two Saskatchewan tills: II. Occurrence of sulfate and implications for salinity. J. Hydrol. 101: 123–144.
Khan, M.G., Silberbush, M., and Lips, S.H. 1994. Physiological study on salinity and nitrogen interaction in alfalfa II photosystem and transpiration. J. Plant Nutr. 17: 669–684.
Khavarinejad, R.A., and Chaparzadeh, N. 1998. The effects of NaCl and CaCl2 on photosynthesis and growth of alfalfa plants. Photosynthetica. 35: 461–466.
Kilic, S., and Aca, H.T. 2016. Role of exogenous folic acid in alleviation of morphological and anatomical inhibition on salinity-induced stress in barley. Ital. J. Agron. 11(4): 246–251.
Kumar, S., Beena, A.S., Awana, M., and Singh, A. 2017. Salt-induced tissue-specific cytosine methylation downregulates expression of HKT genes in contrasting wheat (*Triticum aestivum* L.) genotypes. DNA Cell Biol. 36: 283–294.
Lahlali, R., Jiang, Y., Kumar, S., Karunakaran, C., Liu, X., Borondics, F., Hallin, E., and Bueckert, R. 2014. ATR-FTIR spectroscopy reveals involvement of lipids and proteins of intact pea pollen grains to heat stress tolerance. Front. Plant Sci. 5: 747.
Lahlali, R., Karunakaran, C., Wang, L., Willick, I., Schmidt, M., Liu, X., Borondics, F., Forseille, L., Fobert, P.R., Tanino, K., Peng, G., and Hallin, E. 2015. Synchrotron based phase contrast X-ray imaging combined with FTIR spectroscopy reveals structural and biomolecular differences in spikelets play a significant role in resistance to Fusarium in wheat. BMC Plant Biol. 15: 24.
Lahlali, R., Kumar, S., Wang, L., Forseille, L., Sylvain, N., Korbas, M., Muir, D., Swerhone, G., Lawrence, J.R., Fobert, P.R., Peng, G., and Karunakaran, C. 2016. Cell wall biomolecular composition plays a potential role in the host type II resistance to Fusarium head blight in wheat. Front. Microbiol. 7: 910.
Langmead, B., Trapnell, C., Pop, M., and Salzberg, S. 2009. Ultrafast and memory-efficient alignment of short DNA sequences to the human genome. Genome Biol. 10: 25.
Lauchli, A., and Grattan, S.R. 2007. Plant growth and development under salinity stress. Pages 1–32. In: Jenks, M.A., Hasegawa, P.M., and Jain, S.M. (eds) Advances in molecular breeding toward drought and salt tolerant crops. Springer, Dordrecht, the Netherlands.
Lee, G., Carrow, R.N., Duncan, R.R. Eiteman, M.A., and Rieger, W. 2008. Synthesis of organic osmolytes and salt tolerance mechanisms in *Paspalum vaginatum*. Environ. Exp. Bot. 63: 19–27.
Lei, Y., Hannoufa, A., Christensen, D., Shi, H., Prates, L.L., and Yu, P. 2018b. Molecular structural changes in alfalfa detected by ATR-FTIR spectroscopy in response to silencing of TT8 and HB12 genes. Int. J. Mol. Sci. 19: 1046.
Lei, Y., Xu, Y., Hettenhausen, C., Lu, C., Shen, G., Zhang, C., Li, J., Song, J., Lin, H., and Wu, J. 2018a. Comparative analysis of alfalfa (*Medicago sativa* L.) leaf transcriptomes reveals genotype-specific salt tolerance mechanisms. BMC Plant Biol. 18: 35.
Lesins, K.A., and Lesins, I. 1979. Genus *Medicago* (Leguminosae): A taxogenetic study. Dr. W. Junk by, The Hague, The Netherlands, p. 228.
Li, B., and Dewey, C. 2011. RSEM: Accurate transcript quantification from RNA-Seq data with or without a reference genome. BMC Bioinform.12: 323.
Li, H., Wang, Z., Ke, Q., Ji, C.Y., Jeong, J.C., Lee, H., Lim., Y.P., Xu, B., Deng X.P., and Kwak, S.S. 2014. Overexpression of codA gene confers enhanced tolerance to abiotic stresses in alfalfa. Plant Physiol Biochem. 85: 31–40.

Li, R., Shi, F., Fukuda, K., and Yang, Y. 2010. Effects of salt and alkali stresses on germination, growth, photosynthesis and ion accumulation in alfalfa (*Medicago sativa* L.). Soil Sci. Plant Nutr. 56(5): 725–733.

Li, W., Wang, D., Jin, T., Chang, Q., Yin, D., Xu, S., Liu, B., and Liu, L. 2011. The Vacuolar Na+/H+ antiporter gene SsNHX1from the halophyte salsola soda confers salt tolerance in transgenic alfalfa (*Medicago sativa* L.). Plant Mol. Biol. Report. 29: 278–290

Liu, J., Ishitani, M., Halfter, U., Kim, C.S., and Zhu, J.K. 2000. The Arabidopsis thaliana SOS2 gene encodes a protein kinase that is required for salt tolerance. Proc. Natl. Acad. Sci. U S A. 97(7): 3730–3734.

Liu, N., Karunakaran, C., Lahlali, R., Warkentin, T., and Bueckert, R.A. 2019b. Genotypic and heat stress effects on leaf cuticles of field pea using ATR-FTIR spectroscopy. Planta. 249(2): 601–613.

Liu, X.-P., and Yu, L.-X. 2017. Genome-wide association mapping of loci associated with plant growth and forage production under salt stress in alfalfa (*Medicago sativa* L.). Front Plant Sci. 8: 853.

Liu, X.P., Hawkins, C., Peel, M.D., and Yu, L.X. 2019a. Genetic loci associated with salt tolerance in advanced breeding populations of tetraploid alfalfa using genome wide association studies. Plant Genome. 12: 180026.

Liu, Z., Chen, T., Ma, L., Zhao, Z., Zhao, P.X., Nan, Z., and Wang, Y. 2013. Global Transcriptome sequencing using the illumina platform and the development of EST-SSR markers in autotetraploid alfalfa. PLoS ONE 8(12): e83549.

Liu, Z.P., Yang, Q. C., Hu, T. M., and Yan, L. F. 2006. Genetic diversity of autotetraploid alfalfa with different salt-tolerant traits based on SSR marker analysis. Acta Agron. Sin. 32: 630–632.

Llanes, A., Reinoso, H., and Luna, V. 2005. Germination and early growth of *Prosopis strombulifera* seedlings in different saline solutions. World J. Agric. Sci. 1: 120–128

Long, R., Li, M., Zhang, T., Kang, J., Sun, Y., Cong, L., Gao, Y., Liu, F., and Yang, Q. 2016. Comparative proteomic analysis reveals differential root proteins in *Medicago sativa* and *Medicago truncatula* in response to salt stress. Front. Plant Sci. 7: 424.

Longhese, M.P., Plevani, P., and Lucchini, G. 1994. Replication factor A is required in vivo for DNA replication, repair, and recombination. Mol. Cell. Biol. 14(12): 7884–7890.

Luo, D., Zhou, Q., Wu, Y.G., Chai, X.T., Liu, W.X., Wang, Y.R., Yang, Q.C., Wang, Z.Y., and Liu, Z.P. 2019. Full length transcript sequencing and comparative transcriptomic analysis to evaluate the contribution of osmotic and ionic stress components towards salinity tolerance in the roots of cultivated alfalfa (*Medicago sativa* L.). BMC Plant Biol. 19: 32.

Luo, M., Cheng, K., Xu, Y., Yang, S., and Wu, K. 2017. Plant Responses to Abiotic Stress Regulated by Histone Deacetylases. Frontiers in plant science. 8: 2147.

Lv, S., Jiang, P., Chen, X., Fan, P., Wang, X., and Li, Y. 2012. Multiple compartmentalization of sodium conferred salt tolerance in *Salicornia europaea*. Plant Physiol. Bioch. 51: 47–52.

Maas, E.V., and Hoffman, G.J. 1977. Crop salt tolerance-current assessment. J. Irrig. Drain. Div. 103: 115–134.

Magidin, M., Pittman, J.K., Hirschi, K.D., and Bartel, B. 2003. ILR2, a novel gene regulating IAA conjugate sensitivity and metal transport in Arabidopsis thaliana. Plant J. 35: 523–534.

Magome, H., Yamaguchi, S., Hanada, A., Kamiya, Y., and Odadoi, K. 2004. Dwarf and delayed-flowering 1, a novel *Arabidopsis* mutant deficient in gibberellin biosynthesis because of over expression of a putative AP2 transcription factor. Plant J. 37: 720–729.

Maldonado, A.M., Doerner, P., Dixon, R.A., Lamb, C.J., and Cameron R.K. 2002. A putative lipid transfer protein involved in systemic resistance signalling in Arabidopsis. Nature. 419: 399–403.

Mansour, M. 2000. Nitrogen containing compounds and adaptation of plants to salinity stress. Biologia Plantarum 43: 491–500.

Marschner, H. 1995. Mineral nutrition of higher plants. London: Academic Press.

Martinez, J., and Manzur, C.L. 2005. Overview of salinity problems in the world and FAO strategies to address the problem. Proceedings of the international salinity forum. Riverside, California. p. 311–313.

McKimmie, T., and A.K. Dobrenz. 1991. Ionic concentrations and water relations of alfalfa seedlings differing in salt tolerance. Agron. J. 83: 363–367.

Meuwissen, T.H., Hayes, B.J., and Goddard, M.E. 2001. Prediction of total genetic value using genome-wide dense marker maps. Genetics. 157: 1819–1829.

Mezni, M., Albouchi, A., Bizid, E., and Hamza, M. 2010. Minerals uptake, organic osmotica contents and water balance in alfalfa under salt stress. J. Phytol. 2: 1–12.

Munns, R. 1992. A leaf elongation assay detects an unknown growth inhibitor in xylem sap from wheat and barley. Aust. J. Plant Physiol. 19: 127–135.

Munns, R. 2002. Comparative physiology of salt and water stress. Plant Cell Environ. 25: 239–250.

Munns, R. 2005. Genes and salt tolerance: Bringing them together. New Phytol. 167: 654–663.

Munns, R., and James, R.A. 2003. Screening methods for salinity tolerance: A case study with tetraploid wheat. Plant Soil. 253: 201–218.

Munns, R., and Tester, M. 2008. Mechanisms of salinity tolerance. Annu. Rev. Plant Biol. 59: 651–681.

Munns, R., Greenway, H., Delane, R., and Gibbs, J. 1982. Ion concentration and carbohydrate status of the elongating leaf tissue of *Hordeum vulgare* growing at high external NaCl. II. Cause of the growth reduction. J. Exp. Bot. 33: 574–83.

Munns, R., James, R.A., and Lauchli, A. 2006. Approaches to increasing the salt tolerance of wheat and other cereals. J. Exp. Bot. 57: 1025–1043.

National Alfalfa and Forage Alliance. 2020. Alfalfa variety ratings. 2020. Available online: https://www.alfalfa.org/pdf/2020_Alfalfa_Variety_Leaflet.pdf [15 January 2020].

Naumann, J.C., Young, D.R., and Anderson, J.E. 2009. Spatial variations in salinity stress across a coastal landscape using vegetation indices derived from hyperspectral imagery. Plant Ecol. 202: 285–297.

Peel, M.D., Waldron, B.L., Jensen, K.B., Chatterton, N.J., Horton, H., and Dudley, L.M. 2004. Screening for salinity tolerance in alfalfa. Crop Sci. 44: 2049–2053.

Pessarakli, M., Huber, T.C., and Nakabayashi, K. 1991. Growth response of barley and wheat to salt stress. J. Plant Nutr. 14: 331–340.

Postnikova, O.A., Shao, J., and Nemchinov, L.G. 2013. Analysis of the alfalfa root transcriptome in response to salinity stress. Plant Cell Physiol. 54: 1041–1055.

Quan, W.L., Liu, X., Wang, H.Q., and Chan, Z.L. 2016. Physiological and transcriptional responses of contrasting alfalfa (*Medicago sativa* L.) varieties to salt stress. Plant Cell Tissue Organ Cult. 126: 105–115.

Rahayu, Y.S., Walch-Liu, P., Neumann, G., von Wirén, N., and Bangerth, F. 2005. Root-derived cytokinins as long-distance signals for NO_3^- induced stimulation of leaf growth. J. Exp. Bot. 56: 1143–1152.

Rahman, M.A., Alam, I., Kim, Y.G., Ahn, N.Y., Heo, S.H., Lee, D.G., Liu, G., and Lee, B.H. 2015. Screening for salt responsive proteins in two contrasting alfalfa cultivars using a comparative proteome approach. Plant Physiol. Biochem. 89: 112–122.

Ramagopal S. 1987a. Salinity stress induced tissue-specific proteins in barley seedling. Plant Physiol. 84: 324–331.

Ramagopal S. 1987b. Differential mRNA transcription during salinity stress in barley. Proc. Natl. Acad. Sci. U S A. 84: 94–98.

Rathert, G. 1984. Sucrose and starch content of plant parts as a possible indicator for salt tolerance of crops. Aust. J. Plant Physiol. 11: 491–495.

Rengasamy, P. 2002. Transient salinity and subsoil constraints to dryland farming in Australian sodic soils: An overview. Aust. J. Exp. Agric. 42: 351–361.

Robinson, M.D., McCarthy, D.J., and Smyth, G.K. 2010. edgeR: A Bioconductor package for differential expression analysis of digital gene expression data. Bioinformatics. 26: 139–140.

Robinson, P.H., Grattan, S.R., Getachew, G., Grieve, C.M., Poss, J.A., Suarez, D.L., and Benes, S.E. 2004. Biomass accumulation and potential nutritive value of some forages irrigated with saline-sodic drainage water. Anim. Feed Sci. Technol. 111: 175–189.

Romer, C., Wahabzada, M., Ballvora, A., Pinto, F., Rossini, M., Panigada, C., Behmann, J., Léon, J., Thurau, C., Bauckhage, C., Kersting, K., Rascher, U., and Plumer, L. 2012. Early drought stress detection in cereals: Simplex volume maximisation for hyperspectral image analysis. Funct. Plant Biol. 39: 878–890.

Roy, S.J., Negrão, S., and Tester, M. 2014. Salt resistant crop plants. Curr. Opin. Biotechnol. 26: 115–124.

Ryu, H., and Cho, Y.G. 2015. Plant hormones in salt stress tolerance. J. Plant Biol. 58: 147–155.

Sanders D. 2020. The salinity challenge. New Phytol. 225(3): 1047–1048.

Sandhu, D., Cornacchione, M.V., Ferreira, J.F.S., and Suarez, D.L. 2017. Variable salinity responses of 12 alfalfa genotypes and comparative expression analyses of salt-response genes. Sci. Rep. 7: 42958.

Schachtman, D., and Liu, W.H. 1999. Molecular pieces to the puzzle of the interaction between potassium and sodium uptake in plants. Trends Plant Sci. 4: 282–287.

Schmieder, R., and Edwards, R. 2011. Quality control and preprocessing of metagenomic datasets. Bioinformatics. 27: 863–864.

Shannon, M.C., Grieve, C.M., and Francois, L.E. 1994. Whole-plant response to salinity. In: R. E. Wilkinson, ed. Handbook of plant-environment interactions. Marcel Dekker Inc., New York, NY. p. 199–244.

Shen, Q., Fu, L., Qiu, L., Xue, F., Zhang, G., and Wu, D. 2016. Time course of ionic responses and proteomic analysis of a Tibetan wild barley at early stage under salt stress. Plant Growth Regul. 81: 1–11.

Shone, M.G.T., and Gale, J. 1983. Effects of sodium chloride stress and nitrogen source on respiration, growth and photosynthesis in lucerne (*Medicaqo sativa* L.). J. Exp. Bot. 34: 1117–1125.

Shrivastava, P., and Kumar, R. 2015. Soil salinity: A serious environmental issue and plant growth promoting bacteria as one of the tools for its alleviation. Saudi J. Biol. Sci. 22: 123–131.
Sibole, J.V., Cabot, C., Poschenrieder, C., and Barcelo, J. 2003. Ion allocation in two different salt-tolerant Mediterranean *Medicago* species. J. Plant Physiol. 160: 1361–1365.
Smethurst, C.F., Rix, K., Garnett, T., Auricht, G., Bayart, A., Lane, P., Wilson, S.J., and Shabala, S. 2008. Multiple traits associated with salt tolerance in lucerne: Revealing the underlying cellular mechanisms. Funct. Plant Biol. 35: 640–650.
Smith, S.E. 1993. Salinity and the production of alfalfa (*Medicago sativa* L.). In: Pessarakli, M., (eds) Handbook of Crop Stress. Marcel Dekker, Inc., New York. p. 431–448.
Sole, V.A., Papillon, E., Cotte, M., Walter, P., and Susini, J. 2007. A multiplatform code for the analysis of energy-dispersive X-ray fluorescence spectra. Spectrochim. Acta -Part B At. Spectrosc. 62: 63–68.
Soltani, A., Khodarahmpour, Z., Jafari, A.A., and Nakhjavan, S. 2012. Selection of alfalfa (*Medicago sativa* L.) cultivars for salt stress tolerance using germination indices. Afr. J. Biotechnol. 11: 7899–7905.
Soltanpour, P.N., Ippolito, J.A., Rodriguez, J.B., Self, J., Gillaume, M., Al-Wardy, M.M., and Mathews, D. 1999. Chloride versus sulfate salinity effects on alfalfa shoot growth and ionic balance. Soil Sci. Soc. Am. J. 63: 111–116.
Statistics Canada. 2016. Census of Agriculture, Hay and Field Crops. Table 32-10-0416-01. Available online: http://www.statcan.gc.ca/eng [5 February 2020].
Steppuhn, H. 1996. What is soil salinity? Pages 1–5. In: Proceedings Soil Salinity Assessment Workshop, Alberta Agriculture, March 1996, Lethbridge, AB.
Steppuhn, H., Acharya, S.N., Iwaasa, A.D., Gruber, M., and Miller, D.R. 2012. Inherent responses to root-zone salinity in nine alfalfa populations. Can. J. Plant Sci. 92: 235–248.
Suyama, H., Benes, S.E., Robinson, P.H., Grattan, S.R., Grieve, C.M., and Getachew, G. 2007. Forage yield and quality under irrigation with saline-sodic drainage water: Greenhouse evaluation. Agric. Water Manage. 88: 159–172.
Sytar, O., Brestic, M., Zivcak, M., Olsovska, K., Kovar, M., Shao, H.B., and He, X.L. 2017. Applying hyperspectral imaging to explore natural plant diversity towards improving salt stress tolerance. Sci. Total Environ. 578: 90–99.
Szabolcs, I. 1989. Salt-affected soils. CRC Press, Boca Raton, FL.
Tang, L., Cai, H., Ji, W., Luo, X., Wang, Z., Wu, J., Wang, X., Cui, L., Wang, Y., Zhu, Y., and Bai, X. 2013. Overexpression of GsZFP1enhances salt and drought tolerance in transgenic alfalfa (*Medicago sativa* L.). Plant Physiol. Biochem. 71: 22–30
Tang, L., Cai, H., Zhai, H., Luo, X., Wang, Z., Cui, L., and Bai, X. 2014. Overexpression of *Glycine soja* WRKY20 enhances both drought and salt tolerance in transgenic alfalfa (*Medicago sativa* L.). Plant Cell Tissue Organ Cult. 118: 77–86.
Tanji, K.K. 1990. Nature and extent of agricultural salinity. Pages 1–13. In: Tanji, K.K. (eds) Agricultural Salinity Assessment and Management. Am. Soc. Civil Engineers, New York.
Teakle, N.L., and Tyerman, S.D. 2010. Mechanisms of Cl- transport contributing to salt tolerance. Plant, Cell and Environment 33: 566–589.
Thalmann, M., Pazmino, D., Seung, D., Horrer, D., Nigro, A., Meier, T., Kölling, K., Pfeifhofer, H.W., Zeeman, S.C., and Santelia, D. 2016. Regulation of leaf starch degradation by

abscisic acid is important for osmotic stress tolerance in plants. Plant Cell. 28: 1860–1878.
Thomas, D.S.G., and Middleton, N.J. 1993. Salinization: new perspectives on a major desertification issue. J. Arid Environ. 24: 95–105.
Tilbrook, J., and Roy, S.J. 2014. Salinity tolerance. In Jenks, M.A., Hasewaga, P.M. (eds) Plant abiotic stress. Second edition. Wiley-Blackwell, New York. p. 134–178.
Tiwari, R., and Mamrutha, H.M. 2013. Precision phenotyping for mapping of traits for abiotic stress tolerance in crops. In: Salar, R., Gahlawat, S., Siwach, P., Duhan, J. (eds) Biotechnology: Prospects and Applications. Springer, New Delhi.
Tootoonchi, M., and Gettys, L.A. 2019. Testing salt stress on aquatic plants: Effect of salt source and substrate. Aquat. Ecol. 53: 325–334.
Torabi, M., and Halim, M.R.A. 2010. Variation of root and shoot growth and free proline accumulation in Iranian alfalfa ecotypes under salt stress. J. Food Agric. Environ. 8: 323–327.
Türker-Kaya, S., and Huck, C. 2017. A review of mid-infrared and near-infrared imaging: Principles, concepts and applications in plant tissue analysis. Molecules. 22(1): 168.
Tuteja, N. 2007. Mechanisms of high salinity tolerance in plants. Methods Enzymol. 428: 419–138.
USDA–NASS. 2018. Crop production 2018 summary. Available online: http://www.nass.usda.gov [9 February 2020].
Valizadeh, M., Moharamnejad, S., Ahmadi, M., and Jalaly, H.M. 2013. Changes in activity profile of some antioxidant enzymes in alfalfa half-sib families under salt stress. J. Agr. Sci. Tech. 15: 801–809.
van der Werf, A., and Nagel, O.W. 1996. Carbon allocation to shoots and roots in relation to nitrogen supply is mediated by cytokinins and sucrose: Opinion. Plant and Soil. 185: 21–32.
Vijayan, P., Willick, I.R., Lahlali, R., Karunakaran, C., and Tanino, K.K. 2015. Synchrotron radiation sheds fresh light on plant research: The use of powerful techniques to probe structure and composition of plants. Plant Cell Physiol. 56: 1252–1263.
Villarino, G.H., Hu, Q., Scanlon, M.J., Mueller, L., Bombarely, A., and Mattson, N.S. 2017. Dissecting tissue-specific transcriptomic responses from leaf and roots under salt stress in *Petunia hybrida* Mitchell. Genes. 8: 195.
Wang, X.S., and Han, J.G. 2007. Effects of NaCl and silicon on ion distribution in the roots, shoots and leaves of two alfalfa cultivars with different salt tolerance. Soil Sci. Plant Nutr. 53: 278–285.
Wang, X.S., and Han, J.G. 2009. Changes of proline content, activity, and active isoforms of antioxidative enzymes in two alfalfa cultivars under salt stress. Agric. Sci. China. 8: 431–440.
Wang, Y., Yang, L., Chen, X., Ye, T., Zhong, B., Liu, R., Wu, Y., and Chan, Z. 2016. Major latex protein-like protein 43 (MLP43) functions as a positive regulator during abscisic acid responses and confers drought tolerance in *Arabidopsis thaliana*, J. Exp. Bot. 67: 421–434.
Wang, Z., Li, H., Ke, Q., Jeong, J.C., Lee, H.S., Xu, B., Deng, X.P., Lim Y.P., and Kwak, S.S. 2014. Transgenic alfalfa plants expressing AtNDPK2 exhibit increased growth and tolerance to abiotic stresses. Plant Physiol. Biochem. 84: 67–77.

Wei, T.J., Jiang, C.J., Jin, Y.Y., Zhang, G.H., Wang, M.M., and Liang, Z.W. 2020. Ca2+/Na+ ratio as a critical marker for field evaluation of saline-alkaline tolerance in alfalfa (*Medicago sativa* L.). Agronomy. 10(2): 191.

Wetzel, D.L., Srivarin, P., and Finney, J.R. 2003. Revealing protein infrared spectral detail in a heterogeneous matrix dominated by starch. Vib. Spectrosc. 31: 109–114.

Wiebe, B.H., Eilers, R.G., Eilers, W.D., and Brierley, J.A. 2007. Application of a risk indicator for assessing trends in dryland salinization risk on the Canadian Prairies. Can. J. Soil Sci. 87: 213–224.

Willick, I.R., Lahlali, R., Vijayan, P., Muir, D., Karunakaran, C., and Tanino, K.K. 2017. Wheat flag leaf epicuticular wax morphology and composition in response to moderate drought stress are revealed by SEM, FTIR-ATR and synchrotron X-ray spectroscopy. Physiol. Plant. 162: 316–332.

Winicov, I. 2000. Alfin1 transcription factor overexpression enhances plant root growth under normal and saline conditions and improves salt tolerance in alfalfa. Planta. 210(3): 416–422.

Wu, D., Shen, Q., Cai, S., Chen, Z.H., Dai, F., and Zhang, G. 2013. Ionomic responses and correlations between elements and metabolites under salt stress in wild and cultivated barley. Plant Cell Physiol. 54: 1976–1988.

Wu, S.J., Ding, L., and Zhu, J.K. 1996. SOS1, a genetic locus essential for salt tolerance and potassium acquisition. Plant Cell. 8: 617–627.

Xiong, J., Sun, Y., Yang, Q., Tian, H., Zhang, H., Liu, Y., and Chen, M. 2017. Proteomic analysis of early salt stress responsive proteins in alfalfa roots and shoots. Proteome Sci. 15: 19.

Yacoubi, R., Job, C., Belghazi, M., Chaibi, W., and Job, D. 2013. Proteomic analysis of the enhancement of seed vigour in osmo-primed alfalfa seeds germinated under salinity stress. Seed Sci. Res. 23: 99–110.

Younesi, O., and Moradi, A. 2014. Effect of priming of seeds of *Medicago sativa* 'Bami' with gibberellic acid on germination, seedlings growth and antioxidant enzymes activity under salinity stress. J. Hortic. Res. 22(2): 167–174.

Yu, L., Ma, J., Niu, Z., Bai, X., Lei, W., Shao, X., Chen, N., Zhou, F., and Wan, D. 2017. Tissue-specific transcriptome analysis reveals multiple responses to salt stress in *Populus euphratica* seedlings. Genes. 8: 372.

Yu, L.X., Liu, X., Boge, W., and Liu, X.P. 2016. Genome-wide association study identifies loci for salt tolerance during germination in autotetraploid alfalfa (*Medicago sativa* L.) using genotyping-by-sequencing. Front. Plant Sci. 7: 956.

Yuegao, H., and Cash, D. 2009. Global status and development trends of alfalfa. In: Cash D, editor. Alfalfa Management. Guide For Ningxia. Beijing, China: United Nations Food and Agriculture Organization, p. 1–14.

Zeng, F., Biligetu, B., Coulman, B., Schellenberg, M.P., and Fu, Y.-B. 2017. RNA-seq analysis of plant maturity in crested wheatgrass (*Agropyron cristatum* L.). Genes. 8(11): 291.

Zhang, L.Q., Niu, Y.D., Huridu H., Hao, J.F., Qi, Z., and Hasi, A. 2014b. *Salicornia europaea* L. Na+/H+ antiporter gene improves salt tolerance in transgenic alfalfa (*Medicago sativa* L.). Genet. Mol. Res. 13: 5350–5360.

Zhang, Q., Ma, C., Xue, X., Xu, M., Li, J., and Wu, J.X. 2014a. Overexpression of a cytosolic ascorbate peroxidase gene, OsAPX2, increases salt tolerance in transgenic Alfalfa. J. Integr. Agric. 13(11): 2500–2507.

Zhang, T., Yu, L.-X., Zheng, P., Li, Y., Rivera, M., Main, D., and Greene, S.L. 2015. Identification of loci associated with drought resistance traits in heterozygous autotetraploid alfalfa (*Medicago sativa* L.) using genome-wide association studies with genotyping by sequencing. PLoS One. 10: e0138931.

Zhang, Y.M., Liu, Z.H., Wen, Z.Y., Zhang, H.M., Yang, F., and Guo, X.L. 2012. The vacuolar Na+/H+ antiport geneTaNHX2 confers salt tolerance on transgenic alfalfa (*Medicago sativa* L.). Funct. Plant Biol. 39: 708–716.

Zhichang, Z., Wanrong, Z., Jinping, Y., Jianjun, Z., Zhen, L., Xufeng, L., and Yang, Y. 2010. Over-expression of *Arabidopsis* DnaJ (Hsp40) contributes to NaCl-stress tolerance. Afr. J. Biotechnol. 9: 972–978.

Zhu, J.K., Liu, J.P., and Xiong, L.M. 1998. Genetic analysis of salt tolerance in *Arabidopsis*: Evidence for a critical role of potassium nutrition. Plant Cell. 10: 1181–1191.

Appendices

Appendix A.1. Heatmap of top 10 differentially expressed genes in each sample showing variations in biological and technical replicates.
Each column represents an experimental sample and each row represents a gene. Expression differences are shown in different colors. Purple means low expression and yellow means high expression.

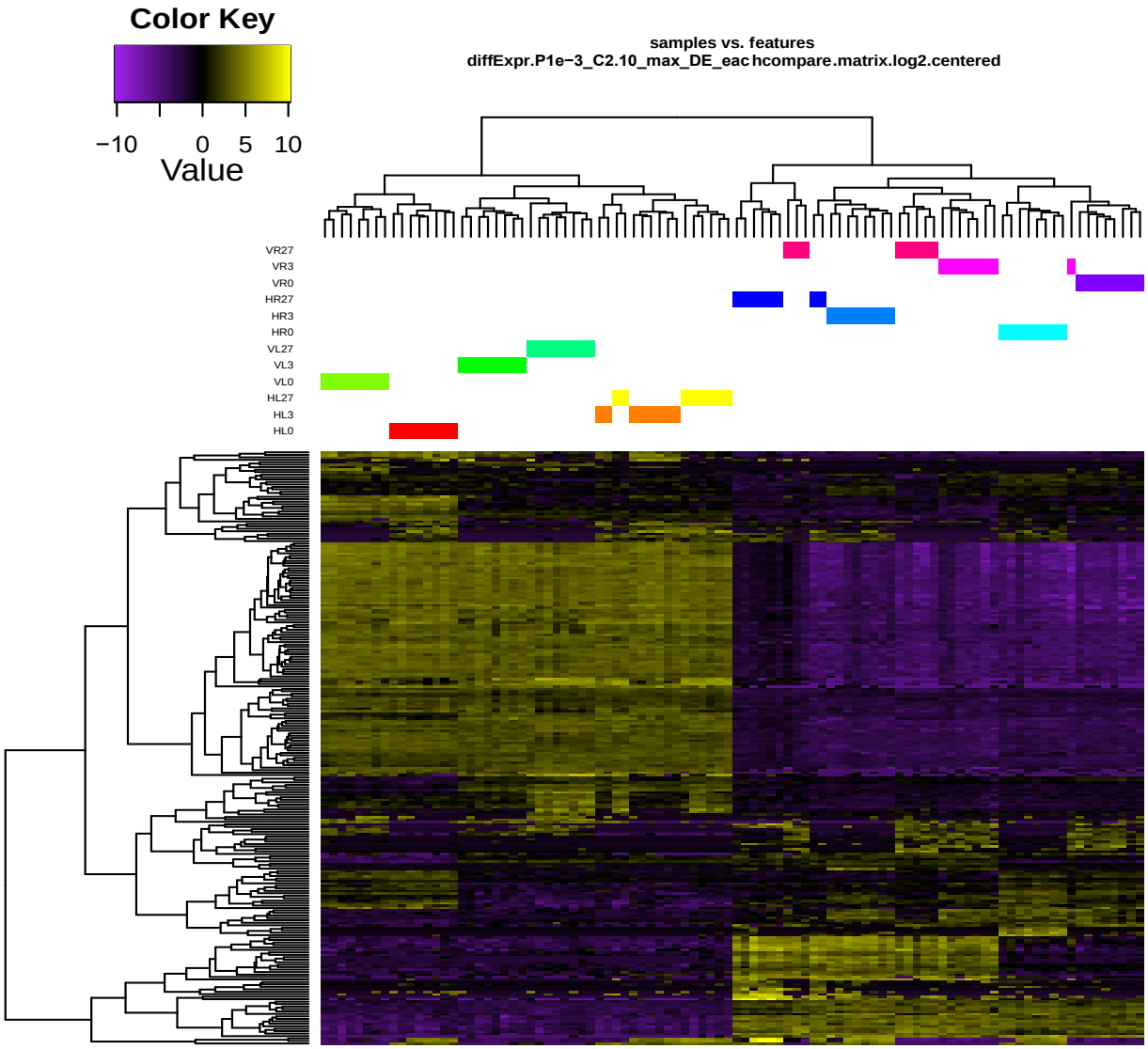

Appendix A.2. List of differentially expressed genes in leaf tissue at control (0h), 3h, 27h of salt stress between salt tolerant 'Halo' and salt intolerant 'Vernal' cultivars of alfalfa.

Time (h)	Gene ID	Putative function[1]	Nr ID[2]	Halo	
				log_2FC[3]	FDR[4]
0	TRINITY_DN13099_c1_g1	NA	NA	10.50	1.32E-27
0	TRINITY_DN3671_c0_g1	histone H2A.6-like [*Arachis duranensis*]	XP_015953769.1	8.51	9.12E-06
0	TRINITY_DN13099_c0_g1	NA	NA	8.12	6.74E-16
0	TRINITY_DN1680_c0_g1	NA	NA	8.03	1.43E-14
0	TRINITY_DN274030_c0_g1	DNA gyrase subunit B, putative [*Medicago truncatula*]	AES88004.1	7.97	3.40E-04
0	TRINITY_DN12165_c0_g1	GTP cyclohydrolase [*Arachis hypogaea*]	QHO24156.1	7.95	3.99E-04
0	TRINITY_DN2746_c0_g1	hypothetical protein MTR_1g064590 [*Medicago truncatula*]	KEH42243.1	7.83	1.30E-05
0	TRINITY_DN4000_c0_g1	putative non-specific serine/threonine protein kinase [*Medicago truncatula*]	RHN41153.1	7.39	3.99E-04
0	TRINITY_DN165162_c0_g1	NA	NA	7.30	3.99E-04
0	TRINITY_DN10576_c0_g1	dnaJ protein ERDJ2A [*Medicago truncatula*]	XP_024632012.1	7.09	5.81E-12
0	TRINITY_DN4396_c1_g1	NA	NA	7.08	1.50E-11
0	TRINITY_DN462_c0_g2	ribosomal RNA small subunit methyltransferase nep-1 [*Medicago truncatula*]	XP_013454067.1	7.07	4.39E-04
0	TRINITY_DN26158_c0_g1	uncharacterized protein LOC112416619 [*Medicago truncatula*]	XP_024626645.1	6.80	5.83E-04
0	TRINITY_DN13735_c0_g1	putative F-box domain-containing protein [*Medicago truncatula*]	RHN73861.1	6.39	1.34E-04
0	TRINITY_DN270143_c0_g1	NA	NA	6.06	8.35E-04
0	TRINITY_DN34220_c0_g1	replication factor A protein [*Trifolium pratense*]	PNY01153.1	5.98	2.87E-05
0	TRINITY_DN13850_c0_g1	transcription factor bHLH128 isoform X1 [*Medicago truncatula*]	XP_003592849.1	5.94	5.09E-05
0	TRINITY_DN16575_c0_g1	protein IAA-LEUCINE RESISTANT 2 [*Trifolium medium*]	MCI04234.1	5.87	4.39E-04

0	TRINITY_DN3009_c1_g1	hypothetical protein TSUD_215660 [*Trifolium subterraneum*]	GAU27755.1	5.15	4.97E-04
0	TRINITY_DN8029_c0_g1	hypothetical protein MTR_6g465600 [*Medicago truncatula*]	KEH26597.1	4.03	1.10E-04
0	TRINITY_DN27543_c0_g1	retrovirus-related Pol polyprotein from transposon TNT 1-94 [*Trifolium pratense*]	PNX92270.1	3.26	4.39E-04
0	TRINITY_DN7561_c0_g1	NA	NA	2.46	7.98E-04
0	TRINITY_DN7669_c0_g1	cationic amino acid transporter 4, vacuolar isoform X1 [*Medicago truncatula*]	XP_024641709.1	-2.09	6.61E-04
0	TRINITY_DN17685_c0_g1	plant/F12A21-30 protein, putative [*Medicago truncatula*]	KEH35275.1	-2.49	3.99E-04
0	TRINITY_DN1302_c0_g1	uncharacterized methyltransferase At1g78140, chloroplastic [*Medicago truncatula*]	XP_013460874.1	-3.09	1.30E-05
0	TRINITY_DN34621_c1_g1	putative transferase, protein kinase RLK-Pelle-LRR-I-1 family [*Medicago truncatula*]	RHN39207.1	-3.20	2.57E-05
0	TRINITY_DN304_c0_g1	Integrase, catalytic region; Zinc finger, CCHC-type; Peptidase aspartic, catalytic [*Medicago truncatula*]	ABD32582.1	-3.36	1.71E-06
0	TRINITY_DN18229_c1_g3	NA	NA	-3.85	6.61E-04
0	TRINITY_DN1205_c0_g1	probable glutathione S-transferase [*Medicago truncatula*]	XP_003623174.1	-4.62	4.39E-04
0	TRINITY_DN69117_c0_g1	SAUR-like auxin-responsive family protein [*Medicago truncatula*]	AES89345.1	-5.57	1.95E-05
0	TRINITY_DN18428_c0_g1	NA	NA	-5.65	3.94E-05
0	TRINITY_DN8352_c0_g1	receptor-like protein EIX2 [*Medicago truncatula*]	XP_003627996.3	-6.01	3.99E-04
0	TRINITY_DN44_c1_g1	replication protein A 70 kDa protein [*Medicago truncatula*]	KEH32028.1	-6.85	1.32E-04
0	TRINITY_DN7794_c0_g1	replication factor A protein 1 [*Medicago truncatula*]	XP_003616287.1	-6.92	1.35E-14
0	TRINITY_DN168591_c0_g1	hypothetical protein TSUD_124940 [*Trifolium subterraneum*]	GAU18661.1	-7.42	3.68E-07

0	TRINITY_DN3690_c0_g1	NADP-dependent alkenal double bond reductase P1-like [*Trifolium medium*]	MCH87509.1	-7.62	9.34E-04
0	TRINITY_DN211142_c0_g1	NA	NA	-7.86	4.84E-04
0	TRINITY_DN31671_c0_g1	GDSL esterase/lipase At1g29670 isoform X4 [*Medicago truncatula*]	XP_024631729.1	-7.87	2.05E-09
0	TRINITY_DN14543_c0_g1	NA	NA	-8.46	6.61E-04
3	TRINITY_DN3671_c0_g1	histone H2A.6-like [*Arachis duranensis*]	XP_015953769.1	9.20	7.62E-05
3	TRINITY_DN153727_c0_g1	NA	NA	8.81	8.32E-05
3	TRINITY_DN12165_c0_g1	GTP cyclohydrolase [*Arachis hypogaea*]	QHO24156.1	8.75	8.25E-05
3	TRINITY_DN3732_c0_g1	putative lipid-transfer protein DIR1 [*Vigna radiata* var. *radiata*]	XP_014492609.1	8.73	2.10E-23
3	TRINITY_DN16210_c0_g1	MLP-like protein [*Trifolium pratense*]	PNX89162.1	8.65	7.62E-05
3	TRINITY_DN40709_c0_g1	seed linoleate 9S-lipoxygenase [*Medicago truncatula*]	XP_013444392.1	8.62	9.42E-05
3	TRINITY_DN165162_c0_g1	NA	NA	8.51	1.94E-04
3	TRINITY_DN10576_c0_g1	dnaJ protein ERDJ2A [*Medicago truncatula*]	XP_024632012.1	8.08	5.75E-14
3	TRINITY_DN274030_c0_g1	DNA gyrase subunit B, putative [*Medicago truncatula*]	AES88004.1	7.91	4.03E-05
3	TRINITY_DN4396_c1_g1	NA	NA	7.75	3.84E-10
3	TRINITY_DN270143_c0_g1	NA	NA	7.50	2.79E-09
3	TRINITY_DN10425_c2_g2	shaggy-like kinase [*Medicago truncatula*]	KEH23337.1	7.47	9.00E-04
3	TRINITY_DN16575_c0_g1	protein IAA-LEUCINE RESISTANT 2 [*Trifolium medium*]	MCI04234.1	7.36	3.84E-10
3	TRINITY_DN13099_c0_g1	NA	NA	7.33	2.99E-08
3	TRINITY_DN462_c0_g2	ribosomal RNA small subunit methyltransferase nep-1 [*Medicago truncatula*]	XP_013454067.1	7.19	4.35E-04
3	TRINITY_DN28868_c0_g1	receptor-like protein kinase At3g21340 isoform X5 [*Medicago truncatula*]	XP_024627896.1	7.18	3.68E-04
3	TRINITY_DN11343_c0_g1	polyubiquitin 3 [*Medicago truncatula*]	AES82697.1	7.12	5.31E-04
3	TRINITY_DN4000_c0_g1	putative non-specific serine/threonine protein kinase [*Medicago truncatula*]	RHN41153.1	7.09	6.00E-04

3	TRINITY_DN19570_c0_g1	probable LRR receptor-like serine/threonine-protein kinase At3g47570 [*Medicago truncatula*]	XP_003616606.1	7.05	7.03E-04
3	TRINITY_DN205405_c0_g1	threonine--tRNA ligase, mitochondrial 1 [*Medicago truncatula*]	XP_003613276.1	6.99	7.05E-04
3	TRINITY_DN2664_c0_g1	NA	NA	6.80	1.33E-06
3	TRINITY_DN26083_c0_g1	uncharacterized protein LOC11405977 isoform X1 [*Medicago truncatula*]	XP_003613312.3	6.23	8.32E-05
3	TRINITY_DN26158_c0_g1	uncharacterized protein LOC112416619 [*Medicago truncatula*]	XP_024626645.1	6.19	9.00E-04
3	TRINITY_DN129905_c0_g1	NA	NA	5.52	1.69E-06
3	TRINITY_DN9868_c0_g1	F-box/kelch-repeat protein At3g06240 [*Medicago truncatula*]	XP_013442975.1	5.39	2.21E-04
3	TRINITY_DN24_c8_g1	LEAF RUST 10 DISEASE-RESISTANCE LOCUS RECEPTOR-LIKE PROTEIN KINASE-like 1.2 isoform X2 [*Cicer arietinum*]	XP_004512900.1	5.35	5.38E-04
3	TRINITY_DN34220_c0_g1	replication factor A protein [*Trifolium pratense*]	PNY01153.1	5.22	1.26E-05
3	TRINITY_DN5865_c0_g1	uncharacterized protein LOC101494494 isoform X4 [*Cicer arietinum*]	XP_012571787.1	3.86	4.46E-05
3	TRINITY_DN34892_c0_g1	NA	NA	3.78	1.90E-04
3	TRINITY_DN2466_c0_g1	transmembrane protein, putative [*Medicago truncatula*]	AES79519.2	2.99	1.42E-04
3	TRINITY_DN944_c0_g1	endochitinase [*Medicago truncatula*]	XP_003629191.3	2.29	1.69E-06
3	TRINITY_DN15802_c0_g1	uncharacterized protein LOC11438954 [*Medicago truncatula*]	XP_003601780.1	-2.08	1.42E-05
3	TRINITY_DN7515_c0_g1	NA	NA	-2.59	5.91E-04
3	TRINITY_DN1302_c0_g1	uncharacterized methyltransferase At1g78140, chloroplastic [*Medicago truncatula*]	XP_013460874.1	-2.99	1.85E-04

3	TRINITY_DN17030_c0_g1	putative 1-phosphatidylinositol-3-phosphate 5-kinase FAB1D isoform X2 [*Vigna radiata* var. *radiata*]	XP_014513696.1	-3.02	2.53E-04
3	TRINITY_DN789_c0_g1	two-component response regulator [*Medicago truncatula*]	KEH35774.1	-3.19	1.42E-04
3	TRINITY_DN4121_c0_g1	putative calcium-transporting ATPase 13, plasma membrane-type [*Vigna unguiculata*]	XP_027917970.1	-3.46	9.18E-04
3	TRINITY_DN7715_c0_g1	probable cytokinin riboside 5'-monophosphate phosphoribohydrolase LOGL10 [*Medicago truncatula*]	XP_003603739.1	-3.67	7.83E-05
3	TRINITY_DN69117_c0_g1	SAUR-like auxin-responsive family protein [*Medicago truncatula*]	AES89345.1	-4.44	2.39E-04
3	TRINITY_DN1205_c0_g1	probable glutathione S-transferase [*Medicago truncatula*]	XP_003623174.1	-5.26	2.35E-05
3	TRINITY_DN15482_c0_g1	alpha-amylase, putative [*Medicago truncatula*]	KEH25578.1	-5.40	1.51E-05
3	TRINITY_DN17276_c0_g1	PREDICTED: transcription factor MYB108-like isoform X2 [*Lupinus angustifolius*]	XP_019432290.1	-5.64	4.56E-07
3	TRINITY_DN7238_c0_g1	uncharacterized protein ECU03_1610 [*Medicago truncatula*]	XP_003593603.1	-5.85	2.23E-05
3	TRINITY_DN42634_c0_g1	replication protein A 70 kDa DNA-binding subunit [*Trifolium pratense*]	PNX99377.1	-6.41	5.31E-04
3	TRINITY_DN7794_c0_g1	replication factor A protein 1 [*Medicago truncatula*]	XP_003616287.1	-6.62	1.47E-08
3	TRINITY_DN4715_c0_g1	uncharacterized protein LOC25493757 [*Medicago truncatula*]	XP_013457801.1	-6.89	4.35E-04
3	TRINITY_DN18_c0_g1	UPF0481 protein At3g47200 [*Medicago truncatula*]	XP_003618477.1	-7.07	2.86E-05
3	TRINITY_DN159_c0_g1	dihydrolipoyl dehydrogenase 2, chloroplastic isoform X1 [*Medicago truncatula*]	XP_003594783.1	-7.48	1.90E-04
3	TRINITY_DN11592_c0_g1	hypothetical protein MtrunA17_Chr6g0468321 [*Medicago truncatula*]	RHN51417.1	-7.98	1.89E-04

3	TRINITY_DN7434_c0_g2	transmembrane protein, putative [*Medicago truncatula*]	AES92409.1	-9.87	7.26E-04
27	TRINITY_DN3671_c0_g1	histone H2A.6-like [*Arachis duranensis*]	XP_015953769.1	9.54	5.45E-05
27	TRINITY_DN13099_c0_g1	NA	NA	8.71	4.99E-16
27	TRINITY_DN153727_c0_g1	NA	NA	8.65	5.28E-05
27	TRINITY_DN165162_c0_g1	NA	NA	8.43	6.57E-05
27	TRINITY_DN270143_c0_g1	NA	NA	8.42	7.41E-10
27	TRINITY_DN274030_c0_g1	DNA gyrase subunit B, putative [*Medicago truncatula*]	AES88004.1	8.14	6.69E-06
27	TRINITY_DN12165_c0_g1	GTP cyclohydrolase [*Arachis hypogaea*]	QHO24156.1	8.08	1.16E-04
27	TRINITY_DN16575_c0_g1	protein IAA-LEUCINE RESISTANT 2 [*Trifolium medium*]	MCI04234.1	7.98	2.41E-10
27	TRINITY_DN462_c0_g2	ribosomal RNA small subunit methyltransferase nep-1 [*Medicago truncatula*]	XP_013454067.1	7.66	1.31E-04
27	TRINITY_DN4000_c0_g1	putative non-specific serine/threonine protein kinase [*Medicago truncatula*]	RHN41153.1	7.66	2.82E-04
27	TRINITY_DN25886_c0_g1	hypothetical protein MtrunA17_Chr6g0479881 [*Medicago truncatula*]	RHN52380.1	7.54	3.85E-04
27	TRINITY_DN36828_c0_g1	beta-amylase 3, chloroplastic [*Medicago truncatula*]	XP_003611408.1	7.52	5.44E-04
27	TRINITY_DN13735_c0_g1	putative F-box domain-containing protein [*Medicago truncatula*]	RHN73861.1	7.08	7.85E-05
27	TRINITY_DN10576_c0_g1	dnaJ protein ERDJ2A [*Medicago truncatula*]	XP_024632012.1	6.83	8.76E-14
27	TRINITY_DN18634_c1_g1	NA	NA	6.22	1.27E-04
27	TRINITY_DN129905_c0_g1	NA	NA	6.11	3.26E-04
27	TRINITY_DN9436_c1_g2	replication factor-A carboxy-terminal domain protein [*Medicago truncatula*]	AET03044.2	6.03	8.88E-05
27	TRINITY_DN62284_c0_g1	mitochondrial Rho GTPase 1 [*Medicago truncatula*]	XP_003591106.1	5.98	6.98E-07
27	TRINITY_DN34220_c0_g1	replication factor A protein [*Trifolium pratense*]	PNY01153.1	5.60	1.46E-06

27	TRINITY_DN2664_c0_g1	NA	NA	5.22	3.11E-08
27	TRINITY_DN41421_c0_g1	hypothetical protein MtrunA17_Chr7g0220081 [*Medicago truncatula*]	RHN44499.1	3.64	7.89E-04
27	TRINITY_DN1725_c0_g1	uncharacterized protein LOC11441722 [*Medicago truncatula*]	XP_003609992.1	-2.01	9.56E-04
27	TRINITY_DN15802_c0_g1	uncharacterized protein LOC11438954 [*Medicago truncatula*]	XP_003601780.1	-2.06	4.53E-05
27	TRINITY_DN35504_c0_g1	glutamyl-tRNA reductase 1 chloroplastic-like [*Trifolium medium*]	MCI22368.1	-2.24	3.85E-06
27	TRINITY_DN1302_c0_g1	uncharacterized methyltransferase At1g78140, chloroplastic [*M. truncatula*]	XP_013460874.1	-2.29	1.86E-05
27	TRINITY_DN31838_c0_g1	hypothetical protein MTR_3g081560 [*Medicago truncatula*]	KEH35199.1	-3.07	1.15E-04
27	TRINITY_DN3109_c0_g1	glutathione S-transferase [*Medicago truncatula*]	XP_003589566.1	-3.59	2.56E-04
27	TRINITY_DN367_c3_g1	hypothetical protein MTR_1g492690 [*Medicago truncatula*]	KEH43411.1	-3.65	3.26E-04
27	TRINITY_DN98502_c0_g1	gibberellin 2-beta-dioxygenase 8 [*Medicago truncatula*]	XP_003596636.2	-3.75	5.44E-04
27	TRINITY_DN15247_c0_g1	uncharacterized protein LOC112705385 [*Arachis hypogaea*]	XP_025612003.1	-3.79	9.50E-04
27	TRINITY_DN3918_c0_g1	uncharacterized protein LOC112419870 [*Medicago truncatula*]	XP_024633687.1	-3.87	4.72E-05
27	TRINITY_DN6788_c0_g4	peroxidase P7 [*Medicago truncatula*]	XP_003602462.1	-4.08	9.55E-04
27	TRINITY_DN34621_c1_g1	putative transferase, protein kinase RLK-Pelle-LRR-I-1 family [*Medicago truncatula*]	RHN39207.1	-4.88	3.70E-12
27	TRINITY_DN4715_c0_g1	uncharacterized protein LOC25493757 [*Medicago truncatula*]	XP_013457801.1	-5.10	9.94E-04
27	TRINITY_DN712_c0_g1	transmembrane protein, putative [*Medicago truncatula*]	KEH28562.1	-5.18	1.51E-05

27	TRINITY_DN14924_c1_g1	hypothetical protein MtrunA17_Chr7g0246661 [*Medicago truncatula*]	RHN46852.1	-5.37	8.88E-05
27	TRINITY_DN22638_c0_g1	peroxidase 15 isoform X2 [*Medicago truncatula*]	XP_013463006.1	-5.56	3.98E-04
27	TRINITY_DN36028_c0_g1	NA	NA	-5.57	6.45E-04
27	TRINITY_DN7238_c0_g1	uncharacterized protein ECU03_1610 [*Medicago truncatula*]	XP_003593603.1	-5.68	6.94E-06
27	TRINITY_DN2809_c0_g3	BURP domain-containing protein BNM2A [*Medicago truncatula*]	XP_003620537.1	-6.00	1.97E-06
27	TRINITY_DN7715_c0_g1	probable cytokinin riboside 5'-monophosphate phosphoribohydrolase LOGL10 [*Medicago truncatula*]	XP_003603739.1	-6.02	5.61E-08
27	TRINITY_DN63_c0_g1	hypothetical protein MTR_6g087780 [*Medicago truncatula*]	KEH27136.1	-6.19	3.85E-04
27	TRINITY_DN6387_c3_g1	transmembrane protein, putative [*Medicago truncatula*]	AES62829.2	-6.28	3.36E-05
27	TRINITY_DN69117_c0_g1	SAUR-like auxin-responsive family protein [*Medicago truncatula*]	AES89345.1	-6.28	6.47E-07
27	TRINITY_DN34249_c0_g1	ubiquitin 5 [*Cicer arietinum*]	NP_001352098.1	-6.33	6.69E-06
27	TRINITY_DN18_c0_g1	UPF0481 protein At3g47200 [*Medicago truncatula*]	XP_003618477.1	-6.35	1.86E-05
27	TRINITY_DN7794_c0_g1	replication factor A protein 1 [*M. truncatula*]	XP_003616287.1	-6.68	6.47E-07
27	TRINITY_DN42634_c0_g1	replication protein A 70 kDa DNA-binding subunit [*Trifolium pratense*]	PNX99377.1	-6.72	2.10E-04
27	TRINITY_DN17508_c0_g1	WAT1-related protein At5g40240-like [*Medicago truncatula*]	XP_024641358.1	-6.89	9.61E-04
27	TRINITY_DN1205_c0_g1	probable glutathione S-transferase [*Medicago truncatula*]	XP_003623174.1	-6.93	1.17E-08
27	TRINITY_DN8121_c0_g1	phospholipid hydroperoxide glutathione peroxidase [*Medicago truncatula*]	AET04997.2	-6.94	9.61E-04
27	TRINITY_DN17954_c0_g1	transcriptional repressor ILP1 [*Medicago truncatula*]	XP_003610832.1	-7.13	6.45E-04

27	TRINITY_DN8211_c0_g2	hypothetical protein MTR_3g060650 [*Medicago truncatula*]	AES70638.1	-7.16	9.49E-04
27	TRINITY_DN364_c0_g1	60S ribosomal protein L34-like [*Cicer arietinum*]	XP_004509966.1	-7.40	2.10E-09
27	TRINITY_DN1811_c2_g1	uncharacterized protein LOC102667171 [*Glycine max*]	XP_006580479.1	-7.44	2.16E-04
27	TRINITY_DN7617_c1_g1	hypothetical protein MTR_0475s0040 [*Medicago truncatula*]	KEH15872.1	-7.59	1.59E-04
27	TRINITY_DN171_c0_g1	NA	NA	-7.92	1.12E-05
27	TRINITY_DN28816_c0_g1	unknown [*Medicago truncatula*]	ACJ86307.1	-8.03	7.06E-09
27	TRINITY_DN10073_c0_g1	hypothetical protein DEO72_LG1g2315 [*Vigna unguiculata*]	QCD78679.1	-8.15	2.82E-04
27	TRINITY_DN2988_c0_g1	putative leucine-rich repeat domain, L domain-containing protein [*Medicago truncatula*]	RHN66971.1	-8.17	3.38E-04
27	TRINITY_DN168591_c0_g1	hypothetical protein TSUD_124940 [*Trifolium subterraneum*]	GAU18661.1	-8.20	2.82E-04
27	TRINITY_DN24998_c0_g1	PREDICTED: probable galacturonosyltransferase 6 [*Lupinus angustifolius*]	XP_019456475.1	-8.35	1.06E-04
27	TRINITY_DN3690_c0_g1	NADP-dependent alkenal double bond reductase P1-like [*Trifolium medium*]	MCH87509.1	-8.36	2.52E-04
27	TRINITY_DN211615_c0_g1	putative protein-synthesizing GTPase [*Medicago truncatula*]	RHN50622.1	-8.56	5.45E-05
27	TRINITY_DN8176_c0_g1	phosphomethylpyrimidine synthase, chloroplastic isoform X3 [*Medicago truncatula*]	XP_024634968.1	-8.95	2.11E-19
27	TRINITY_DN7434_c0_g2	transmembrane protein, putative [*Medicago truncatula*]	AES92409.1	-9.55	3.85E-04

[1]NA represents no homology retrieved upon performing BLASTX.
[2]Nr ID is the protein accession number in NCBI non redundant protein database.
[3]$\log_2$FC stands for log Fold Change, where it is log base 2.
[4]FDR stands for false discovery rate.

Appendix A.3. List of differentially expressed genes in root tissue at control (0h), 3h, 27h of salt stress between salt tolerant 'Halo' and salt intolerant 'Vernal' cultivars of alfalfa.

Time (h)	Gene ID	Putative function[1]	Nr ID[2]	Halo	Vernal
				log_2FC[3]	FDR[4]
0	TRINITY_DN13099_c1_g1	NA	NA	11.10	8.81E-50
0	TRINITY_DN12165_c0_g1	GTP cyclohydrolase [*Arachis hypogaea*]	QHO24156.1	9.31	6.05E-05
0	TRINITY_DN34404_c0_g1	UDP-glycosyltransferase 87A1 [*Medicago truncatula*]	XP_003615830.1	8.87	2.65E-05
0	TRINITY_DN4396_c2_g1	NA	NA	8.55	6.45E-05
0	TRINITY_DN3909_c0_g1	hypothetical protein MtrunA17_Chr2g0290231 [*Medicago truncatula*]	RHN72664.1	8.39	5.74E-05
0	TRINITY_DN23236_c0_g1	Elongation factor 1-alpha [*Lupinus albus*]	KAE9588919.1	8.33	1.31E-14
0	TRINITY_DN13099_c0_g1	NA	NA	8.25	3.11E-11
0	TRINITY_DN16575_c0_g1	protein IAA-LEUCINE RESISTANT 2 [*Trifolium medium*]	MCI04234.1	8.11	2.98E-08
0	TRINITY_DN462_c0_g2	ribosomal RNA small subunit methyltransferase nep-1 [*Medicago truncatula*]	XP_013454067.1	8.06	2.06E-04
0	TRINITY_DN270143_c0_g1	NA	NA	7.72	6.46E-07
0	TRINITY_DN63699_c0_g1	60S ribosomal protein L5 isoform B [*Glycine soja*]	RZB83260.1	7.45	2.39E-04
0	TRINITY_DN26083_c0_g1	uncharacterized protein LOC11405977 isoform X1 [*Medicago truncatula*]	XP_003613312.3	7.32	3.18E-05
0	TRINITY_DN80388_c0_g1	unknown [*Lotus japonicus*]	AFK44937.1	7.31	7.89E-07
0	TRINITY_DN13735_c0_g1	putative F-box domain-containing protein [*Medicago truncatula*]	RHN73861.1	7.01	9.83E-05
0	TRINITY_DN64224_c0_g1	PREDICTED: 40S ribosomal protein S13-like [*Lupinus angustifolius*]	XP_019445342.1	6.98	7.96E-10
0	TRINITY_DN203065_c0_g1	NA	NA	6.98	5.90E-04
0	TRINITY_DN153727_c0_g1	NA	NA	6.97	8.90E-05
0	TRINITY_DN7742_c0_g1	glutathione S-transferase F9 [*Medicago truncatula*]	XP_003617377.1	6.96	5.37E-04

0	TRINITY_DN274030_c0_g1	DNA gyrase subunit B, putative [*Medicago truncatula*]	AES88004.1	6.84	1.35E-04
0	TRINITY_DN72564_c0_g1	ribonuclease P protein subunit p25-like protein isoform X2 [*Cajanus cajan*]	XP_020212223.1	6.63	6.96E-06
0	TRINITY_DN9641_c1_g1	hypothetical protein MtrunA17_Chr2g0293921 [*Medicago truncatula*]	RHN73014.1	6.62	9.63E-04
0	TRINITY_DN10576_c0_g1	dnaJ protein ERDJ2A [*Medicago truncatula*]	XP_024632012.1	6.59	5.31E-15
0	TRINITY_DN25388_c0_g1	NA	NA	6.56	1.31E-04
0	TRINITY_DN87377_c0_g1	40S ribosomal protein S19-1 [*Arachis duranensis*]	XP_015946175.1	6.37	1.39E-06
0	TRINITY_DN10425_c1_g3	unknown [*Medicago truncatula*]	ACJ84779.1	6.32	1.18E-05
0	TRINITY_DN16271_c0_g1	serine carboxypeptidase-like 50 [*Medicago truncatula*]	XP_003617939.1	6.06	2.92E-04
0	TRINITY_DN8840_c0_g1	hypothetical protein E2542_SST21712 [*Spatholobus suberectus*]	TKY57266.1	6.06	3.49E-05
0	TRINITY_DN150256_c0_g1	NA	NA	5.91	8.55E-04
0	TRINITY_DN179897_c0_g1	NA	NA	5.88	2.74E-04
0	TRINITY_DN43225_c0_g1	NA	NA	5.84	7.01E-04
0	TRINITY_DN59254_c0_g2	NA	NA	5.80	7.41E-05
0	TRINITY_DN22187_c1_g3	cathepsin B-like protease 2 [*Arachis ipaensis*]	XP_016205660.1	5.57	3.46E-04
0	TRINITY_DN42116_c0_g1	hypothetical protein TSUD_382410 [*Trifolium subterraneum*]	GAU50776.1	5.57	8.02E-06
0	TRINITY_DN40669_c0_g1	tubulin beta chain [*Prosopis alba*]	XP_028806218.1	5.46	8.59E-06
0	TRINITY_DN119871_c0_g1	NA	NA	5.35	3.90E-05
0	TRINITY_DN12177_c0_g1	NA	NA	5.34	6.24E-04
0	TRINITY_DN18582_c2_g1	heat shock cognate 70 kDa protein 2 [*Arachis duranensis*]	XP_015952265.1	5.20	6.17E-05
0	TRINITY_DN24521_c0_g1	pyrophosphate-energized vacuolar membrane proton pump isoform X1 [*Arachis hypogaea*]	XP_025618926.1	5.12	3.92E-06
0	TRINITY_DN218078_c0_g1	NA	NA	5.09	2.13E-05
0	TRINITY_DN25982_c0_g1	organelle RRM domain-containing protein 6, chloroplastic [*Vigna radiata* var. *radiata*]	XP_014511794.1	5.08	8.54E-04

0	TRINITY_DN62284_c0_g1	mitochondrial Rho GTPase 1 [*Medicago truncatula*]	XP_003591106.1	5.06	9.82E-05
0	TRINITY_DN4844_c1_g1	NA	NA	5.03	6.76E-05
0	TRINITY_DN11783_c0_g1	60S acidic ribosomal protein P2-2-like [*Cajanus cajan*]	XP_020230602.1	5.00	1.55E-04
0	TRINITY_DN18820_c0_g1	Thiol protease SEN102 family [*Cajanus cajan*]	KYP68548.1	4.99	1.64E-04
0	TRINITY_DN181961_c0_g1	NA	NA	4.93	6.46E-07
0	TRINITY_DN19276_c0_g1	Tubulin beta-1 chain [*Glycine soja*]	KHN39147.1	4.90	1.47E-04
0	TRINITY_DN151538_c0_g1	cathepsin B-like protease 2 [*Vigna unguiculata*]	XP_027920507.1	4.87	6.45E-05
0	TRINITY_DN181834_c0_g1	NA	NA	4.84	1.33E-06
0	TRINITY_DN182964_c0_g1	NA	NA	4.82	1.37E-06
0	TRINITY_DN6728_c0_g1	unknown [*Lotus japonicus*]	AFK39823.1	4.79	2.57E-04
0	TRINITY_DN120349_c0_g1	eukaryotic translation initiation factor 5A-like [*Prosopis alba*]	XP_028803634.1	4.75	2.31E-04
0	TRINITY_DN2619_c4_g1	Elongation factor 1-alpha isoform C [*Glycine soja*]	RZB57532.1	4.73	7.73E-05
0	TRINITY_DN183372_c0_g1	60S ribosomal protein L7a [*Glycine soja*]	KHN15384.1	4.66	8.96E-04
0	TRINITY_DN12381_c0_g3	hypothetical protein TSUD_262640 [*Trifolium subterraneum*]	GAU13937.1	4.65	9.95E-08
0	TRINITY_DN243863_c0_g1	40S ribosomal protein S2-3 [*Spatholobus suberectus*]	TKY60984.1	4.57	2.65E-04
0	TRINITY_DN3229_c0_g1	NA	NA	4.56	6.61E-05
0	TRINITY_DN3037_c1_g1	putative ribosomal protein L21e [*Lupinus albus*]	KAE9621707.1	4.50	8.35E-05
0	TRINITY_DN79427_c0_g1	hypothetical protein PHAVU_008G187000g [*Phaseolus vulgaris*]	XP_007141334.1	4.40	6.16E-05
0	TRINITY_DN18582_c0_g1	heat shock 70 kDa protein [*Arachis duranensis*]	XP_015933068.1	4.29	6.20E-05
0	TRINITY_DN18534_c0_g1	cathepsin B-like protease 2 [*Prosopis alba*]	XP_028770964.1	4.28	3.27E-04
0	TRINITY_DN4602_c0_g1	elongation factor 2 [*Prosopis alba*]	XP_028799560.1	4.23	9.21E-04

0	TRINITY_DN33091_c0_g3	ADP, ATP carrier protein 1, mitochondrial isoform X3 [*Vigna radiata* var. *radiata*]	XP_014497934.1	4.23	2.50E-04
0	TRINITY_DN211987_c0_g1	putative ribosomal protein L11/L12 [*Lupinus albus*]	KAE9587950.1	4.15	2.44E-07
0	TRINITY_DN1461_c0_g1	putative leucine-rich repeat-containing, plant-type, leucine-rich repeat domain, L [*Medicago truncatula*]	RHN81975.1	4.12	9.69E-04
0	TRINITY_DN4602_c0_g2	elongation factor 2 [*Vigna unguiculata*]	XP_027928201.1	4.10	1.07E-04
0	TRINITY_DN6685_c0_g1	NA	NA	3.78	2.60E-04
0	TRINITY_DN1118_c0_g2	hypothetical protein LR48_Vigan04g102600 [*Vigna angularis*]	KOM40828.1	3.61	6.59E-05
0	TRINITY_DN2874_c0_g2	abscisic acid receptor PYL4 [*Medicago truncatula*]	XP_003600988.1	2.59	1.32E-06
0	TRINITY_DN5681_c0_g1	DNA replication licensing factor MCM6 isoform X1 [*Medicago truncatula*]	XP_013463311.1	2.48	9.74E-05
0	TRINITY_DN3511_c0_g2	uncharacterized protein LOC25496853 [*Medicago truncatula*]	XP_013453016.1	2.15	9.21E-04
0	TRINITY_DN2557_c0_g1	MACPF domain-containing protein At4g24290 isoform X1 [*Medicago truncatula*]	XP_003630397.1	2.13	3.37E-05
0	TRINITY_DN1302_c0_g1	uncharacterized methyltransferase At1g78140, chloroplastic [*Medicago truncatula*]	XP_013460874.1	-3.73	2.41E-04
0	TRINITY_DN42073_c0_g2	40S ribosomal protein S6 [*Arachis duranensis*]	XP_015956447.1	-4.00	9.52E-04
0	TRINITY_DN3554_c2_g1	60S ribosomal protein L7a-1 [*Prosopis alba*]	XP_028798094.1	-4.04	9.21E-04
0	TRINITY_DN241613_c0_g1	60S ribosomal protein L32-1 [*Medicago truncatula*]	XP_003629717.1	-4.27	1.11E-04
0	TRINITY_DN8119_c0_g1	ribulose bisphosphate carboxylase small chain clone 512-like [*Abrus precatorius*]	XP_027332320.1	-4.49	5.11E-08
0	TRINITY_DN21682_c0_g1	PREDICTED: uncharacterized protein LOC108334719 isoform X1 [*Vigna angularis*]	XP_017426129.1	-4.61	1.07E-04

0	TRINITY_DN151004_c0_g1	40S ribosomal protein S14-like [*Prosopis alba*]	XP_028787038.1	-4.74	5.44E-04
0	TRINITY_DN1151_c2_g1	tubulin alpha-4 chain-like protein [*Trifolium pratense*]	PNX75403.1	-4.77	3.27E-12
0	TRINITY_DN182920_c0_g1	putative chlorophyll A-B binding protein [*Lupinus albus*]	KAE9592472.1	-4.78	9.53E-05
0	TRINITY_DN51410_c0_g1	Photosystem I reaction center subunit III [*Spatholobus suberectus*]	TKY55048.1	-4.87	5.44E-04
0	TRINITY_DN151360_c0_g1	ferredoxin-like [*Vigna unguiculata*]	XP_027931956.1	-4.89	1.63E-04
0	TRINITY_DN240131_c0_g1	ribulose-phosphate 3-epimerase chloroplastic-like [*Trifolium pratense*]	PNX93604.1	-4.90	6.17E-05
0	TRINITY_DN37909_c0_g1	40S ribosomal protein SA-like [*Prosopis alba*]	XP_028799653.1	-4.92	7.01E-04
0	TRINITY_DN253319_c0_g1	hypothetical protein PHAVU_009G247800g [*Phaseolus vulgaris*]	XP_007138908.1	-4.94	9.67E-04
0	TRINITY_DN1205_c0_g1	probable glutathione S-transferase [*Medicago truncatula*]	XP_003623174.1	-5.00	1.60E-11
0	TRINITY_DN212623_c0_g1	ribosome biogenesis protein NSA2 homolog [*Arachis duranensis*]	XP_015951385.1	-5.03	7.71E-04
0	TRINITY_DN275128_c0_g1	NA	NA	-5.06	6.16E-05
0	TRINITY_DN151250_c0_g1	60S ribosomal protein L38 isoform X1 [*Cajanus cajan*]	XP_020224465.1	-5.06	1.07E-04
0	TRINITY_DN213400_c0_g1	hypothetical protein TSUD_95870 [*Trifolium subterraneum*]	GAU51472.1	-5.18	1.37E-06
0	TRINITY_DN11_c0_g1	putative P-loop containing nucleoside triphosphate hydrolase, leucine-rich repeat domain, L [*Medicago truncatula*]	RHN67702.1	-5.19	9.04E-04
0	TRINITY_DN2801_c0_g1	glyceraldehyde-3-phosphate dehydrogenase B, chloroplastic [*Arachis duranensis*]	XP_015934037.1	-5.22	2.96E-04
0	TRINITY_DN120242_c0_g1	chlorophyll a-b binding protein P4, chloroplastic [*Vigna unguiculata*]	XP_027905299.1	-5.32	9.21E-04
0	TRINITY_DN5605_c0_g1	NA	NA	-5.32	6.95E-04

0	TRINITY_DN7687_c0_g1	fructose-bisphosphate aldolase 1, chloroplastic [*Vigna radiata*]	XP_014501159.1	-5.34	9.87E-05
0	TRINITY_DN151735_c0_g1	hypothetical protein TSUD_05790 [*Trifolium subterraneum*]	GAU26909.1	-5.35	1.36E-04
0	TRINITY_DN2149_c0_g1	argininosuccinate synthase, chloroplastic [*Medicago truncatula*]	XP_003602086.1	-5.37	7.76E-04
0	TRINITY_DN153498_c0_g1	PREDICTED: cytochrome b6-f complex iron-sulfur subunit, chloroplastic-like [*Lupinus angustifolius*]	XP_019437042.1	-5.39	1.91E-06
0	TRINITY_DN282944_c0_g1	NA	NA	-5.42	3.39E-04
0	TRINITY_DN12909_c0_g2	elongation factor-1A [*Glycine max*]	ACI42861.1	-5.43	2.35E-04
0	TRINITY_DN211931_c0_g1	40S ribosomal protein S15-4-like [*Cicer arietinum*]	XP_004495132.1	-5.44	9.58E-05
0	TRINITY_DN210714_c0_g1	phosphoglycerate kinase, chloroplastic [*Arachis duranensis*]	XP_015932386.1	-5.48	6.20E-05
0	TRINITY_DN5546_c0_g3	chlorophyll a-b binding protein CP26, chloroplastic-like [*Abrus precatorius*]	XP_027363265.1	-5.59	1.31E-04
0	TRINITY_DN6083_c0_g1	hypothetical protein TSUD_305470 [*Trifolium subterraneum*]	GAU42202.1	-5.60	1.82E-04
0	TRINITY_DN12143_c0_g1	PREDICTED: 60S acidic ribosomal protein P2A-like [*Lupinus angustifolius*]	XP_019451066.1	-5.63	2.12E-05
0	TRINITY_DN1330_c0_g1	hypothetical protein TSUD_184950 [*Trifolium subterraneum*]	GAU44994.1	-5.67	9.63E-04
0	TRINITY_DN121653_c0_g1	40S ribosomal protein S2-3 [*Spatholobus suberectus*]	TKY60984.1	-5.70	6.03E-05
0	TRINITY_DN2097_c0_g1	putative chlorophyll A-B binding protein [*Lupinus albus*]	KAE9610650.1	-5.71	6.56E-06
0	TRINITY_DN270789_c0_g1	hypothetical protein GLYMA_02G255500 [*Glycine max*]	KRH73166.1	-5.74	9.04E-04
0	TRINITY_DN269483_c0_g1	hypothetical protein Lal_00020498 [*Lupinus albus*]	KAF1871704.1	-5.74	4.18E-05
0	TRINITY_DN5605_c0_g2	NA	NA	-5.75	2.11E-04

0	TRINITY_DN150709_c0_g1	myo-inositol 1-phosphate synthase [*Phaseolus vulgaris*]	CAH68559.2	-5.76	6.81E-04
0	TRINITY_DN273563_c0_g1	60S ribosomal protein L19-2 [*Mucuna pruriens*]	RDX86978.1	-5.76	6.61E-05
0	TRINITY_DN23592_c0_g1	unknown [*Glycine max*]	ACU21362.1	-5.81	8.54E-04
0	TRINITY_DN20697_c0_g1	NA	NA	-5.82	8.55E-04
0	TRINITY_DN209506_c0_g1	phosphoribulokinase, chloroplastic [*Vigna unguiculata*]	XP_027907951.1	-5.83	2.11E-04
0	TRINITY_DN6634_c0_g1	NA	NA	-5.83	2.68E-05
0	TRINITY_DN6447_c0_g1	NA	NA	-5.86	1.47E-04
0	TRINITY_DN20615_c0_g1	40S ribosomal protein S12-like [*Prosopis alba*]	XP_028760845.1	-5.86	5.06E-04
0	TRINITY_DN73554_c3_g1	RecName: Full=Plastocyanin, chloroplastic; Flags: Precursor [*Pisum sativum*]	P16002.1	-5.89	1.54E-05
0	TRINITY_DN11798_c0_g1	60S ribosomal protein L6-1 [*Arachis duranensis*]	XP_015971071.1	-5.89	9.74E-05
0	TRINITY_DN247634_c0_g1	40S ribosomal protein S3a [*Medicago truncatula*]	XP_003610736.1	-5.91	2.91E-06
0	TRINITY_DN30069_c0_g1	ABC transporter F family member 4 [*Cajanus cajan*]	KYP63230.1	-5.95	3.39E-04
0	TRINITY_DN33321_c0_g1	PREDICTED: 40S ribosomal protein S4-1 [*Lupinus angustifolius*]	XP_019464787.1	-6.00	8.54E-04
0	TRINITY_DN16578_c0_g1	NA	NA	-6.01	5.37E-04
0	TRINITY_DN120433_c0_g1	photosystem I reaction center subunit psaK, chloroplastic [*Cicer arietinum*]	XP_004498476.1	-6.07	5.48E-05
0	TRINITY_DN22541_c0_g1	40S ribosomal protein S11 [*Glycine max*]	XP_003549708.1	-6.10	5.90E-04
0	TRINITY_DN105946_c0_g4	NA	NA	-6.29	2.03E-04
0	TRINITY_DN22742_c1_g1	Tubulin beta-2 chain [*Glycine soja*]	KHN26219.1	-6.37	2.01E-04
0	TRINITY_DN25204_c0_g1	hypothetical protein [*Trifolium medium*]	MCH80706.1	-6.42	1.36E-06
0	TRINITY_DN16634_c0_g2	PREDICTED: 40S ribosomal protein S15-4-like [*Lupinus angustifolius*]	XP_019424438.1	-6.50	2.73E-06
0	TRINITY_DN187618_c0_g1	hypothetical protein PHAVU_008G118000g [*Phaseolus vulgaris*]	XP_007140501.1	-6.57	1.55E-04

0	TRINITY_DN1949_c0_g1	putative transcription factor B3-Domain family [*Medicago truncatula*]	RHN51852.1	-6.58	2.91E-06
0	TRINITY_DN121843_c0_g1	F-box protein interaction domain protein [*Medicago truncatula*]	KEH31985.1	-6.59	3.99E-05
0	TRINITY_DN8089_c0_g1	60S ribosomal protein L36-3-like [*Prosopis alba*]	XP_028806191.1	-6.59	7.77E-05
0	TRINITY_DN34152_c0_g1	60S ribosomal protein L23a [*Vigna radiata* var. *radiata*]	XP_014494213.2	-6.59	9.92E-05
0	TRINITY_DN13678_c0_g1	NA	NA	-6.63	7.73E-05
0	TRINITY_DN10772_c0_g1	NA	NA	-6.67	1.05E-04
0	TRINITY_DN270920_c0_g1	hypothetical protein TSUD_291620 [*Trifolium subterraneum*]	GAU48477.1	-6.69	4.27E-04
0	TRINITY_DN17900_c0_g1	NA	NA	-6.71	5.11E-08
0	TRINITY_DN2809_c0_g1	dehydration-responsive RD22-like protein [*Medicago truncatula*]	KEH30397.1	-6.73	5.99E-05
0	TRINITY_DN269631_c0_g1	40S ribosomal protein S17-2 [*Cajanus cajan*]	KYP32630.1	-6.75	8.55E-04
0	TRINITY_DN23852_c0_g1	ribulose bisphosphate carboxylase/oxygenase activase, chloroplastic [*Cicer arietinum*]	XP_004490873.1	-6.85	5.95E-06
0	TRINITY_DN242543_c0_g1	40S ribosomal protein S13-like [*Cicer arietinum*]	XP_004511653.1	-6.92	1.07E-04
0	TRINITY_DN152063_c0_g1	60S ribosomal protein L35a-3 [*Cajanus cajan*]	XP_020212327.1	-6.93	1.91E-06
0	TRINITY_DN28291_c0_g1	NA	NA	-6.95	7.15E-04
0	TRINITY_DN12582_c0_g1	PREDICTED: 40S ribosomal protein S6-2-like [*Lupinus angustifolius*]	XP_019425273.1	-7.02	2.65E-07
0	TRINITY_DN10420_c0_g1	putative BURP domain-containing protein [*Medicago truncatula*]	RHN61199.1	-7.02	1.54E-05
0	TRINITY_DN123500_c0_g1	photosystem II reaction center [*Retama raetam*]	AAL32042.1	-7.03	5.59E-05
0	TRINITY_DN25799_c0_g1	ADP, ATP carrier protein 3, mitochondrial isoform X1 [*Prosopis alba*]	XP_028807879.1	-7.06	6.42E-06
0	TRINITY_DN7794_c0_g1	replication factor A protein 1 [*Medicago truncatula*]	XP_003616287.1	-7.09	7.96E-10

0	TRINITY_DN999_c0_g1	60S ribosomal protein L15-1 [*Abrus precatorius*]	XP_027359806.1	-7.21	8.02E-06
0	TRINITY_DN209564_c0_g1	NA	NA	-7.24	1.47E-06
0	TRINITY_DN18237_c0_g1	putative ribosomal protein S12e [*Lupinus albus*]	KAE9616317.1	-7.26	3.89E-04
0	TRINITY_DN271711_c0_g1	60S ribosomal protein L30-like [*Cicer arietinum*]	XP_004516683.1	-7.28	5.48E-05
0	TRINITY_DN11723_c0_g1	NA	NA	-7.32	3.35E-04
0	TRINITY_DN183434_c0_g1	uncharacterized protein LOC100500317 [*Glycine max*]	NP_001236277.1	-7.39	3.61E-06
0	TRINITY_DN18644_c0_g1	60S ribosomal protein L23a [*Vigna radiata* var. *radiata*]	XP_014494213.2	-7.40	5.59E-05
0	TRINITY_DN3323_c0_g1	NA	NA	-7.40	2.06E-04
0	TRINITY_DN168591_c0_g1	hypothetical protein TSUD_124940 [*Trifolium subterraneum*]	GAU18661.1	-7.52	3.39E-04
0	TRINITY_DN24419_c0_g1	40S ribosomal protein S28-1-like isoform X1 [*Prosopis alba*]	XP_028784871.1	-7.52	7.45E-04
0	TRINITY_DN31493_c0_g1	hypothetical protein Lal_00005057 [*Lupinus albus*]	KAF1854648.1	-7.55	6.16E-05
0	TRINITY_DN1587_c7_g1	hypothetical protein MtrunA17_Chr2g0320531 [*Medicago truncatula*]	RHN75378.1	-7.74	9.67E-04
0	TRINITY_DN26193_c0_g1	60S ribosomal protein L15-1 [*Abrus precatorius*]	XP_027359806.1	-7.76	6.77E-08
0	TRINITY_DN3690_c0_g1	NADP-dependent alkenal double bond reductase P1-like [*Trifolium medium*]	MCH87509.1	-7.83	3.27E-04
0	TRINITY_DN12516_c0_g1	NA	NA	-7.88	3.49E-05
0	TRINITY_DN151979_c0_g1	60S ribosomal protein L23 [*Medicago truncatula*]	XP_003625359.2	-7.88	2.73E-06
0	TRINITY_DN4967_c0_g1	60S ribosomal protein L38 [*Spatholobus suberectus*]	TKY71929.1	-7.92	1.11E-04
0	TRINITY_DN48263_c0_g1	PREDICTED: 40S ribosomal protein S21-like [*Lupinus angustifolius*]	XP_019418188.1	-7.96	2.54E-06

0	TRINITY_DN37305_c0_g1	toll interleukin receptor [*Trifolium medium*]	MCI08620.1	-8.07	1.07E-04
0	TRINITY_DN171_c0_g1	NA	NA	-8.27	5.62E-06
0	TRINITY_DN669_c3_g1	hypothetical protein [*Cicer arietinum*]	CAB71132.1	-8.28	6.21E-06
0	TRINITY_DN12438_c0_g1	elongation factor 1-alpha [*Trifolium pratense*]	PNX63146.1	-8.38	3.18E-07
0	TRINITY_DN21696_c0_g1	uncharacterized protein LOC110277292 [*Arachis duranensis*]	XP_020990120.1	-8.99	9.48E-07
0	TRINITY_DN12415_c0_g2	tubulin beta-3 chain-like [*Trifolium medium*]	MCH87073.1	-9.44	1.75E-05
0	TRINITY_DN1045_c0_g2	NA	NA	-10.58	7.05E-04
0	TRINITY_DN11162_c0_g1	dehydration-responsive RD22-like protein [*Medicago truncatula*]	KEH30397.1	-11.43	3.01E-06
3	TRINITY_DN13099_c1_g1	NA	NA	11.02	1.31E-38
3	TRINITY_DN210018_c0_g1	hypothetical protein MtrunA17_Chr1g0149151 [*Medicago truncatula*]	RHN76922.1	10.29	2.62E-04
3	TRINITY_DN16575_c0_g1	protein IAA-LEUCINE RESISTANT 2 [*Trifolium medium*]	MCI04234.1	9.78	6.66E-16
3	TRINITY_DN44062_c0_g1	putative naringenin-chalcone synthase [*Medicago truncatula*]	RHN44508.1	9.47	7.57E-06
3	TRINITY_DN270143_c0_g1	NA	NA	9.33	1.52E-12
3	TRINITY_DN9518_c1_g1	hypothetical protein MTR_8g075380 [*Medicago truncatula*]	AET03761.1	9.01	4.04E-05
3	TRINITY_DN12165_c0_g1	GTP cyclohydrolase [*Arachis hypogaea*]	QHO24156.1	8.86	2.93E-05
3	TRINITY_DN4396_c2_g1	NA	NA	8.81	2.51E-05
3	TRINITY_DN4373_c0_g1	hypothetical protein MTR_4g051502 [*Medicago truncatula*]	KEH29758.1	8.68	5.32E-04
3	TRINITY_DN13099_c0_g1	NA	NA	8.37	5.61E-20
3	TRINITY_DN13735_c0_g1	putative F-box domain-containing protein [*Medicago truncatula*]	RHN73861.1	8.08	2.00E-04
3	TRINITY_DN13677_c1_g1	amino acid transporter AVT1C [*Medicago truncatula*]	XP_024641044.1	7.79	1.68E-04
3	TRINITY_DN2368_c1_g1	hypothetical protein VIGAN_01442200 [*Vigna angularis* var. *angularis*]	BAT76424.1	7.70	1.01E-04

3	TRINITY_DN4452_c1_g1	F-box protein CPR1 isoform X3 [*Medicago truncatula*]	XP_013463143.2	7.68	2.41E-04
3	TRINITY_DN205067_c0_g1	NA	NA	7.68	1.68E-04
3	TRINITY_DN2664_c2_g2	NA	NA	7.58	2.92E-04
3	TRINITY_DN10576_c0_g1	dnaJ protein ERDJ2A [*Medicago truncatula*]	XP_024632012.1	7.28	6.55E-07
3	TRINITY_DN33426_c0_g1	protein FAR1-RELATED SEQUENCE 5-like [*Arachis ipaensis*]	XP_016168211.1	7.23	4.23E-04
3	TRINITY_DN462_c0_g2	ribosomal RNA small subunit methyltransferase nep-1 [*Medicago truncatula*]	XP_013454067.1	7.20	1.01E-04
3	TRINITY_DN26083_c0_g1	uncharacterized protein LOC11405977 isoform X1 [*Medicago truncatula*]	XP_003613312.3	6.88	5.60E-04
3	TRINITY_DN13645_c0_g1	nuclear pore complex protein Nup54-like [*Trifolium pratense*]	PNY13939.1	6.84	3.58E-05
3	TRINITY_DN129905_c0_g1	NA	NA	6.68	1.11E-05
3	TRINITY_DN153727_c0_g1	NA	NA	6.13	6.59E-04
3	TRINITY_DN8157_c0_g2	uncharacterized protein LOC25480725 [*Medicago truncatula*]	XP_024630178.1	4.11	1.62E-05
3	TRINITY_DN18660_c0_g1	AP-5 complex subunit zeta-1 [*Medicago truncatula*]	XP_003607673.2	3.39	9.14E-04
3	TRINITY_DN8029_c0_g1	hypothetical protein MTR_6g465600 [*Medicago truncatula*]	KEH26597.1	2.97	2.64E-04
3	TRINITY_DN10486_c0_g1	dihydroflavonol 4-reductase [*Medicago sativa*]	AEI59122.1	2.92	6.20E-04
3	TRINITY_DN1598_c0_g1	17.9 kDa class II heat shock protein [*Medicago truncatula*]	XP_013465875.1	2.75	6.33E-04
3	TRINITY_DN1194_c0_g1	protein HEAT-STRESS-ASSOCIATED 32 [*Medicago truncatula*]	XP_013457153.1	2.38	4.54E-04
3	TRINITY_DN13789_c0_g1	hypothetical protein MTR_3g050170 [*Medicago truncatula*]	AES70243.2	2.25	2.92E-04
3	TRINITY_DN2212_c0_g1	uncharacterized calcium-binding protein At1g02270 isoform X1 [*Medicago truncatula*]	XP_024629078.1	2.11	5.23E-06

3	TRINITY_DN523_c0_g1	putative 4-hydroxyphenylpyruvate dioxygenase [*Medicago truncatula*]	RHN57659.1	2.01	5.30E-05
3	TRINITY_DN9871_c0_g1	cyclin-dependent kinases regulatory subunit 1 [*Medicago truncatula*]	XP_003606312.1	-2.02	3.55E-04
3	TRINITY_DN1295_c0_g2	putative proteinase inhibitor I12, Bowman-Birk [*Medicago truncatula*]	RHN46929.1	-2.24	8.57E-04
3	TRINITY_DN882_c0_g1	sugar transport protein 5 [*Medicago truncatula*]	XP_013460889.1	-2.58	1.94E-04
3	TRINITY_DN212366_c0_g1	60S ribosomal protein L8-1 [*Abrus precatorius*]	XP_027346504.1	-3.35	1.01E-04
3	TRINITY_DN8119_c0_g1	ribulose bisphosphate carboxylase small chain clone 512-like [*Abrus precatorius*]	XP_027332320.1	-3.40	4.57E-04
3	TRINITY_DN613_c0_g2	embryonic abundant protein VF30.1 isoform X2 [*Medicago truncatula*]	XP_003628215.2	-3.41	1.18E-04
3	TRINITY_DN180291_c0_g1	60S ribosomal protein L3 isoform C [*Glycine soja*]	RZB88573.1	-3.46	7.37E-04
3	TRINITY_DN151735_c0_g1	hypothetical protein TSUD_05790 [*Trifolium subterraneum*]	GAU26909.1	-3.48	5.63E-04
3	TRINITY_DN2387_c0_g2	40S ribosomal protein S5 [*Prosopis alba*]	XP_028752747.1	-3.61	6.33E-04
3	TRINITY_DN244389_c0_g1	hypothetical protein TSUD_132800 [*Trifolium subterraneum*]	GAU45263.1	-3.69	9.14E-04
3	TRINITY_DN16578_c0_g1	NA	NA	-3.84	6.14E-05
3	TRINITY_DN269483_c0_g1	hypothetical protein Lal_00020498 [*Lupinus albus*]	KAF1871704.1	-3.88	5.98E-05
3	TRINITY_DN270267_c0_g1	eukaryotic translation initiation factor 5a-2-like protein [*Trifolium pratense*]	PNX72413.1	-3.92	1.11E-05
3	TRINITY_DN210714_c0_g1	phosphoglycerate kinase, chloroplastic [*Arachis duranensis*]	XP_015932386.1	-3.97	3.58E-05
3	TRINITY_DN270789_c0_g1	hypothetical protein GLYMA_02G255500 [*Glycine max*]	KRH73166.1	-4.04	9.14E-04
3	TRINITY_DN12143_c0_g1	PREDICTED: 60S acidic ribosomal protein P2A-like [*Lupinus angustifolius*]	XP_019451066.1	-4.04	8.57E-04

3	TRINITY_DN18644_c0_g1	60S ribosomal protein L23a [*Vigna radiata* var. *radiata*]	XP_014494213.2	-4.15	3.80E-04
3	TRINITY_DN182920_c0_g1	putative chlorophyll A-B binding protein [*Lupinus albus*]	KAE9592472.1	-4.19	3.80E-04
3	TRINITY_DN151360_c0_g1	ferredoxin-like [*Vigna unguiculata*]	XP_027931956.1	-4.19	3.08E-04
3	TRINITY_DN2097_c0_g1	putative chlorophyll A-B binding protein [*Lupinus albus*]	KAE9610650.1	-4.33	2.77E-04
3	TRINITY_DN27158_c0_g1	glycerol-3-phosphate dehydrogenase [NAD(+)]-like [*Vigna unguiculata*]	XP_027902060.1	-4.37	2.00E-04
3	TRINITY_DN31461_c0_g1	pathogenesis-related protein 1B [*Medicago truncatula*]	XP_024637244.1	-4.39	1.02E-05
3	TRINITY_DN23852_c0_g1	ribulose bisphosphate carboxylase/oxygenase activase, chloroplastic [*Cicer arietinum*]	XP_004490873.1	-4.61	4.23E-04
3	TRINITY_DN37909_c0_g1	40S ribosomal protein SA-like [*Prosopis alba*]	XP_028799653.1	-4.64	7.38E-04
3	TRINITY_DN1205_c0_g1	probable glutathione S-transferase [*Medicago truncatula*]	XP_003623174.1	-4.65	2.10E-07
3	TRINITY_DN150554_c0_g1	group 2 truncated hemoglobin-like protein [*Trifolium pratense*]	PNX80972.1	-4.71	4.46E-04
3	TRINITY_DN151979_c0_g1	60S ribosomal protein L23 [*Medicago truncatula*]	XP_003625359.2	-4.72	1.13E-05
3	TRINITY_DN151250_c0_g1	60S ribosomal protein L38 isoform X1 [*Cajanus cajan*]	XP_020224465.1	-4.75	4.01E-04
3	TRINITY_DN3554_c2_g1	60S ribosomal protein L7a-1 [*Prosopis alba*]	XP_028798094.1	-4.81	4.28E-04
3	TRINITY_DN3849_c0_g1	hypothetical protein PHAVU_005G090400g [*Phaseolus vulgaris*]	XP_007149685.1	-4.86	2.30E-04
3	TRINITY_DN59038_c1_g1	60S ribosomal protein L5 [*Glycine max*]	XP_003548576.2	-4.96	1.70E-04
3	TRINITY_DN242304_c0_g1	40S ribosomal protein S10-1 [*Spatholobus suberectus*]	TKY70970.1	-4.99	6.15E-04
3	TRINITY_DN125398_c0_g1	photosystem I subunit VIII [*Bauhinia binata*]	YP_009486638.1	-5.02	4.37E-05
3	TRINITY_DN18040_c0_g1	NA	NA	-5.10	1.06E-04
3	TRINITY_DN1949_c0_g1	putative transcription factor B3-Domain family [*Medicago truncatula*]	RHN51852.1	-5.20	1.46E-05

3	TRINITY_DN11798_c0_g1	60S ribosomal protein L6-1 [*Arachis duranensis*]	XP_015971071.1	-5.34	5.94E-04
3	TRINITY_DN5605_c0_g2	NA	NA	-5.35	6.70E-06
3	TRINITY_DN180826_c0_g1	hypothetical protein TSUD_161670 [*Trifolium subterraneum*]	GAU29762.1	-5.41	3.80E-04
3	TRINITY_DN7794_c0_g1	replication factor A protein 1 [*Medicago truncatula*]	XP_003616287.1	-5.56	6.78E-08
3	TRINITY_DN17752_c0_g1	thymidine kinase a [*Medicago truncatula*]	XP_003601580.1	-5.84	1.13E-05
3	TRINITY_DN2801_c0_g1	glyceraldehyde-3-phosphate dehydrogenase B, chloroplastic [*Arachis duranensis*]	XP_015934037.1	-5.90	2.31E-06
3	TRINITY_DN1_c4_g1	hypothetical protein KK1_029344 [*Cajanus cajan*]	KYP48943.1	-5.94	4.04E-05
3	TRINITY_DN2809_c0_g1	dehydration-responsive RD22-like protein [*Medicago truncatula*]	KEH30397.1	-5.95	1.75E-05
3	TRINITY_DN239610_c0_g1	hypothetical protein MTR_3g035620 [*Medicago truncatula*]	AES69825.1	-6.25	1.36E-05
3	TRINITY_DN213400_c0_g1	hypothetical protein TSUD_95870 [*Trifolium subterraneum*]	GAU51472.1	-6.37	1.96E-05
3	TRINITY_DN20615_c0_g1	40S ribosomal protein S12-like [*Prosopis alba*]	XP_028760845.1	-6.48	1.68E-04
3	TRINITY_DN168591_c0_g1	hypothetical protein TSUD_124940 [*Trifolium subterraneum*]	GAU18661.1	-6.84	7.29E-04
3	TRINITY_DN98432_c0_g1	PHD finger protein Alfin1-like isoform X2 [*Abrus precatorius*]	XP_027352369.1	-6.87	6.33E-04
3	TRINITY_DN1760_c0_g1	arabinogalactan protein 16 [*Medicago truncatula*]	XP_013447162.1	-6.99	1.62E-05
3	TRINITY_DN187377_c0_g1	PPR containing plant-like protein [*Medicago truncatula*]	AES89729.2	-7.09	7.02E-04
3	TRINITY_DN51318_c0_g1	ferredoxin, root R-B1 isoform X2 [*Medicago truncatula*]	XP_013470267.1	-7.22	3.80E-04
3	TRINITY_DN1607_c2_g1	LINE-1 reverse transcriptase like [*Trifolium medium*]	MCH79506.1	-7.51	2.15E-04

3	TRINITY_DN15675_c0_g1	leguminosin proline-rich group669 secreted peptide [*Medicago truncatula*]	KEH37994.1	-7.59	1.19E-04
3	TRINITY_DN41037_c0_g1	NA	NA	-7.71	6.48E-04
3	TRINITY_DN275015_c0_g1	Hypothetical protein glysoja_045180 [*Glycine soja*]	KHN01270.1	-8.11	7.06E-04
3	TRINITY_DN30254_c0_g1	hypothetical protein MtrunA17_Chr4g0029041 [*Medicago truncatula*]	RHN60734.1	-8.26	1.05E-04
3	TRINITY_DN56244_c0_g1	hypothetical protein Ahy_B01g055549 [*Arachis hypogaea*]	RYR30781.1	-8.60	1.05E-07
3	TRINITY_DN155676_c0_g1	NA	NA	-8.82	3.67E-04
3	TRINITY_DN5862_c0_g1	PREDICTED: uncharacterized protein LOC109358019, partial [*Lupinus angustifolius*]	XP_019457628.1	-8.90	1.25E-08
3	TRINITY_DN11162_c0_g1	dehydration-responsive RD22-like protein [*Medicago truncatula*]	KEH30397.1	-9.49	7.30E-04
27	TRINITY_DN16289_c0_g1	unknown [*Medicago truncatula*]	ACJ84593.1	11.47	6.02E-10
27	TRINITY_DN270143_c0_g1	NA	NA	10.98	2.02E-06
27	TRINITY_DN16575_c0_g1	protein IAA-LEUCINE RESISTANT 2 [*Trifolium medium*]	MCI04234.1	10.73	6.66E-08
27	TRINITY_DN13099_c1_g1	NA	NA	10.28	2.09E-25
27	TRINITY_DN2368_c1_g1	hypothetical protein VIGAN_01442200 [*Vigna angularis* var. *angularis*]	BAT76424.1	10.12	2.02E-06
27	TRINITY_DN242242_c0_g1	PREDICTED: uncharacterized protein LOC109348129 isoform X2 [*Lupinus angustifolius*]	XP_019443917.1	9.63	2.35E-05
27	TRINITY_DN11429_c0_g1	two-component response regulator-APRR2-like protein [*Medicago truncatula*]	KEH31561.1	9.33	5.25E-12
27	TRINITY_DN25665_c0_g1	elongation factor 1-beta [*Medicago truncatula*]	KEH28966.1	9.31	5.74E-05
27	TRINITY_DN165162_c0_g1	NA	NA	8.65	7.82E-04
27	TRINITY_DN2655_c1_g1	hypothetical protein VIGAN_UM160600, partial [*Vigna angularis* var. *angularis*]	BAU03701.1	8.52	6.96E-05

27	TRINITY_DN14324_c1_g1	NA	NA	7.90	2.98E-04
27	TRINITY_DN2664_c2_g2	NA	NA	7.86	6.05E-04
27	TRINITY_DN5865_c0_g3	NA	NA	7.75	8.78E-04
27	TRINITY_DN30638_c0_g2	22.7 kDa class IV heat shock protein-like [*Vigna unguiculata*]	XP_027923157.1	7.70	9.93E-07
27	TRINITY_DN12165_c0_g1	GTP cyclohydrolase [*Arachis hypogaea*]	QHO24156.1	7.68	2.65E-04
27	TRINITY_DN13278_c0_g1	small subunit ribosomal protein S7 [*Vigna unguiculata*]	QCD92443.1	7.67	9.43E-04
27	TRINITY_DN462_c0_g2	ribosomal RNA small subunit methyltransferase nep-1 [*Medicago truncatula*]	XP_013454067.1	7.52	7.55E-04
27	TRINITY_DN23505_c0_g1	LEAF RUST 10 DISEASE-RESISTANCE LOCUS RECEPTOR-LIKE PROTEIN KINASE-like 2.1 [*Medicago truncatula*]	XP_024627079.1	7.22	6.73E-07
27	TRINITY_DN3739_c0_g4	hypothetical protein MTR_2g084200 [Medicago truncatula]	KEH38861.1	7.14	2.75E-04
27	TRINITY_DN19418_c0_g1	hypothetical protein DEO72_LG11g759 [*Vigna unguiculata*]	QCE13761.1	7.04	5.42E-05
27	TRINITY_DN32103_c0_g1	putative senescence-associated protein [*Pisum sativum*]	BAB33421.1	7.01	4.43E-08
27	TRINITY_DN10576_c0_g1	dnaJ protein ERDJ2A [*Medicago truncatula*]	XP_024632012.1	6.46	2.65E-04
27	TRINITY_DN34811_c0_g3	NA	NA	6.38	2.35E-05
27	TRINITY_DN14165_c0_g1	putative Heat shock protein 70 family [*Medicago truncatula*]	RHN73567.1	6.26	9.09E-04
27	TRINITY_DN11666_c0_g1	NA	NA	6.25	1.10E-05
27	TRINITY_DN13099_c0_g1	NA	NA	5.48	6.90E-06
27	TRINITY_DN2664_c0_g1	NA	NA	5.16	2.50E-05
27	TRINITY_DN27481_c0_g2	uncharacterized protein At2g33490 isoform X2 [*Vigna radiata* var. *radiata*]	XP_014497890.1	5.12	9.09E-04
27	TRINITY_DN274030_c0_g1	DNA gyrase subunit B, putative [*Medicago truncatula*]	AES88004.1	5.00	3.58E-04
27	TRINITY_DN13068_c0_g1	hypothetical protein TSUD_237040 [*Trifolium subterraneum*]	GAU41453.1	4.73	9.93E-07

27	TRINITY_DN672_c2_g1	uncharacterized protein LOC110272781 [*Arachis duranensis*]	XP_020980766.1	4.39	2.65E-04
27	TRINITY_DN1991_c0_g2	hypothetical protein MtrunA17_Chr6g0470871 [*Medicago truncatula*]	RHN51632.1	3.99	1.53E-04
27	TRINITY_DN1903_c0_g1	poly(U)-specific endoribonuclease-B [*Medicago truncatula*]	XP_013457556.1	3.34	1.21E-10
27	TRINITY_DN2_c0_g1	hypothetical protein [*Vicia faba*]	AGC78890.1	3.04	4.90E-05
27	TRINITY_DN293_c1_g1	hypothetical protein L195_g035870 [*Trifolium pratense*]	PNX79880.1	2.59	7.55E-04
27	TRINITY_DN47996_c0_g1	uncharacterized protein LOC11416135 isoform X2 [*Medicago truncatula*]	XP_003625101.1	2.17	7.60E-04
27	TRINITY_DN12817_c0_g1	MtN4 [*Medicago truncatula*]	CAA75594.1	-2.28	1.10E-05
27	TRINITY_DN12475_c0_g1	40S ribosomal protein S4 [*Trifolium medium*]	MCI19247.1	-2.69	5.08E-04
27	TRINITY_DN4147_c0_g1	aspartyl protease AED3 [*Medicago truncatula*]	XP_003602931.1	-2.77	7.97E-05
27	TRINITY_DN23626_c0_g1	cytosolic aldehyde dehydrogenase RF2C [*Medicago truncatula*]	KEH21359.1	-2.88	3.41E-05
27	TRINITY_DN7794_c0_g1	replication factor A protein 1 [*Medicago truncatula*]	XP_003616287.1	-3.92	2.80E-04
27	TRINITY_DN249347_c0_g1	PREDICTED: histone H3 [*Lupinus angustifolius*]	XP_019435472.1	-4.67	3.49E-04
27	TRINITY_DN32509_c0_g1	pentatricopeptide repeat-containing protein At2g01390 [*Medicago truncatula*]	XP_003631109.2	-6.54	2.65E-04
27	TRINITY_DN6002_c0_g1	hypothetical protein LR48_Vigan08g017200 [*Vigna angularis*]	KOM49345.1	-6.64	6.05E-04
27	TRINITY_DN27772_c0_g1	dof zinc finger protein DOF1.4 [*Medicago truncatula*]	XP_003593614.1	-6.76	3.94E-04
27	TRINITY_DN77210_c1_g1	hypothetical protein MTR_7g026530 [*Medicago truncatula*]	AES78259.1	-7.18	9.43E-04
27	TRINITY_DN31461_c0_g1	pathogenesis-related protein 1B [*Medicago truncatula*]	XP_024637244.1	-7.29	2.97E-08
27	TRINITY_DN2229_c0_g1	putative exostosin [*Medicago truncatula*]	RHN78237.1	-7.90	8.44E-07

27	TRINITY_DN168591_c0_g1	hypothetical protein TSUD_124940 [*Trifolium subterraneum*]	GAU18661.1	-8.04	4.63E-10
27	TRINITY_DN60356_c0_g2	NA	NA	-8.14	2.98E-04
27	TRINITY_DN17451_c0_g2	soyasaponin III rhamnosyltransferase [*Medicago truncatula*]	XP_003593144.1	-8.52	5.61E-05
27	TRINITY_DN164403_c0_g1	paired amphipathic helix protein [*Medicago truncatula*]	KEH24936.1	-8.80	1.14E-04
27	TRINITY_DN53_c6_g1	NYN domain protein [*Medicago truncatula*]	AET01316.1	-9.92	1.57E-09

[1]NA represents no homology retrieved upon performing BLASTX.
[2]Nr ID is the protein accession number in NCBI non redundant protein database.
[3]$\log_2$FC stands for log Fold Change, where it is log base 2.
[4]FDR stands for false discovery rate.

Appendix A.4. Mean value (2-yr) and analysis of variance of the germination parameters of five alfalfa cultivars under five gradients of salt stress (0 dS m^{-1}, 4 dS m^{-1}, 8 dS m^{-1}, 12 dS m^{-1}, and 16 dS m^{-1}).

Salinity	Cultivars	germination percentage	germination rate	seedling length (mm)	seed vigor
0 dS m^{-1}	Halo	87.5±2.97	13.8±0.48	24.7±0.33	21.5±0.66
	Rugged	61.5±3.29	8.7±0.59	34.8±0.97	21.6±1.57
	Bridgeview	81.0±2.59	12.0±0.31	24.7±0.45	20.0±0.79
	Rangelander	40.0±3.02	5.0±0.39	20.6±0.79	8.2±0.61
	Vernal	90.0±2.14	13.4±0.54	28.1±1.25	25.2±0.92
4 dS m^{-1}	Halo	86.5±3.11	10.2±0.56	24.1±0.74	20.8±1.05
	Rugged	58.0±3.38	6.7±0.51	33.5±2.22	19.7±2.22
	Bridgeview	83.0±2.48	9.3±0.28	25.4±1.08	21.2±1.29
	Rangelander	39.0±3.68	3.3±0.32	15.7±0.89	6.3±0.80
	Vernal	81.5±3.46	8.7±0.54	25.0±0.64	20.4±0.92
8 dS m^{-1}	Halo	80.0±2.93	9.3±0.38	23.8±0.98	19.0±1.06
	Rugged	60.5±3.58	6.1±0.32	33.6±3.00	20.6±2.57
	Bridgeview	76.0±2.83	7.9±0.27	23.8±0.73	18.1±0.82
	Rangelander	34.0±3.78	2.6±0.25	13.8±0.77	4.8±0.61
	Vernal	74.5±3.54	8.3±0.54	24.1±1.30	18.2±1.68
12 dS m^{-1}	Halo	71.0±3.76	7.5±0.57	20.7±0.57	14.7±0.91
	Rugged	58.0±3.30	5.5±0.39	30.6±1.79	17.9±1.70
	Bridgeview	71.0±3.91	7.3±0.39	21.1±0.76	15.0±0.98
	Rangelander	33.5±4.34	2.5±0.40	12.6±1.11	4.1±0.56
	Vernal	66.5±3.62	6.6±0.40	22.9±0.95	15.2±0.83
16 dS m^{-1}	Halo	73.0±3.98	7.2±0.49	23.8±2.40	17.8±2.81
	Rugged	61.5±1.68	5.6±0.24	29.6±2.17	18.3±1.54
	Bridgeview	55.0±2.36	5.3±0.41	17.1±1.68	9.6±1.22
	Rangelander	21.0±3.68	1.5±0.23	10.7±1.73	3.3±0.64
	Vernal	53.5±5.07	5.2±0.59	17.3±0.88	9.2±0.99
Salinity		<0.001	<0.001	<0.001	<0.001
Cultivar		<0.001	<0.001	<0.001	<0.001
Salinity : Cultivar		<0.001	<0.001	0.043	<0.001

Appendix A.5. Mean value (2-yr) and analysis of variance of the plant height of five alfalfa cultivars grown under five gradients of salt stress (0 dS m^{-1}, 4 dS m^{-1}, 8 dS m^{-1}, 12 dS m^{-1}, and 16 dS m^{-1}) measured at five time points.

Salinity	Cultivars	PH1	PH2	PH3	PH4	PH5
0 dS m^{-1}	Halo	6.0±0.96	15.4±1.22	30.5±2.2	43.7±5.17	48.3±5.53
	Rugged	3.7±0.36	12.9±1.64	28.4±2.87	43.8±4.55	51.0±6.23
	Bridgeview	4.3±0.62	13.1±1.20	26.0±1.39	38.6±4.46	45.1±5.90
	Rangelander	3.2±0.38	9.6±1.26	20.0±1.63	33.7±3.39	40.6±4.93
	Vernal	5.9±0.79	17.9±1.88	35.6±2.62	49.3±6.06	54.3±6.80
4 dS m^{-1}	Halo	7.7±1.38	18.4±2.88	28.7±3.30	34.6±3.63	37.5±4.36
	Rugged	8.0±1.47	20.4±2.32	32.8±1.40	40.3±3.17	41.8±3.57
	Bridgeview	5.1±0.85	14.3±1.83	23.3±2.95	30.9±4.16	34.3±4.90
	Rangelander	6.1±1.16	16.3±2.23	25.5±2.76	32.3±3.02	36.6±3.45
	Vernal	8.3±0.98	21.3±2.05	32.1±2.64	36.9±3.50	39.0±4.14
8 dS m^{-1}	Halo	9.3±1.00	20.3±1.59	26.0±2.21	27.7±2.70	28.2±2.49
	Rugged	7.7±0.63	19.3±1.26	25.8±1.07	28.6±1.82	31.3±2.31
	Bridgeview	5.9±0.33	17.2±1.18	24.7±2.90	26.8±3.58	28.9±3.62
	Rangelander	6.2±1.36	16.6±2.07	24.2±1.73	24.8±1.00	28.1±2.01
	Vernal	9.3±0.99	23.0±2.17	30.9±2.73	33.4±3.87	33.6±3.88
12 dS m^{-1}	Halo	7.9±0.99	17.3±1.15	21.1±1.22	22.6±1.40	25.5±1.96
	Rugged	6.3±1.02	15.6±1.91	21.7±1.36	23.5±1.15	27.3±1.36
	Bridgeview	6.1±0.98	13.7±1.49	17.6±1.45	19.8±1.28	23.0±1.35
	Rangelander	4.8±0.89	12.6±1.48	16.9±1.53	19.6±1.34	25.8±4.02
	Vernal	8.0±0.73	19.7±1.37	25.9±2.12	27.2±2.38	29.3±3.17
16 dS m^{-1}	Halo	7.0±0.25	16.6±0.90	21.5±1.85	22.6±1.82	24.4±1.92
	Rugged	7.0±0.50	18.9±1.70	23.4±2.37	24.1±2.22	23.5±2.81
	Bridgeview	5.2±0.62	13.6±1.39	17.9±2.48	20.7±2.73	20.2±3.04
	Rangelander	4.7±0.64	13.1±1.83	19.0±2.08	20.6±2.01	22.3±2.57
	Vernal	7.0±0.36	18.1±1.69	24.3±2.80	25.9±3.32	27.7±3.46
Salinity		<0.001	<0.001	<0.001	<0.001	<0.001
Cultivar		<0.001	<0.001	<0.001	<0.001	<0.001
Salinity : Cultivar		0.88	0.82	0.64	0.97	0.92

Data are means ± standard errors of means; PH1, plant height on 4th week of growth; PH2, plant height on 6th week of growth; PH3, plant height on 8th week of growth; PH4, plant height on 10th week of growth; PH5, plant height on 12th week of growth.

Appendix A.6. Mean value (2-yr) and analysis of variance of the chlorophyll content of five alfalfa cultivars grown under five gradients of salt stress (0 dS m^{-1}, 4 dS m^{-1}, 8 dS m^{-1}, 12 dS m^{-1}, and 16 dS m^{-1}) measured at five time points.

Salinity	Cultivars	CH1	CH2	CH3	CH4	CH5
0 dS m^{-1}	Halo	43.6±3.46	44.3±6.33	49.1±5.79	50.8±5.18	51.4±3.08
	Rugged	51.3±1.63	56.1±1.78	56.3±2.71	55.4±3.03	54.5±2.73
	Bridgeview	45.9±2.79	48.7±4.26	46.8±5.14	50.1±4.46	50.4±3.28
	Rangelander	43.9±2.00	45.6±1.31	45.9±3.94	46.0±3.44	45.2±2.79
	Vernal	49.4±2.17	48.6±4.26	51.6±3.53	49.1±4.02	48.7±2.54
4 dS m^{-1}	Halo	49.2±4.83	46.4±6.24	47.9±6.29	49.6±5.25	49.8±4.75
	Rugged	60.6±2.05	60.4±3.71	55.8±2.67	56.2±2.86	57.5±3.46
	Bridgeview	47.8±4.64	44.6±6.73	44.3±6.81	49.2±4.89	47.7±4.48
	Rangelander	43.0±2.53	42.8±4.40	41.8±4.36	41.1±4.15	43.5±3.04
	Vernal	46.4±5.25	47.9±6.08	49.1±6.26	49.9±4.70	54.0±2.27
8 dS m^{-1}	Halo	46.0±5.67	42.1±7.35	42.2±6.44	46.4±5.08	46.2±4.01
	Rugged	56.5±1.94	56.1±3.82	52.8±5.54	56.8±3.45	53.7±4.09
	Bridgeview	48.6±5.04	47.9±5.13	44.7±5.83	47.4±4.59	47.5±3.80
	Rangelander	43.6±3.08	43.1±3.24	35.0±4.67	43.8±3.52	41.8±2.80
	Vernal	51.1±3.27	51.4±4.44	44.1±6.37	49.1±4.54	48.1±4.40
12 dS m^{-1}	Halo	42.0±5.44	43.0±6.99	43±7.87	45.0±6.75	44.7±6.54
	Rugged	56.8±1.09	53.7±4.25	47.0±4.70	52.1±2.82	46.2±5.33
	Bridgeview	44.3±4.27	44.1±4.78	37.3±6.67	45.6±4.54	40.1±5.02
	Rangelander	42.5±3.11	35.7±4.37	38.2±4.61	38.0±3.78	38.0±5.00
	Vernal	49.1±4.00	47.5±5.43	43.1±5.87	48.5±4.55	41.3±6.73
16 dS m^{-1}	Halo	42.7±4.75	42.0±5.36	40.7±6.94	45.1±4.69	40.5±4.82
	Rugged	52.7±1.29	48.1±4.04	39.5±6.19	43.7±3.84	42.6±3.86
	Bridgeview	46.6±4.12	45.3±5.18	46.8±6.39	48.1±3.86	43.8±4.80
	Rangelander	42.9±3.56	42.4±3.36	33.9±4.63	42.9±3.17	34.3±3.45
	Vernal	47.2±3.75	45.6±4.25	43.5±5.40	48.4±3.81	43.5±3.48
Salinity		0.35	0.02	0.003	0.056	<0.001
Cultivar		<0.001	<0.001	<0.001	<0.001	<0.001
Salinity : Cultivar		0.74	0.26	0.23	0.03	0.82

Data are means ± standard errors of means; CH1, chlorophyll on 8th week of growth; CH2, chlorophyll on 9th week of growth; CH3, chlorophyll on 10th week of growth; CH4, chlorophyll on 11th week of growth; CH5, chlorophyll on 12th week of growth.

Appendix A.7. Mean value (2-yr) and analysis of variance of the plant injury (PI) (1=no injury, 5= >75% injury), survival percentage, leaf relative water content (RWC), crude protein (CP) percentage, fresh (FSB) and dry (DSB) shoot biomass (g plant^{-1}), fresh (FRB) and dry (DRB) root biomass (g plant^{-1}) of five alfalfa cultivars grown under five gradients of salt stress.

Salinity	Cultivar	PI	Survival	RWC	CP	FSB	FRB	DSB	DRB
0 dS m^{-1}	Halo	1.0±0.02	100±0	80.8±6.12	14.0±2.16	15.2±4.79	13.3±5.39	4.4±1.42	2.5±1.17
	Rugged	1.1±0.06	100±0	82.8±0.88	13.8±0.96	12.1±3.27	8.7±1.38	4.0±1.23	2.0±0.39
	Bridgeview	1.1±0.04	100±0	82.9±2.04	12.8±1.43	9.5±2.00	9.4±1.08	2.6±0.6	1.8±0.29
	Rangelander	1.2±0.11	100±0	84.8±1.05	13.4±1.50	6.9±1.67	5.2±1.32	1.8±0.43	1.0±0.19
	Vernal	1.1±0.07	100±0	82.3±3.58	14.4±2.04	11.8±2.82	8.7±1.64	3.9±1.04	1.7±0.43
4 dS m^{-1}	Halo	1.7±0.16	100±0	74.5±3.43	14.6±0.86	8.3±2.02	6.4±2.14	2±0.52	1.8±0.51
	Rugged	2.3±0.13	100±0	78.2±3.61	14.8±0.43	9.1±2.37	7.6±2.75	2.1±0.53	2.3±0.52
	Bridgeview	1.8±0.16	100±0	75.3±5.75	14.8±0.43	6.2±1.56	4.9±1.28	1.4±0.35	1.3±0.23
	Rangelander	2.1±0.13	100±0	78.9±1.71	13.6±0.5	7.2±2.62	3.9±0.91	1.8±0.74	1.3±0.35
	Vernal	1.8±0.13	100±0	77.4±0.97	13.4±0.66	8.8±2.39	7.8±2.49	2.2±0.6	2.4±0.76
8 dS m^{-1}	Halo	2.1±0.14	97.9±2.08	74.4±1.73	18.1±1.20	5.2±1.24	3.4±0.72	1.3±0.30	1.0±0.23
	Rugged	2.6±0.30	93.8±4.38	73.7±0.83	18.7±0.57	6.2±1.17	2.7±0.33	1.5±0.24	1.0±0.11
	Bridgeview	2.7±0.27	95.8±4.17	71.1±2.80	17.1±1.33	5.9±1.53	2.8±0.47	1.4±0.36	1.0±0.20
	Rangelander	2.9±0.25	87.5±4.17	75.2±4.83	17.6±0.87	5.0±1.26	2.1±0.49	1.2±0.28	0.6±0.09
	Vernal	2.4±0.25	97.9±2.08	70.4±4.49	15.9±0.71	6.5±1.99	3.7±1.45	1.2±0.31	1.2±0.47
12 dS m^{-1}	Halo	2.7±0.22	60.4±12.96	74.0±2.53	21.7±0.88	5.6±1.55	3.5±0.74	1.4±0.37	0.9±0.12
	Rugged	3.3±0.38	83.3±9.45	76.7±1.80	18.7±0.86	3.4±0.71	2.0±0.37	0.9±0.14	0.5±0.06
	Bridgeview	3.1±0.28	68.8±10.65	74.1±1.40	19.6±0.68	3.0±0.61	3.0±0.75	0.9±0.18	0.7±0.11
	Rangelander	2.8±0.35	66.7±11.36	78.0±1.73	17.2±0.96	5.2±2.45	2.2±0.42	1.2±0.58	0.7±0.21
	Vernal	2.7±0.28	87.5±8.18	75.8±3.35	20.0±0.88	4.9±1.83	2.7±0.48	1.2±0.41	0.8±0.17
16 dS m^{-1}	Halo	3.0±0.38	64.6±11.11	NA	NA	NA	NA	NA	NA
	Rugged	3.6±0.43	56.3±15.08	NA	NA	NA	NA	NA	NA
	Bridgeview	2.7±0.28	56.3±14.06	NA	NA	NA	NA	NA	NA
	Rangelander	3.1±0.28	52.1±10.18	NA	NA	NA	NA	NA	NA
	Vernal	3.0±0.28	58.3±11.79	NA	NA	NA	NA	NA	NA
Salinity		<0.001	<0.001	0.03	<0.001	<0.001	<0.001	<0.001	<0.001
Cultivar		0.007	0.494	0.44	0.233	0.022	0.01	0.038	0.013
Salinity : Cultivar		0.53	0.777	0.99	0.493	0.66	0.74	0.64	0.46

Appendix A.8. Salt tolerance index of alfalfa cultivars based on dry shoot biomass yield.

Cultivar	Salinity		
	4 dS m^{-1}	8 dS m^{-1}	12 dS m^{-1}
Halo	0.90	0.58	0.56
Rugged	0.77	0.63	0.36
Bridgeview	0.37	0.36	0.27
Rangelander	0.34	0.28	0.22
Vernal	0.79	0.45	0.42

Appendix A.9. Welch two-sample t-test (*P values*) indicating the cultivar difference for the salt tolerance index.

Cultivars	Salinity		
	4 dS m^{-1}	8 dS m^{-1}	12 dS m^{-1}
Halo - Rugged	0.67	0.72	0.02
Halo - Bridgeview	0.10	0.07	0.002
Halo - Rangelander	0.08	0.02	<0.001
Halo - Vernal	0.73	0.32	0.15
Rugged - Bridgeview	0.02	0.04	0.20
Rugged - Rangelander	0.01	0.01	0.05
Rugged - Vernal	0.92	0.19	0.50
Bridgeview - Rangelander	0.81	0.20	0.45
Bridgeview - Vernal	0.03	0.25	0.11
Rangelander - Vernal	0.01	0.06	0.04

Appendix A.10. Mean value and analysis of variance of Sodium (Na), Chlorine (Cl), Potassium (K) and Calcium (Ca) elemental concentrations (mg L^{-1}) in leaf, stem and root tissues of alfalfa varieties under five gradients of salt stress (0 dS m^{-1}, 4 dS m^{-1}, 8 dS m^{-1}, 12 dS m^{-1} and 16 dS m^{-1}) as revealed by inductively coupled plasma-mass spectroscopy.

Salinity	Tissue	Cultivar	Na	Cl	K	Ca
0 dS m^{-1}	Leaf	Halo	944	625	19262	17950
		Rugged	746	795	21796	19180
		Bridgeview	357	737	21302	21936
		Rangelander	310	790	21556	15713
		Vernal	684	640	19024	18484
	Stem	Halo	878	686	23048	6282
		Rugged	797	841	20046	4478
		Bridgeview	576	1069	25196	5615
		Rangelander	611	661	22309	4655
		Vernal	993	838	20188	4931
	Root	Halo	3466	823	20562	2249
		Rugged	3040	832	13659	2660
		Bridgeview	4940	939	21137	2194
		Rangelander	5002	1021	17114	2109
		Vernal	4662	929	15134	2800
4 dS m^{-1}	Leaf	Halo	24578	9779	29464	11322
		Rugged	19442	9656	29002	11332
		Bridgeview	14041	7421	34442	12638
		Rangelander	20292	12398	40535	13129
		Vernal	22016	10078	25769	11104
	Stem	Halo	13365	10188	24906	5900
		Rugged	13685	10810	22228	6119
		Bridgeview	14438	9662	21294	5573
		Rangelander	15543	12660	19627	5641
		Vernal	12674	10226	14765	6355
	Root	Halo	21921	11491	23183	3291
		Rugged	19358	7086	16973	2601
		Bridgeview	21258	8922	20698	2569
		Rangelander	23528	12398	18527	2566
		Vernal	22315	11636	20235	3358
8 dS m^{-1}	Leaf	Halo	38863	16842	30206	10551
		Rugged	23179	9471	41329	10042
		Bridgeview	27516	17140	35693	10791
		Rangelander	43055	23244	30063	8630
		Vernal	36746	22476	31170	9254
	Stem	Halo	26972	11729	15638	6804
		Rugged	17859	7117	16772	6274
		Bridgeview	14773	9970	18281	4969
		Rangelander	32185	13609	14881	6105
		Vernal	17714	9503	9937	4967

	Root	Halo	24570	14343	14837	2956
		Rugged	17248	11749	15787	2324
		Bridgeview	16349	10604	13739	1829
		Rangelander	24185	12514	13585	2689
		Vernal	19005	10034	13425	3049
12 dS m^{-1}	Leaf	Halo	43142	22072	31690	10663
		Rugged	59205	21695	27216	9252
		Bridgeview	51264	25237	33291	10333
		Rangelander	53166	28643	36915	10091
		Vernal	39192	22911	40941	9070
	Stem	Halo	27947	11545	17441	6149
		Rugged	37601	12517	17448	6783
		Bridgeview	40015	16770	21983	7938
		Rangelander	34864	15522	17085	5586
		Vernal	31148	15307	19543	6161
	Root	Halo	29964	17245	16635	3059
		Rugged	29521	16616	15014	2723
		Bridgeview	33877	18761	14702	2819
		Rangelander	40405	28900	16093	3488
		Vernal	38947	21222	18670	3323
16 dS m^{-1}	Leaf	Halo	47356	24662	29410	9700
		Rugged	44123	26250	28233	6461
		Bridgeview	56392	25810	32030	8293
		Rangelander	57445	35728	29312	7501
		Vernal	28083	21092	39883	10448
	Stem	Halo	41429	17430	14819	6988
		Rugged	37202	21498	17683	6740
		Bridgeview	48431	21684	18373	7232
		Rangelander	42327	18596	15782	5731
		Vernal	25105	9830	14257	7827
	Root	Halo	35143	22183	11749	2012
		Rugged	33436	22143	13015	2502
		Bridgeview	34100	19726	13118	2128
		Rangelander	29783	19110	11657	2103
		Vernal	30766	19220	14825	2966

Salinity	<0.001	<0.001	<0.001	<0.001
Cultivar	0.003	0.007	0.22	0.22
Tissue	<0.001	<0.001	<0.001	<0.001
Salinity × Cultivar	<0.001	0.27	0.002	0.60
Salinity × Tissue	<0.001	<0.001	<0.001	<0.001
Cultivar × Tissue	0.57	0.63	0.034	0.44
Salinity × Cultivar × Tissue	0.65	0.94	0.25	0.81